Universidad de Navarra

Facultad de Ciencias

ANALYSIS OF AAV9 BIODISTRIBUTION, TRANSDUCTION EFFICIENCY AND AAV-MIR-935 CARDIO-SPECIFIC OVEREXPRESSION IN A MURINE MODEL OF MYOCARDIAL INFARCTION

Paula García Olloqui

PhD Thesis

2019

Universidad de Navarra

Facultad de Ciencias

ANALYSIS OF AAV9 BIODISTRIBUTION, TRANSDUCTION EFFICIENCY AND AAV-MIR-935 CARDIO-SPECIFIC OVEREXPRESSION IN A MURINE MODEL OF MYOCARDIAL INFARCTION

Paula García Olloqui

Universidad de Navarra

Facultad de Ciencias

Analysis of AAV9 biodistribution, transduction efficiency and AAV-miR-935 cardio-specific overexpression in a murine model of myocardial infarction

Memoria presentada por D./Dª Paula García Olloqui para aspirar al grado de Doctor por la Universidad de Navarra

Dña. Paula García Olloqui

El presente trabajo ha sido realizado bajo mi dirección en el Departamento de Medicina Regenerativa y autorizo su presentación ante el Tribunal que lo ha de juzgar.

Pamplona, 22 de Mayo de 2019

Dr. Beatriz Pelacho Samper

Me gustaría comenzar agradeciendo al CIMA, a la CUN y a la Universidad de Navarra por brindarme la posibilidad de realizar esta tesis doctoral y formarme tanto profesional como personalmente.

Sois muchos los que de una forma u otra me habéis acompañado a lo largo de este camino, gracias de corazón a todos y cada uno de los que habéis hecho que esto sea posible.

Quiero dar las gracias de manera especial a Felipe y Beatriz. Felipe, gracias por confiar en mí, por darme la oportunidad de realizar este trabajo y por apoyarme en el camino. Bea, muchísimas gracias por tu implicación en la dirección de esta tesis, por tu apoyo, tu paciencia y tus consejos. Gracias por preocuparte por mí, por la motivación y por todo lo que me has enseñado. Muchas gracias de corazón.

Quiero dar las gracias al grupo de Cardio. Gracias a Edu y a Saray por ser las mejores manos para ayudarme a llegar donde no podía; pero sobre todo, gracias por ser un gran apoyo y formar parte de tantos buenos momentos. Gracias a Iñigo por los ánimos y el apoyo a lo largo de todo este tiempo. Gracias a Laura, el mejor regalo que me deparaba este último año de tesis. No imaginas cuánto he aprendido de ti. Gracias por transmitir tu fuerza, tus ganas y tu ilusión. Gracias también a Ainhoa, la nueva incorporación, por su frescura y alegría.

Gracias a Gloria González y a todo laboratorio de Terapia Génica del CIMA, en especial a África y a Cristina O. Gracias Gloria por adentrarme en el mundo de los virus, por tu confianza, por tu optimismo e ilusión ante cada resultado. Gracias África y Cristina por vuestro trabajo, vuestra paciencia, por todo lo que he podido aprender con vosotras.

Gracias a Antonio Bernad y a Susana. Gracias Antonio por transmitir tus ganas y pasión por la ciencia, por darle la vuelta a cualquier resultado buscando nuevas preguntas. Gracias Susana por hacerlo todo fácil, por estar siempre dispuesta a ayudar, por tu cariño. Gracias por enseñarme lo bonito que es colaborar.

Muchísimas gracias a mis mellizas, Raquel y Javi. Gracias por vivir esta aventura a mi lado. Sois sin duda lo mejor que me llevo de estos años. Gracias por todos los momentos vividos tanto dentro como fuera del laboratorio, por la complicidad, porque sé que os llevo conmigo para siempre. Gracias por estar siempre ahí y hacer el camino especial.

Muchas gracias a la gran familia de Terapia Celular y Oncohematologia. Gracias por ser el mejor equipo que podía imaginar, es un placer compartir el día a día con vosotros. Gracias Adri y Silvia, por preocuparos por mí y por esta tesis, gracias por vuestro apoyo incondicional. Gracias Juanro, por tu infinita paciencia con mis dudas y por todo lo que me has enseñado. Gracias Isa y Miriam por estar siempre dispuestas a ayudar, por transmitir tanta alegría. Gracias a Arantxa C. y Arantxa B. por tener siempre las palabras adecuadas, por cada sonrisa y por todo el apoyo.

Agradecimientos

Gracias a Eva, Rebeca, Teresa, Oscar, Giulia, Esti Miranda, Leyre y Edurne por vuestro cariño y generosidad. Gracias a Xabi Aranguren, Xonia, Ana Perez, Xabi Agirre, Ana Pardo, Borja, Manu, Quique, Elena y Froi por ser ejemplo de trabajo y permitirnos aprender tanto. Gracias a los nuevos fichajes: Leyre, Jose, Pilar, María, Marta, Laura V., Ana Cris, Ángel, Paula, Ane, Naroa y Juan Antonio por llenar de energía el laboratorio. Disfrutad el camino porque es largo, pero pasa volando! Quiero dar las gracias de manera especial a Gloria y Elena. Sin vosotras esta tesis no hubiese sido posible. Gracias por vuestro trabajo, vuestra paciencia y dedicación. Gracias por tanta ayuda y cariño en todo este tiempo.

Gracias a todos los que formáis parte de los laboratorios de Biología Celular y Molecular de la CUN. En especial, gracias a Tania y Adriana por los buenos momentos compartidos.

No puedo olvidarme de dar las gracias a quien me ayudó a comenzar esta aventura. Gracias a Olalla, Laura M. y Natalia, por la acogida, por cuidarme y enseñarme tanto. No pude imaginar un inicio mejor, mil gracias.

Gracias a todos los que han formado parte del laboratorio. Gracias Esti A. por todos los momentos vividos, por tu alegría innata, por hacernos el día a día mejor y por hacer que parezca que no pasa el tiempo cuando nos volvemos a ver. Gracias a Zapata, Emma, Mentxu, Nico y Andoni, es un lujo haber compartido momentos con todos vosotros.

Gracias a todos los que de una forma u otra me han regalado su ayuda y su cariño durante este tiempo. Gracias Amaia por tus consejos, tu cariño y tus abrazos. Gracias Marien por tu alegría y generosidad. Gracias a Sarai S., Marta L., Erika y Yoli por tener siempre una sonrisa y una palabra de cariño.

Gracias al servicio de Citometría, en especial a Diego, Idoia y Sonia, por su paciencia y su ayuda infinitas. Gracias a los servicios de Imagen y Morfología. Gracias Sylvie, por recibirnos cada día con una sonrisa. Gracias a Marisol por su paciencia y generosidad. Gracias a Alberto, Mari y Ana por su simpatia y amabilidad. Gracias Carol, por preocuparte por mí y por este trabajo, por tu dedicación y cariño.

Gracias a todo el departamento de Bioquímica y Genética de la UNAV. Gracias a Mª Jesús, por iniciarme en el mundo de la investigación y animarme a empezar esta aventura. Gracias a Silvia Cenoz e Iñigo por tanta organización y ayuda. Y gracias a todos y cada uno de los que me habéis permitido colaborar en la docencia, gracias por todo lo aprendido.

Gracias a mis amigas. A las de toda la vida, a mis chicas Diferencia. Gracias también a las que de una forma u otra se cruzaron en mi camino y por suerte se quedaron: Ana I., Alba, Ana M., Jenny, Laura, Silvia, Amaia y Naza. Gracias por estar siempre ahí. Por vuestro apoyo en todo momento, por entender mis ausencias y por hacer que parezca que no ha pasado el tiempo cuando volvemos a vernos. Gracias por ser mi mejor vía de escape. ¡Gracias de corazón!

Gracias Javi, por crecer a mi lado, por cuidarme y entenderme, por confiar en mí. Gracias por formar parte de mi vida, por hacerme feliz. Gracias también a toda tu familia, por su apoyo y su cariño.

Muchísimas gracias a mi familia, el pilar fundamental de mi vida. A mis tíos y primos, a los que siempre han estado y están, gracias. Gracias a mis hermanos, Javier e Ignacio. Gracias por preocuparos por mí, por protegerme, por hacerme saber que siempre puedo contar con vosotros. Gracias por estar siempre, para todo. Gracias Vero y Marta, por vuestro apoyo y vuestro cariño desde el primer día. Gracias por formar parte de la familia, gracias de verdad. Infinitas gracias a Aitor, Mario y Nacho. Gracias por llenar nuestras vidas de ilusión y alegría, por multiplicar los buenos momentos y hacernos olvidar los que no lo son tanto. Gracias por ser tan especiales, por dejarme disfrutar a vuestro lado, siempre seréis el mejor regalo.

Gracias a mis padres por ser los primeros en confiar en mí, por acompañarme siempre. Gracias Papá por ser el mejor ejemplo de trabajo y dedicación, gracias por tus consejos y tu cariño. Gracias Mamá por escucharme y entenderme como nadie. Gracias por luchar siempre por todos, por guiarme, por estar a mi lado. Gracias a los dos por todo lo que hacéis por mí. En el fondo este trabajo es vuestro, por eso, gracias y enhorabuena!

Gracias a todos los que habéis estado, estáis y estaréis.

Gracias porque sin vosotros no lo hubiese logrado.

He aquí mi secreto,
que no puede ser más simple:
sólo con el corazón se puede ver bien;
lo esencial es invisible para los ojos.

El Principito
Antoine de Saint-Exupéry

AAP: Assembly activating protein

AAV: Adeno-associated viral vectors

AGO: Argonaute

ALP: Alkaline phosphatase

ALT: Alanine aminotransferase

AMI: Acute myocardial infarction

Ang-1: Angiopoietin-1

ARL: ADP-ribosylation factor-like

ASS-1: Argininosuccinate synthase 1

BCL6: B-cell lymphoma 6 protein

bFGF: Basic fibroblast growth factor

Bim: Bcl-2 like protein 11

BMI1: B lymphoma Mo-MLV insertion region 1 homolog

BMSC: Bone marrow stem cells

bp: Base pairs

BSA: Bovine serum albumin

Cap: Capsid protein

CDC: Cardiosphere-derived cells

CK: Creatine kinase

c-kit: Tyrosine kinase receptor

CMs: Cardiomyocytes

CMV: Cytomegalovirus

CPC: Cardiac progenitor cells

CSC: Cardiac stem cells

CTGF: Connective tissue growth factor

CVD: Cardiovascular diseases

DMEM: Dulbecco's modified Eagle's medium

ECM: Extracellular matrix

EF: Ejection fraction

EF1α: Elongation factor -1 alpha

EPC: Endothelial progenitor cells

Abbreviations

ESCRT: Endosomal sorting complex required for transport

ESC: Embryonic stem cells

FAC: Fractional area change

FBS: Fetal bovine serum

FS: Fractional shortening

GFP: Green fluorescent protein

GO: Gene ontology

HDF: Human dermal fibroblasts

HGF: Hepatocyte growth factor

HSC: Hematopoietic stem cells

IF: Immunofluorescence

IGF: Insulin-like growth factor

IL: Interleukins

Imyo: Intramyocardial

iPSC: Induced pluripotent stem cells

I/R: Ischemia/reperfusion

ITRs: Inverted terminal repeats

IV: Intravenous

IZ: Infarct zone

LAD: Left anterior descendent

LAMPs: Lysosomal-associated membrane proteins

Ldbr: Lariat debranching enzyme

LDH: Lactate dehydrogenase

LV: Left ventricular

LVEF: Left ventricular ejection fraction

Luc: Luciferase

MCP-1: Monocyte chemoattractant protein-1

MHC: Histocompatibility complex

MI: Myocardial infarction

miRNAs: MicroRNAs

MLC: Myosin light chain

MMP: Metalloproteinases

MSC: Mesenchymal stem cells

MVEs: Multivesicular endosomes

Nabs: Neutralizing antibodies

NTA: Nanoparticle tracking analysis

ORF: Open reading frame

PCA: Principal component analysis

PDGF: Platelet derived growth factor

PEG: Poly-ethylene glycol

PEI: Poly-ethylene imine

POFUT1: GDP-fucose protein O-fucosyltransferase 1

PPP1R10: serine/threonine-protein prosphatase 1 regulatory subunit 10

Rep: Replication protein

RISC: RNA-induced silencing complex

RLUs: Relative light units

R/T: Room temperature

RZ: Remote zone

Sca-1: Stem cell antigen-1

SCF: Stem cell factor

SDF1: Stromal derived factor-1

SEMA4B: Semaphorin-4b

SIRT1: Sirtuin-1

SM: Skeletal myoblasts

ssDNA: Single-stranded DNA

SSEA1: Stage-specific embryonic antigen-1

SV: Stroke volume

TGF-β: Transforming growth factor-β

TIMPs: Tissue inhibitors of metalloproteinases

TNF-α: Tumoral necrosis factor-α

Abbreviations

TnT: Cardiac troponin T

Tβ4: Thymosin-β4

VD: Volume in diastole

VEGF: Vascular endothelial growth factor

Vg: viral genomes

VS: Volume in systole

WPRE: Woodchuck hepatitis virus post-transcriptional regulatory element

XPO5: Exportin-5

αMHC: α-myosin heavy chain

Table of contents

TABLE OF CONTENTS

Introduction

1. CARDIOVASCULAR DISEASES

1.1 EPIDEMIOLOGY AND RISK FACTORS

Cardiovascular diseases (CVD) are the main cause of morbidity and mortality worldwide. According to the World Health Organization, CVD are the leading cause of death, accounting for 30% of all of them (**Figure 1A**), approximately 17 million per year (https://www.who.int/news-room/fact-sheets). Ischemic heart disease, in particular, represents one of the most important hurdles for health systems in high- or middle-income countries, whilst it is also increasing in underdeveloped ones. According to statistics, 50% of patients suffering a first infarct, will die within the next 5 years, which gives an idea of the magnitude of the problem both at the human and economic level. Unfortunately, predictions are not favorable and it is estimated that by 2030, about 24 million people will die from these diseases, representing 42% of deaths worldwide [1].

The major risk factors associated with ischemic heart disease include behavioral ones such as a high cholesterol-diet, physical inactivity, smoking and alcoholism; as well as physiological factors like hypertension and high cholesterol or glucose blood levels (**Figure 1B**). These can be associated with social determinants but also with non-modifiable factors like aging, family history, gender or ethnic origin.

Pharmacological therapies and revascularization techniques have allowed to improve symptoms and to slow down the adverse progress of cardiac remodeling, improving patient's quality of life and survival. However, myocardial infarction (MI) still represents an increasingly common disorder that carries a poor long-term prognosis, being heart transplantation the only real option for severe cases of cardiac dysfunction, with the concomitant immunological and organ availability limitations.

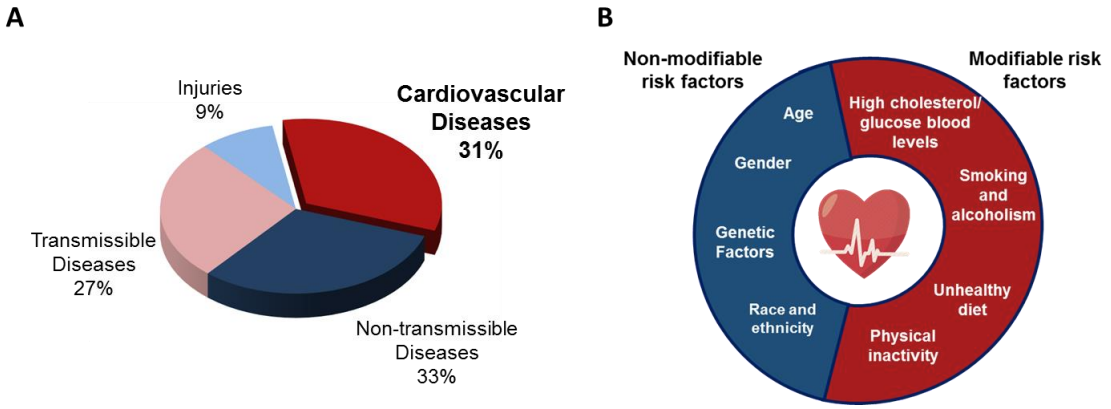

Figure 1. Epidemiology and risk factors of CVD. *Distribution of major causes of death including CVD* ***(A).*** *Major risk factors associated with cardiac ischemic pathology* ***(B).***

1.2 MYOCARDIAL INFARCTION

MI is most often caused by cholesterol plaque rupture and thrombus formation in a coronary vessel, resulting in the acute reduction of blood supply to a portion of the myocardium (ischemia) that eventually leads to irreversible damage and death of the heart muscle. After the ischemic event, cardiomyocytes (CMs) die due to hypoxia, triggering a compensatory mechanism that initiates and modulates the reparative processes. These ones include dilatation, hypertrophy and collagen scar formation, and can be divided into three overlapping phases (**Figure 2**):

- **Inflammatory phase.** Acute inflammation takes place between 1 hour and 4 days after MI. This phase starts with a massive necrotic cell death in the infarct area. Damaged CMs release many intracellular molecules and numerous pro-inflammatory cytokines like tumoral necrosis factor-a (TNF-α), interleukins (IL)-1β and IL-6 [2], and chemotactic active molecules such as monocyte chemoattractant protein-1 (MCP-1) or stem cell factor (SCF) [3]. On the other hand, interstitial fibroblasts produce metalloproteinases (MMP) to degrade the extracellular matrix (ECM) favoring inflammatory cells migration into the damaged tissue. Pro-inflammatory monocytes and macrophages modulate inflammatory cytokines and chemokines activity that promotes clearance of debris and the deposition of a temporary fibrin matrix that replaces the dead tissue [4].

- **Proliferative phase.** This phase occurs between 4 and 14 days after MI. The repression of inflammation is essential for the activation of this following phase. Cardiac endothelium and inflammatory cells are key regulators in this process inducing the revascularization of the damaged tissue [5]. They regulate the secretion of cytokines, chemokines and growth factors such as stromal derived factor-1 (SDF1) or IL-8 [6], which are involved in the recruitment of vascular progenitors to the injured area. Other factors like transforming growth factor β1 (TGF-β), vascular endothelial growth factor (VEGF), insulin-like growth factor (IGF) or IL-10 stimulate the differentiation of fibroblasts into myofibroblasts and the secretion of collagen and fibronectin, producing large amounts of ECM (composed mainly by Collagen-III, laminin and adhesion proteins) and resulting in the formation of the so called granulation tissue [7], [8].

- **Maturation of the infarct scar.** Finally, the granulation tissue matures in the infarcted heart 14 days after MI. Scar maturation is characterized by disappearance of inflammatory cells, regression of blood vessels and persistence of myofibroblasts. Myofibroblasts release tissue inhibitors of MMPs (TIMPs) that inhibit the degradation of the ECM and induce deposition of new collagen fibers [9]. At this stage, type-III collagen is replaced by type-I collagen, which is

further modified by LOX-catalyzed cross-linking [10]. A large accumulation of mature collagen fibers and extensive remodeling lead to increased tensile strength and contraction of the scar that finally, leaves a non-contracting region in the ventricular wall. Thereby, although this fibrotic tissue is essential for avoiding initial tissue rupture, it gets chronic, impairing tissue elasticity and therefore leading to a deleterious decline of heart function.

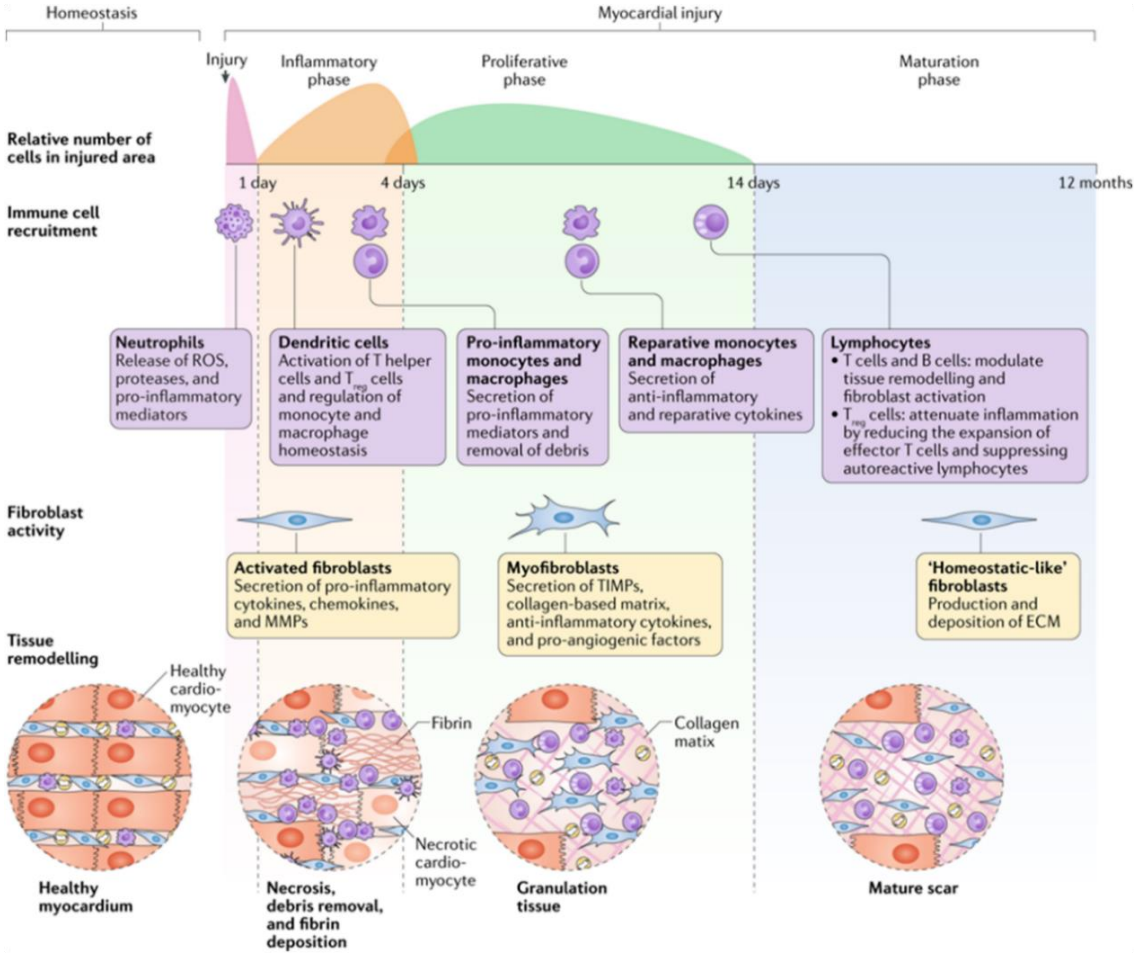

Figure 2. Phases of cardiac remodeling after myocardial injury. *The repair response after cardiac damage can be subdivided into three overlapping phases: inflammatory, proliferative and maturation phase. In the inflammatory phase, CMs death leads to the release of damage-associated molecular patterns and activate the inflammatory cells infiltration, which promote clearance of debris and the deposition of temporary fibrin matrix to replace dead cells. In the proliferative phase, inflammation is contained by the pro-healing subset of monocytes and macrophages, while myofibroblasts and collagen-based matrix replaces the initial fibrin. Finally, myofibroblast activation recedes in a dense collagen network form the mature scar tissue. Image reproduced from Forte E et al. Nat. Rev. Cardiol, 2018* [11].

2. CELL-BASED THERAPIES FOR CARDIAC REPAIR

After an ischemic event, there is a massive loss of contractile cells, which cannot be compensated by the survival CMs. This fundamental problem has not been solved by current therapies that are based on the application of palliative (drugs) or in the most severe cases, in radical (heart transplantation) strategies. Thus, a deeper understanding of cardiac development and the pathological processes that occur in the heart is required in order to promote new alternative therapies that advance cardiac regeneration.

In this context, cardiac development and post-natal heart regeneration have been broadly studied topics. After damage, the ability to re-generate mature cells, including CMs, occurs to a different extent in each developmental stage. In embryonic mice stages, compensatory CMs growth is able to restore up to 50% of the lost tissue, replacing the majority of tissue with minimal scarring; however, in adult mice, CMs proliferation is minimal and ECM deposition leads to an extensive scar [12]. For this reason, the adult mammalian heart was long considered a terminally differentiated organ with no regeneration capacity. To treat the failing heart, scientists have focused on different approaches to promote heart protection and repair. In this scenario, **stem cell-based therapy** was born, involving the transplant of progenitor cells or multi/pluripotent stem cells to replace the lost myocardium. Initial cell candidates tested were **skeletal myoblasts (SM), bone marrow stem cells (BMSC) and mesenchymal stem cells (MSC).**

SM were initially expected to remuscularize the damaged heart and restore the contractile function. Their use was motivated by their easy accessibility from autologous muscle biopsies, their rapid *in vitro* expansion, their superior resistance to the ischemic environment and their lack of tumorogenicity [13]. Different research groups tested these cells in both ischemic and non-ischemic cardiomyopathies either in small as well as in large animal models. Despite that transplanted SM did not differentiate into CMs, they were able to improve myocardial function, attenuating the deleterious progression of ventricular remodeling [14] [13]. SM were rapidly translated to the clinic. Initial trials showed improvement in heart function, but unfortunately, long-term follow-up studies did not show significant beneficial effects [15], [16]. Furthermore, ventricular arrhythmias were reported in some of these trials, probably resulting from the lack of electromechanical integration between SM and resident CMs [17]. Although posterior pre-clinical works with lower cell doses did not provoke such problem [18], the use of SM in clinical studies was relegated by the use of other cell types. Meanwhile, **BMSC** have constituted one of the most used cell sources due to their none-low morbidity and

their facile tissue isolation and culture from bone marrow or blood. BMSC include hematopoietic stem cells (HSC) and endothelial progenitor cells (EPC) populations. HSC are isolated via surface markers (CD34 and CD45) whilst EPC can also be harvested from a blood sample based on the expression of CD34 and CD133. Originally, these cells were credited with the ability to differentiate into cardiovascular cells [19], although this point was later disapproved, at least for the CM-lineage [20]. Interestingly, the first preclinical studies performed with BMSC demonstrated a beneficial contribution, promoting cardiac repair. An increase in angiogenesis/vasculogenesis was described, potentially due to paracrine effects on the host vasculature. However, results regarding therapeutic effects were inconsistent among groups when analyzed in the long-term [21], [22]. In this way, early clinical trials showed modest but significant improvement in cardiac function [23], [24]. However, trials with larger randomized patient populations did not reproduce these results [25]–[27]. A lot of controversy remains in this field and the most accepted theory suggests a variable and modest improvement due to paracrine mechanisms while the low engraftment and limited differentiation potential continues to be a restriction of this therapeutic approach.

The third candidate, **MSC**, are a subpopulation of stromal cells that can be easily derived from various tissues, like bone marrow or adipose tissue after expansion *in vitro*. The capacity of MSC for self-renewal and multipotent differentiation into different cell types like adipocytes, cartilage and bone cell-types has been fully demonstrated [28]. Differentiation into CMs was also described for MSC in presence of the DNA methyltransferase inhibitor 5-azacytidine or by co-culture with primary CMs [29], [30], however, the successful rate of differentiation into functional CMs remains unclear. Several preclinical studies have shown that injection of MSC into the injured heart leads to improved cardiac function. Their transplant was able to induce angiogenesis, mainly by paracrine action and in a low degree by differentiation into endothelial cells [31]. Genetic engineering has been used to improve the angiogenic properties of these cells. Thus, the overexpression of granulocyte chemotactic protein 2, angiopoietin-1 (Ang-1) or hepatocyte growth factor (HGF) in MSC, have demonstrated to enhance their beneficial effects [32]–[34]. Additionally, it has been described that transplanted MSC induce CD73 expression on host macrophages, promoting M2 monocyte/macrophage polarization [35]. This effect allows to decrease inflammation in the ischemic cardiac tissue.

Furthermore, at the clinical level, one of the most relevant trials with MSC was the so-called POSEIDON, a phase I/II randomized trial that demonstrated certain beneficial effect after acute MI (AMI). Remarkably, this study compared autologous and allogenic MSC and demonstrated similar therapeutic effects [36]. In addition, different cell doses were assessed,

showing a greatest reduction in left ventricular (LV) volumes and increased ejection fraction (EF) with a lower concentration cell dose (20 *vs.* 200 million cells). Thus, the use of MSC in clinical trials has demonstrated to be safe but with modest benefits for patients [37].

Motivated by the lack of cardiac differentiation and the limited regenerative potential of first-generation stem cell types, **a second generation** with greater cardiovascular differentiation capacity was born, including **pluripotent stem cells** and **cardiac stem cells (CSC) or cardiac progenitor cells (CPC).**

Pluripotent stem cells have been broadly assayed with the aim to generate functional CMs that could regenerate the injured heart. The first cell source studied was the embryonic stem cells (ESC). ESC are clonogenic, self-renewing and pluripotent cells [38] and numerous protocols have already been optimized for their cardiac differentiation *in vitro*. Rodent and human ESC-derived CMs have demonstrated the expression of cardiac markers and a contractile cardiac phenotype [39]. Moreover, when transplanted into the damaged heart (and despite the low engraftment rates), ESC have demonstrated improved cardiac function [40], [41]. Furthermore, transplanted cells electromechanically coupled with resident CMs, although the induction of arrhythmias was reported in some studies [42], [43]. For their clinical application, major issues such as immune rejection or risk of tumorogenesis go hand in hand with ethical concerns. Therefore, only one clinical trial using ESC-derived CMs is ongoing [44]. In 2006, induced pluripotent stem cells (iPSC) were first described by Yamanaka and colleagues. They reported mouse and human fibroblasts reprogramming to an ESC-like pluripotent state, by forced expression of four genes encoding pluripotent transcription factors (either Oct3/4, Sox2, Klf4 and c-Myc, or Oct3/4, Sox2, Nanog and Lin-28) [45], [46]. Since then, different protocols for iPSC cardiac differentiation have been developed, and positive effects in cardiac function and remodeling have been shown after transplantation of iPS-derived CMs into small and large animal models of MI [47], solving the ethical issues of using ESC. However, in cases where cells survived in the long term (up to 12 weeks), substantial incidence of ventricular tachycardia was evidenced, probably as a consequence of the immature state of the transplanted iPSC-derived CMs [48]. Inconsistencies in the reported engraftment rate and putative risk of arrhythmias or tumorogenesis were initially the main limitations of this therapy [49], [50]. Many advances have been made to enhance the cell retention (like combination with different scaffolds) [51], [52] and to reduce the risk of tumorogenesis and arrhythmias associated with the undifferentiated immature state of the cells (improving CMs differentiation and selection protocols) [53], [54]. However, regardless of these key advancements, new studies in large-animal models are needed before translation to the clinic.

On the other hand, several studies have already demonstrated the low but intrinsic CMs turnover in the adult mouse heart [55], [56]. De novo cardiomyogenesis is limited to ~1% per year and the cellular source of endogenous CMs renewal continues to be debated. Adult multipotent **CPC** were first defined based on surface expression of the tyrosine kinase receptor c-kit [57]. Other cell surface markers were later proposed to describe resident subpopulations including stem cell antigen 1 (Sca-1) [58], [59], insulin gene enhancer protein ISL1 [60] platelet derived growth factor α (PDGFα) [61], ATP-binding cassette ABCG2 [62] or combinations of these. Among them, the c-kit$^+$ as well as Sca-1$^+$ cardiac cell populations have been the most broadly described.

Murine c-kit$^+$-CPC were initially proposed as necessary and sufficient for cardiac regeneration and repair [63], however, later lineage tracing studies for c-kit$^+$ CPC failed to demonstrate a significant contribution of them to the cardiac lineage [64], [65]. Despite this fact, these cells have demonstrated to improve cardiac function in rodent as well as in large animal models, probably due to trophic effects [66], [67]. Therefore, nowadays, c-kit expression is considered necessary but not sufficient to define CPC [68]. On the other hand, Sca-1 is a specific surface marker for somatic stem cells, with a crucial role in activation and differentiation of CPC *in vivo* [69], [70]. Matsuura *et al.* demonstrated how Sca-1$^+$ cells isolated from adult mice hearts were differentiated into contractile CMs after oxytocin treatment [71]. Several subpopulations of Sca-1$^+$ CPC combined with different stem cell markers have been reported too. Thus, transplantation of Sca-1$^+$/CD31$^-$ cells after MI, resulted in positive cardiac remodeling and improvement in LV ejection fraction in a mouse model [72]. Unlike c-kit, Sca-1 lacks an equivalent in human. Another cell population with adult cardiac progenitor characteristics has been recently identified, such as CPC with high expression levels of B lymphoma Mo-MLV insertion region 1 homolog (BMI1) protein [73]. BMI1 is a transcription factor, member of the polycomb complex BMI1, involved in many biological processes including embryonic development, stem cell stabilization and differentiation [74]. Interestingly, BMI1$^+$ cells have been described to contribute to the three main heart lineages in homeostasis and markedly, after damage [75], [76]. Furthermore, genetic ablation of the BMI1$^+$ progenitors before MI induction, has shown their involvement in cardiac physiological remodeling, mainly by intervening in the revascularization processes [77]. On the other hand, a mixed population of CPC (mainly c-kit$^+$ CPC) derived from cardiac explants has the ability to form cardiospheres which can be dissociated to yield **cardiosphere-derived cells (CDC).** It has been also reported a substantial cardiomyogenic potential of CDC in several MI models [78], [79]. Interestingly,

positive effects on myocardial repair were initially reported after intracoronary infusion of CDC in a pig model of MI [79].

In general, the unsuitable homing and engraftment of progenitor cells after transplantation has been a substantial limitation, so strategies to improve the engraftment and survival of the transplanted cells have been thoroughly studied. Transgenic CPC with an extra copy of p53 have demonstrated an increased tolerance to oxidative stress, improving their engraftment in the damaged tissue [80]. Other groups have used multiple CPC injections [81] or chemical pretreatments to CPC to improve their survival and homing [82], [83]. The *in situ* CPC stimulation for cardiac regeneration through specific cytokines and growth factors has been also assayed [84], [85].

The therapeutic role of these cells has been already assessed in the clinic**.** SCIPIO was the first clinical trial in which c-kit$^+$ CPC were used to treat patients with ischemic cardiomyopathy, although conflicting findings about their potential have been reported [86]. A second clinical trial where CDC were transplanted into patients after MI (CADUCEUS), reported a reduction in infarct size and an increase in viable myocardium, nonetheless, no changes could be observed in left ventricular ejection fraction (LVEF) [87]. Other clinical trials have combined CDC with basic fibroblast growth factor (bFGF)-gelatin hydrogel sheets (ALCADIA) or with autologous BMSC (CONCERT-HF). ALCADIA clinical trial has shown an increased LVEF and decreased scar size after 6 months of treatment in patients with ischemic cardiomyopathy. However, the results are not very conclusive as only 6 patients were treated and a control group was not included in the study [88]. CONCERT-HF is an ongoing clinical trial performed with the aim to investigate the feasibility/safety and the therapeutic effect of c-kit$^+$ CPC and BMSC (alone or in combination) in patients with ischemic cardiomyopathy [89]. All these trials have been performed with autologous cells that carry concomitant limitations, such as the requirement of patient-specific myocardial biopsy (that can be affected by age and disease), delays in therapy application due to cell processing, culture and performance of quality controls, and increase in logistical and economic constraints. In order to expand CPC/CDC indications, allogenic cells have been already tested as alternative to the autologous ones [90]–[92]. Therefore, clinical evaluation of allogenic CDC is nowadays being performed for the treatment of MI (ALLSTAR) or dilated cardiomyopathy (DYNAMIC) with no major adverse cardiac events reported until now [93], [94]. Meanwhile, allogenic CPC are also currently tested in the CAREMI trial, where safety and efficacy of intracoronary infusion have been already proved in patients with MI, six months after treatment [95].

In summary, stem cell therapy has demonstrated to be feasible and safe but with limited efficacy in the clinic, being their benefit troubled by a number of constraints like the low cell retention/engraftment and poor survival rates, the immunogenicity of some allogenic cell populations and the tumorogenicity of pluripotent stem cells, which minimizes their long-term treatment efficacy [96]. Furthermore, it has been demonstrated that the therapeutic effects found are not mainly mediated by cell differentiation but by paracrine effects. A next generation therapy has been born as a result of the study of this trophic capacity, identifying specific factors that may exert a therapeutic action for cardiac repair and/or protection (**Figure 3**).

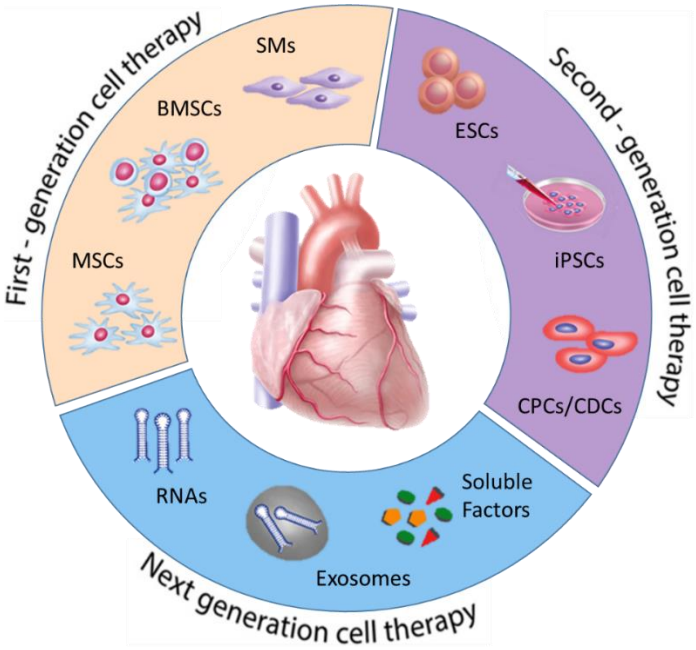

Figure 3. Evolution of alternative cardiac regenerative therapies. *First-generation cell types such as SM, BMSC and MSC demonstrated feasibility and safety but limited efficacy in the clinical setting. Second-generation cell therapies based on the use of ESC, iPSC and CSC/CDC were proposed in order to regenerate the target organ. Emerging next-generation therapies directed toward cell-free concepts (Secretory factors, non-coding RNAs or extracellular vesicles) are being explored also. Image adapted from Cambria et al. NPJ Regen Med. 2017* [97].

3. SECRETORY FACTORS FOR CARDIAC REPAIR

Cell-based therapy was initially expected to regenerate the ischemic heart through differentiation of the transplanted cells into functional cardiovascular cells. Some studies did provide cardioprotective benefits but, paradoxically, transplanted cells rarely differentiated into CMs and a large body of evidences have shown that their paracrine products were the main contributors to the beneficial effects. Thus, it has been demonstrated that soluble factors and microRNAs (free released or encapsulated in exosomes) are secreted by stem cells promoting cardiac repair at many different levels, inducing neovascularization, activation of endogenous progenitor cells and CMs proliferation, inhibition of apoptosis or modulating ECM secretion, fibrosis and inflammation.

In this context, the principal secretory factors involved in cardiac repair are briefly described below.

3.1 SOLUBLE FACTORS

Many studies have dedicated their efforts towards the identification of growth factors and cytokines that contribute to cardiac regeneration. A wide variety of these cell-secreted trophic factors have been already described as modulators of different cardiac repair mechanisms (**Table 1**). Initially, a large number of studies tested the pro-angiogenic potential of different factors, including VEGF and bFGF among others. VEGF binds to a tyrosine kinase receptor on endothelial cells inducing their proliferation [98], as well as endothelial progenitor cells differentiation and angiogenesis post-MI [99]. Another angiogenic factor, bFGF, also mediates endothelial cell proliferation, migration and tube structure formation. The protective effects of bFGF against hypoxic-ischemic events have been also largely reported *in vitro* and *in vivo* [100]. Furthermore, bFGF can modulate angiogenesis by a direct effect on endothelial cells but also indirectly by the up-regulation of VEGF in vascular smooth muscle cells [101]. Thus, the combined administration of VEGF and bFGF results in a synergistic effect on angiogenesis *in vivo* [102]. The chemokine SDF-1 has been also shown to be an effective recruiter of endothelial progenitors to the ischemic tissue [103], able to preserve viable CMs and increase vascular density by stimulating the SDF-1/CXCR4 axis [104]. IGF-1 has also been reported for its role in preventing angiotensin II-induced cardiac inflammation and fibrosis by stimulation of the Akt/Foxo pathway [105], [106]. Other molecules have been described for their implication in cardioprotective effects or fibrosis including HGF, protein thymosin-β4 (Tβ4) or MMPs. HGF was first identified as a hepatocyte mitogen, with chemotactic and anti-apoptotic actions in different cell types [107]. This growth factor is found in elevated levels in the heart and its intravenous

administration has demonstrated to reduce apoptosis in CMs in a rat model of ischemia/reperfusion (I/R) [108]. Similarly, other studies reported how CDC release HGF, which helps to prevent oxidative stress after MI and promote self-repair through the HGF/Met signaling pathway [109], [110]. Tβ4 can be also secreted by stem cells and contribute to cardiac repair after MI [111], [112]. After damage, this protein suppresses the epigenetic repressor methyl-CpG binding protein 2 and this triggers downregulation of fibrogenic genes, platelet-derived growth factor (PDGF)-β receptor, α-smooth muscle actin, collagen I and fibronectin, resulting in reduced fibrosis [113]. Regarding remodeling, the expression of collagen types I and III in the ECM are modulated by paracrine signaling. After damage, MMPs expressed by infiltrated macrophages and fibroblasts, trigger regenerative signals. A balance between MMPs and TIMPs mediates ECM degradation, cell proliferation and migration [114]. Endogenous mechanisms can be also involved in mobilization and homing of progenitor cells to the cardiac lesion, activate them and promote muscular regeneration. On the other hand, extracellular factors have also been identified for their ability to activate CMs proliferation. Thus, neuregulin 1 has been described to induce CMs proliferation and improve cardiac function in the injured heart [115].

Thereby, soluble factors mediate stem cell paracrine effects and contribute to cardiac regeneration, representing a promising alternative therapeutic approach for myocardial repair.

Table 1. Stem cell-secreted paracrine factors and proposed cardiac repair mechanisms. *Table adapted from Mirotsou M et al. J Mol Cell Cardiol. 2011* [116]**.**

Cardiac Repair Mechanisms	*Paracrine Mediators*
Neovascularization / Angiogenesis	VEGF, bFGF, IGF-1, TNFα, IL-1, HGF, SDF-1, Ang-1, Ang-2, TGF-β, PDGF- β, PIGF, MCP-1
Cell Survival	HGF, Tβ4, VEGF, TGF-β, SDF-1, IGF-1, bFGF, STC-1, SFRP2
Remodeling	Tβ4, MMP-2, MMP-9, TIMP-1, TIMP-2, TIMP-9, IL-10, TGF-β, HGF, NGF, TSPI, IL-1, ErbB2
Cardiovascular differentiation	VEGF, IGF-1, HGF, TNFα
Contractility	bFGF, FGF2, HGF, Tβ4

3.2 MICRORNAs

A large body of studies have shown the key role that microRNAs (miRNAs) play in the homeostasis and pathology of the heart. Experimental results have demonstrated that the lack/overexpression of just one miRNA can be sufficient to cause a specific CVD, and importantly, how that disease can be reverted by restoring miRNA physiological levels, suggesting their therapeutic potential. The structure and biogenesis of miRNAs as well as their role in the homeostasis and pathological context is detailed below.

3.2.1 STRUCTURE AND BIOGENESIS

miRNAs are highly conserved, single-stranded, small non-coding RNAs that are involved in the post-transcriptional regulation of gene expression by affecting both the stability and translation of specific mRNAs. The first miRNA assigned to a specific function was lin-4, which targets lin-14 during *C.elegans* development [117]. Since then, many miRNAs have been identified and nowadays, miRBase (http://www.mirbase.org/) contains around 48860 mature miRNAs sequences from 271 organisms [118]. Among these, around 2654 mature sequences are from the human genome, which may target approximately 60% of human protein-coding genes. Each miRNA regulates from tens to hundreds of different target genes and is itself regulated by various mechanisms, including epigenetic changes [119]. These regulatory capabilities make them key molecules for novel therapies or candidate clinical disease biomarkers.

The structure of miRNA consists on a single stranded RNA of 19 to 24 base pairs (bp) that includes a defined seed region of 2 to 8 nucleotides. This region provides specificity for targeting mRNAs, through binding itself to complementary sequences in the 3'UTR untranslated region of target mRNAs and repressing the expression of specific proteins. The rest of the miRNA sequence can also interact with the mRNA giving a stronger complementarity to its target, that increases the probability to be degraded.

Before becoming a single stranded molecule, the miRNAs suffer a series of modifications. The original molecule is an RNA hairpin or loop structure (pri-miRNA) synthesized by RNA polymerase II (**Figure 4A**). These molecules, the pri-miRNAs, can be classified into five groups according to their genomic locations, relative to introns and exons [120]. Thus, we can differentiate among intergenic miRNAs, which are located between two consecutive protein-coding genes; intronic miRNAs (included in non-coding or in protein-coding transcripts) and exonic miRNAs (included in non-coding or in protein-coding transcripts). The intronic genomic location is the most common one for miRNAs, followed by the intergenic and finally by the exonic location (**Figure 4B**). miRNA biogenesis will depend on this genomic localization.

Intergenic miRNAs are processed by a canonical pathway. In this process pri-miRNAs are cropped by the Drosha/DGCR8 complex which permits cleavage into a 70-100 bp stem-loop hairpin (pre-miRNA). The pre-miRNA is exported to the cytoplasm, binding to Exportin-5 (XPO5), complexing next with Ran-GTPase, and being exported through the nuclear pore. Once in the cytoplasm, further enzymatic cleavage by Dicer/TRBP complex produces a miRNA double strand (22 bp long). This duplex serves as a guide that pairs with mRNA. First, duplex is dissociated, followed by assimilation of one of the miRNA strands with Argonaute (AGO), thus forming the RNA-induced Silencing Complex (RISC) which binds to the complementary sequence of the mRNA, promoting post-translational degradation or downregulation of expression [121] (**Figure 4C.1**). **Intronic miRNAs** can be processed by Drosha after assembly of the early spliceosome complex but before (or during) intron excision [122]. Thus, pre-miRNA enters in the mRNA pathway and continue the process. miRtrons are non-canonical intronic miRNAs produced from spliced introns and debranching. Their processing bypasses Drosha cleavage and the lariat debranching enzyme (Ldbr) resolves the secondary structure of the excised intron into a hairpin structure resembling pre-miR, that can be transferred to the cytoplasm by XPO5 and act as a canonical miRNA (**Figure 4C.2**). **Exonic miRNAs** biogenesis is poorly understood. Some works suggest that unspliced nuclear transcripts are mainly processesed to pre-miRNAs and transported into the cytoplasm to follow classical miRNA biogenesis. Moreover, it has been shown that alternatively, the spliced transcripts (still containing the miRNA hairpin) can be exported to the cytoplasm, although it is still not clear how they are processed to a mature form [123] (**Figure 4C.3**).

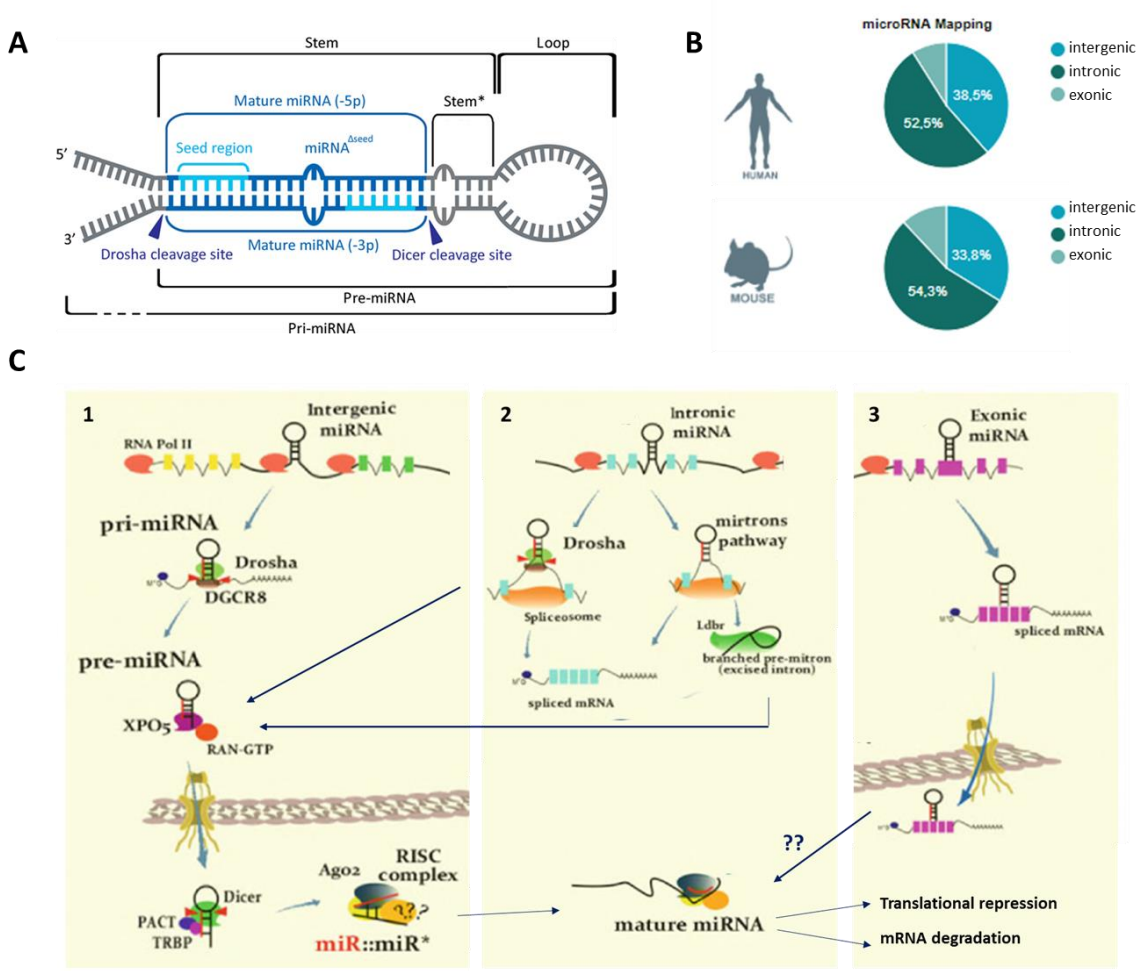

Figure 4. Structure, genomic localization and biogenesis of miRNAs. *Different forms of miRNAs along its biogenesis process, including pri-miRNA, pre-miRNA and mature miRNA* ***(A).*** *miRNA mapping of genomic localization: intergenic, intronic and exonic miRNAs in human and mouse* ***(B)****. Biogenesis of miRNA depending on the genomic localization: intergenic* ***(C.1)****, intronic* ***(C.2)*** *and exonic (****C.3)*** *transcription process. Images adapted from different sources: A) Jevsinek Skok, D et al. Animal Genetics 2007* [124] *B) http://bmi.ana.med.uni-muenchen.de/miriad/ and C) Greene C. Progress in Inflammation Research, Springer 2015* [125].

Once the mature miRNAs are on the cytoplasm they can regulate the expression of targeted genes in two ways. One process requires full complementarity between the miRNA and the targeted mRNA and very rarely occurs in animal cells. This process is known as post-transcriptional gene silencing, and the miRNA blocks protein synthesis through degradation of mRNA. The other process, typically occurs in animal cells and does not depend on full complementarity. In this case, miRNA binds to the 3' UTR of the mRNA and blocks proteins synthesis through inhibition of translation [126]. The classical mechanism suggests the difficult progression of the ribosome along the mRNA that is bound to the miRNA by complementarity, stalling the protein synthesis. When the complementarity is high, the protein complex recruited by miRNA (RISC) can force cleavage of the mRNA, eliminating the expression of the gene. Other

reported mechanisms include the impairment of the pre-initiation complex formation, required for the translation of mRNA from the ribosome, the recruitment of proteases that may degrade the protein synthesized by the ribosome, or the binding blocking of the 80S ribosome to the nucleotide chain [126].

3.2.2 miRNAs IN CARDIOVASCULAR DEVELOPMENT, HOMEOSTASIS AND PATHOLOGY

To date, miRNAs have been described in virtually all the basic cellular processes and cell types, including those relevant to the cardiovascular system. In the cardiac field, miRNAs have demonstrated to play and important role in heart development as well as in heart homeostasis and pathology.

Studies of individual miRNAs using heart developmental models have led to discover that miR-1/miR-133 are fundamental to both the control of proliferation and the regulation of muscle transcriptional networks. Thus, a variation of expression or deletion of miR-1 in mice has been found to be lethal to 50% of embryos, while around 20% of survivors have major cardiac defects [127]–[129]. The cluster of miR-17-92 has been shown to be implicated in cardiac proliferation during heart development [130], [131], whereas miR-15 seems to balance proliferation by repression of cell cycle regulators [130]. Moreover, the regulation of the conduction system of CMs have been associated to miR-208 [132], [133].

Several miRNAs have been described to control important processes responsible of the pathophysiological consequences of MI. miRNAs that can either promote or inhibit CMs cell death, regulate CMs proliferation, neovascularization, fibrosis or interfere in cardiac remodeling with cardioprotective effects, have been extensively described (**Figure 5**).

- **Cardiomyocyte survival**

A potential intervention to improve cardiac function after MI is to induce CMs survival. Several miRNAs have been reported to promote or impair this process. On one hand, various miRNAs were shown to induce or aggravate CMs cell death *in vitro*, including miR-1/miR-206 [134], miR-92a [135], [136], miR-122 [137], miR-150 [138], miR-181a [139] or miR-376b-5p [140]. Furthermore, some miRNA families have been described to be especially relevant in this role. Members of the miR-15 family were the first described as being upregulated after ischemia and to induce CMs apoptosis [141]. Their cell-death-promoting activity has been attributed to targeting Bcl-2, downregulating the ADP-ribosylation factor-like protein (ARL) or the NAD-dependent protein deacetylase sirtuin-1 (SIRT1) [142], [143]. Thus, the inhibition of miR-15 family members have demonstrated to reduce infarct size after I/R injury [141]. The miR-34

family is also known to be upregulated after MI and to contribute to CMs cell death both *in vitro* and *in vivo* [144], [145]. In these studies, the miR-34 inhibition improved CMs survival and preserved cardiac contractile function after MI. Mechanistically, this family have been shown to target multiple mRNAs of genes that promote cell survival, like SIRT1, B-cell lymphoma 6 protein (BCL6), GDP-fucose protein O-fucosyltransferase 1 (POFUT1), serine/threonine-protein prosphatase 1 regulatory subunit 10 (PPP1R10) or semaphorin-4b (SEMA4B) [144]–[146]. Also the inhibition of miR-140 has been described to reduce infarct size *in vivo*, by regulation of apoptotic programs [147]. Others like miR-320 have been shown to be downregulated after I/R in mice. Interestingly, miR-320 overexpression in CMs demonstrated to increase CMs cell death *in vitro* as well as in a transgenic mice, whereas its inhibition induced a reduced infarct size in an infarct model [148].

In contrast, other miRNAs have been described for their *in vitro* CMs-protective effect, including miR-7a/b [149], miR-20a [150], miR-138 [151], miR-144/451 [152], miR-210 [153], miR-499 [154] or miR-874 [155]. Furthermore, the cardioprotective role of miR-24 has been also reported *in vivo.* Its overexpression was found to attenuate infarct size and improve heart function after MI by targeting the pro-apoptotic Bcl-2 like protein 11 (Bim) [156], [157]. However, its regulation after ischemia demonstrated to be controversial for cardiac therapy as miR-24 exhibited also anti-angiogenic effects [158], [159]. Another cardioprotective miRNA is miR-214, which is upregulated after cardiac stress. Its overexpression protected against H_2O_2-induced CMs apoptosis [160], and its genetic deletion aggravated cell death induced by I/R injury [161]. Sodium/calcium exchanger 1, cyclophilin D, Bim, or phosphatase inhibitor PI3K/Akt are regulated by this miRNA and might contribute to the observed protective effect [160], [161]. Importantly, it has been demonstrated transient induction of miR-214 after MI that provides a protective effect, whereas long-term chronic overexpression might induce dilated cardiomyopathy.

- **Cardiomyocyte proliferation**

CMs only retain their proliferative capacity for a short postnatal period, impairing the heart´s capacity to regenerate after injury. Thus, the induction of CMs proliferation could be an interesting strategy to contribute to therapeutic cardiac regeneration. In this process, one miRNA family in particular, the miR-15 family (including miR-15a, miR-15b, miR-16, miR-195 and miR-497) has been shown to be expressed at low levels after birth but to increase with time, inducing the loss of the CMs proliferative capacity [162]. One of the first miRNAs to be described as being cardiac-enriched, miR-133, has been also shown to inhibit proliferation of CMs by targeting cell cycle regulators. Genetic deletion of this miRNA was lethal or provoked heart

failure due to aberrant proliferation [163]. In a zebrafish model its deletion enhanced regeneration of the heart whereas transgenic expression inhibited this process [164]. By contrast, the inhibition of miR-15b and miR-16 was shown to prolong the postnatal CMs proliferation period [162], [165]. Furthermore, in a relevant study with a high throughput overexpression approach for 875 miRNAs analysis, miR-199a and miR-590 highlighted by induced proliferation in neonatal rat CMs. The forced expression of these two miRNAs by adeno-associated virus was demonstrated to induce proliferation of CMs in adult mice, promoting cardiac regeneration after MI [166]. Other important miRNA cluster involved in proliferation of CMs is the miR-17-92 cluster. It has been shown that this family affects CMs proliferation and heart weight after birth [167]. This effect persists in adult mice, contributing to improved cardiac recovery after MI. These effects are predominantly due to two members, miR-19a and miR-19b, which downregulate PTEN, a negative regulator of survival and proliferation. However, overexpression of miR-17-92 has also demonstrated to induce arrhythmias and hypertrophy, which has been associated to the aberrant expression of connexin-43 [131].

- **Angiogenesis and smooth muscle cell proliferation**

Tissue revascularization is a key mechanism that contributes to the regeneration of the heart after ischemic injury. Interestingly, many miRNAs have already been reported to modulate the angiogenic process. Members of the miR-17-92 cluster, previously described for their role in CMs proliferation have been described to control angiogenesis and neovascularization after MI [168]. miR-92a is the most representative member and its inhibition demonstrated to increase endothelial-cell migration, increased capillary density and improved cardiac function in a mouse model of MI [168], [169]. Furthermore, in large animal models, its inhibition reported a decrease in infarct size attributing a protective role to this miRNA. This effect has been related with targets such as integrin α5 or the vasculo-protective genes KLF2 and SIRT1 [170]. Other members of the cluster, like miR-20a, are more controversial, as inhibition of miR-20a has been shown to either promote [171], [172] or block [173] endothelial-cell proliferation and migration. Furthermore, an attractive therapeutic strategy was based on miR-24 inhibition. Different studies demonstrated that inhibition of miR-24 improved neovascularization after MI by repressing endothelial nitric oxide synthase, endothelial transcription factor GATA-2, and serine/threonine-protein kinase PAK 4 [158], [159]. Notwithstanding this therapeutic benefit, miR-24 inhibition also demonstrated a pro-apoptotic effect on CMs, so cell-specific targeting strategies are necessary for miRNAs specific therapeutic effect. On the other hand, the inhibition of miR-26a also induced robust angiogenesis and improved heart function, by regulation of the SMAD1 signaling pathway [174]. Finally, miR-15 family, previously described for its role in CMs cell death

and proliferation, has demonstrated to inhibit angiogenesis, via targeting proangiogenic and endothelial survival factors such a VEGF-A or FGF-2 [175], [176]. Thus, the inhibition of miR-15 represents an attractive strategy to prevent post-ischemic heart failure.

Aberrant proliferation and migration of vascular smooth muscle cells also play an important role in the pathogenesis of CVD. Some miRNAs have also been reported to play a critical role in this process. In this context, miR-145 and miR-143 were found to be downregulated in injured or atherosclerotic vessels. Cordes *et al*. demonstrated that both miRNAs can direct the smooth muscle fate to regulate the quiescent *versus* proliferative phenotype of smooth muscle cells [177]. Furthermore, the regulation of smooth muscle proliferation and migration by these miRNAs has also been reported in other pathologies such as pulmonary arterial hypertension [178]. In a recent study, miR-23 was found upregulated in peripheral blood of coronary heart diseased patients. This work demonstrated that overexpression of this miRNA promoted smooth muscle cell proliferation and inhibited apoptosis, identifying BCL2L11 as a direct target [179].

- **Cardiac hypertrophy and Fibrosis**

The non-coding RNA miR-208 (a cardiac-enriched miRNA encoded by an intron of the α-myosin heavy chain 6 gene) was the first link between miRNAs and cardiac remodeling, being responsible for CMs hypertrophy and fibrosis development in response to cellular stress [180]. Since then, many other miRNAs have been studied for their involvement in cardiac fibrosis. miR-21 was found to be more enriched in cardiac fibroblasts than in CMs, being overexpressed during cardiac remodeling in mice [181] as well as in patients with aortic stenosis [182]. The increased expression of this miRNA leads to fibrosis development. The endogenous MAPK inhibitor, MMP-2 or TGF-β receptor type 3 have been described as targets involved in this process [181], [183], [184] Moreover, pharmacological inhibition of miR-21 has demonstrated to inhibit fibrosis in the heart [181], [185]. However, this effect was not consistent in a knock-out mouse for this miRNA, where under stress conditions, still developed fibrosis [186]. These differences highlight the complex underlying molecular events in miRNAs regulatory processes. Another well-studied miRNA involved in fibrosis is miR-29, which targets a broad collection of mRNAs encoding collagens and ECM genes involved in this process [187], [188]. The miR-29 family has been shown to be downregulated in the injured area of the heart after MI in mice, and its inhibition resulted in de-repression of several fibrosis-related target genes [187]. Inhibition of miR-29 has been proposed as a way to enhance ECM production for the treatment of aneurysms [189]. Other CM-enriched miRNAs, miR-1 and miR-133, have demonstrated to be also involved in cardiac hypertrophy and fibrosis. miR-1 is found repressed in models of heart failure [190] and

its cardiac delivery prevented cardiac hypertrophy and fibrosis development in a rat model [191]. On the other hand, miR-133 has been reported to directly regulate expression of collagen-α1 chain [192] or connective tissue growth factor (CTGF) [193], suggesting a direct link with cardiac fibrosis. Furthermore, silencing of miR-133 demonstrated increased cardiac hypertrophy and fibrosis [194]. By contrast, when miR-133 was overexpressed, an improvement in fibrosis without affecting the extent of hypertrophy was found [195], [196]. Several other miRNAs with an important role in cardiac hypertrophy and fibrosis have been reported, including miR-378, miR-199b, miR-155, miR-101, miR-30, miR-34 and miR-122 among others [197].

- **Inflammatory response**

Regarding the inflammatory processes, several miRNAs have been described to modulate the activity of macrophages and the expression of several pro-inflammatory cytokines. miR-155 is one of the most representative miRNAs playing multiple roles in the inflammatory process. This miRNA has been reported to regulate macrophage polarization by controlling the SOCS1 and Akt1 axis [198]. Furthermore, macrophage derived miR-155 acts as a regulator of both cardiac fibroblast proliferation and inflammatory response following MI-induced injury [199]. By contrast, other groups have reported a negative feedback regulation for miR-155, by reducing the expression of cytokines by CMs during myocarditis [200] or by blocking the activity of macrophages by targeting NF-Kβ in the atherosclerotic plaque [201]. Other miRNA family considered as therapeutic targets for the prevention of inflammation is the miR-125 family, which has been reported to stimulate alternative pathways of macrophage polarization and activation [202]. Different groups have shown the potential of this miRNA to suppress the activity and stability of TNF-α and TNF-α-induced protein 3 and thereby to reduce inflammatory responses [202], [203].

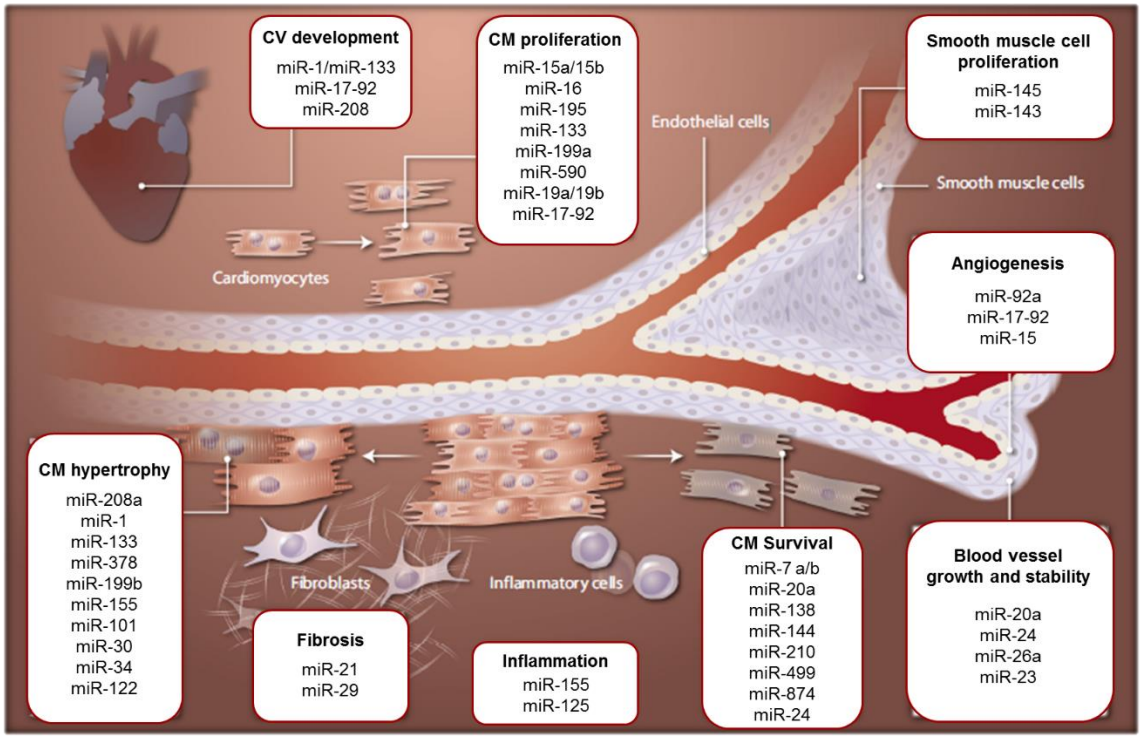

Figure 5. miRNAs involved in different pathological process in CVD. *Image represents the pathological processes in the cardiovascular system and the miRNAs that control these processes. miRNAs regulate CMs proliferation and survival. Other miRNAs regulate cardiac hypertrophy and fibrosis and others participate in angiogenesis, smooth muscle cell proliferation process and inflammatory response (Image adapted from Olson E. Sci Transl Med. 2014)* [204].

3.2.3 miRNAs as POTENTIAL BIOMARKERS

miRNAs have been detected in blood and other body fluids, raising interest for their potential use as disease markers. Furthermore, distinct expression patterns of extracellular miRNAs have been associated with a variety of cardiovascular disorders, including MI. An ideal biomarker needs to be non-invasive, specific, sensitive, stable and robust. Currently, serum troponin is being used as a standard diagnostic marker for MI. However, its instability and delayed release has led to the search for new markers. Circulating miRNAs have emerged as potential biomarkers for diagnosis or prognosis of MI due to their specificity and stability in plasma. Several studies have already explored the miRNAs leaked from the heart to the circulation after MI [205], [206] and analyzed their dynamic expression [207], [208]. Among these abundant miRNAs, four cardiac-enriched miRNAs, miR-208, miR-499, miR-1 and miR-133, have been consistently found increased in the plasma of MI patients and are currently being tested as diagnostic biomarkers [209]. Further research is required in any case to determine whether there is one single trustable miRNA or a combination of these non-coding molecules for diagnostic application in clinical practice.

In summary, extensive data has already confirmed the key role of different miRNAs in post-infarct heart remodeling and failure, so, nowadays, miRNAs are seen as potential diagnostic/prognostic markers as well as potential therapeutic molecules for CVD. The known relationship between different miRNAs and the different processes involved in myocardial ischemia have paved the way to a deeper analysis of the pathological mechanisms involved and to identify the miRNAs' potential use for future therapeutic approaches.

3.3 EXOSOMES

Exosome-mediated intercellular communication has been demonstrated to play a substantial role in the mechanisms involved in CVD. Importantly, these exosomes transfer non-coding RNA (such miRNAs) from the parent to the recipient cells, modulating their phenotype and protein expression.

The characteristics of exosomes and their association with exosomal-miRNAs derived from (stem) cells are described below.

3.3.1 DEFINITION, BIOGENESIS AND RELEASE

It is well known that living cells are able to secrete vesicles of different sizes and intracellular origins. The main difference between these populations is the diameter, which allows to define apoptosomes (vesicles with a diameter range between 50-5000 nm), microvesicles (diameter range: 50-1000 nm) and exosomes (diameter range: 30-150 nm). Also, their mechanisms of generation are different. While apoptosomes originate as fragments of cells undergoing programmed death (**Figure 6A**), microvesicles are formed by direct budding of injured cell plasma membrane (**Figure 6B**). Exosomes by contrast, are generated by internal budding of plasma membranes.

Focusing on exosomes, these particles arise from multivesicular endosomes (MVEs), which are formed from invaginations of the plasma membrane. Two different populations of MVEs have been described: cholesterol-poor and cholesterol-rich secretory MVEs [210]. The cholesterol-poor MEVs are prone to fuse with ubiquitinated products and lysosomes as part of a degradation pathway, whereas, cholesterol-rich secretory MVEs are fused with the payload processed in the Golgi complex to form multivesicular endosomes. Late endosomes mature through acidification, and fuse with the plasma membrane for their release into the extracellular space as exosomes (**Figure 6C**).

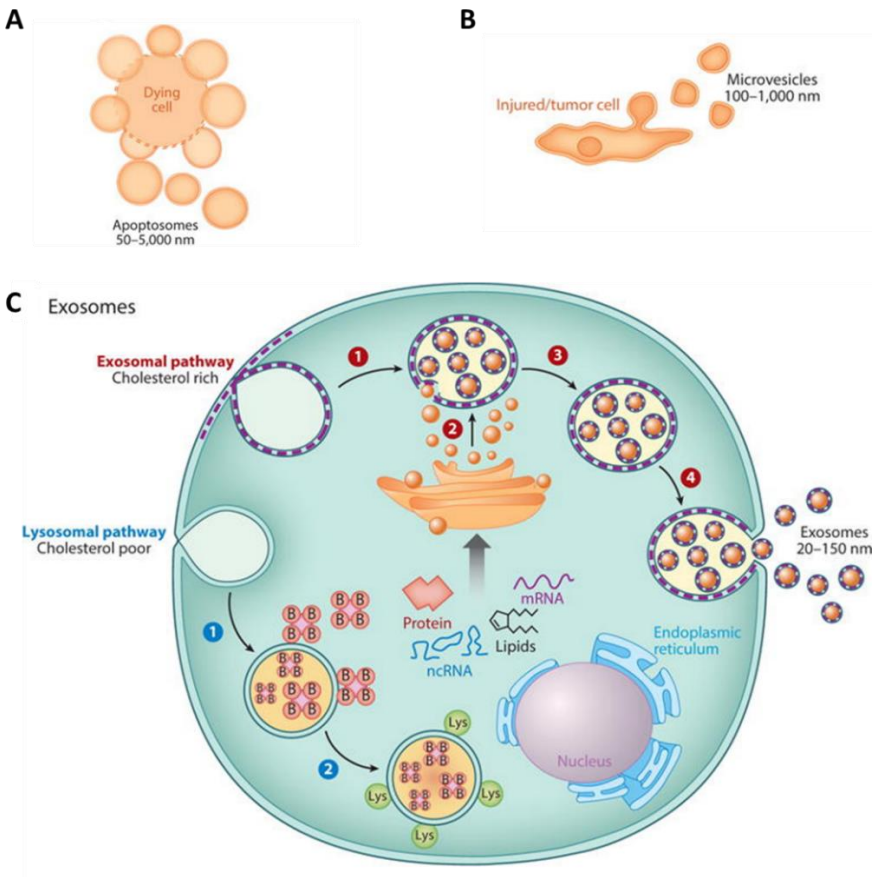

Figure 6. Extracellular vesicles and their mode of secretion. *Apoptosomes that bleb from dead cells* ***(A)****. Microvesicles that shed from injured cells* ***(B)****. Formation of two different multivesicular endosomes (MVEs) through invagination of the plasma membrane* ***(C)****. Steps 1-4 (red numbers): invagination of the plasma membrane to form a secretory endosome (1), followed by budding of payload into the endosomal membrane to form multivesicular endosome (2). Maturation of the late endosome through acidification (3) triggers fusion with the plasma membrane and release of exosomes (4). Steps 1 and 2 (blue numbers): invagination of the plasma membrane to form lysosomal membrane (1), followed by fusion of ubiquitinated products for lysosomal degradation (2). "B" represents the addition of ubiquitin to protein substrates and "Lys" denotes fusion of lysosomes. Image reproduced from Ibrahim et al. Annu Rev Physiol. 2016* [211].

Thus, due to this different intracellular origin, the membrane lipid content of extracellular vesicles is more similar to that of the cell of origin. Exosomes, by contrast, are more distinct from the plasma membrane since they include lipids from the Golgi complex. In fact, exosomes are a unique class of extracellular vesicles by virtue of their biogenesis. It has been demonstrated that exosomes contain fragments of the endosomal sorting complex required for transport (ESCRT). This complex is involved in the process by which the molecular payload populates the multivesicular body. Four members of the ESCRT complex have been described. ESCRT 0, I and II recognize and sequester ubiquitinated protein products at the endosomal delimiting membrane, concentrate them in microdomains and trigger membrane involution. On the other hand, complex III is responsible for the membrane budding and release of vesicles

[212]–[214]. Other conserved exosome markers have been described, such as lysosomal-associated membrane proteins (LAMPs) [215] or tetraspanins (CD63, CD81 and CD9) [216]. However, the markers associated with the ESCRT are not entirely exclusive, LAMPs are also abundantly found in the lysosomal compartment, and tetraspanins, due to their multifunctional capacities (cell activation, proliferation, adhesion, motility and differentiation) are present on the plasma membrane or in the cytosol. The process of distinguishing exosomes from lysosomal vesicles has become highly complicated, so different studies have been focused on defining the structurally conserved components of these vesicles, including lipid composition and membrane proteins. Interestingly, the exceptional rigidity of exosome membranes compared with that of the plasma membrane, can be explained in part by the difference in lipid composition. Exosomes are bound by a lipid bilayer membrane consisting of cholesterol, diglycerides, sphingolipids, phospholipids, glycerophospholipids and polyglycerophospholipids [217]. Some of these lipids also participate in trafficking during biogenesis, recognition and internalization [217], [218], aside from structural functions. Furthermore, other bioactive lipids, including prostaglandins, leukotrienes, and active enzymes that can generate these lipids [219] can also be found in exosomes. Regarding membrane proteins, the most commonly defined ones are related to membrane transport and fusion, heat shock proteins (e.g., Hspa8, Hsp90), GTPases (e.g., EEF1A1, EEF2) or endosomal proteins and markers (e.g., Alix). Cytoskeletal, metabolic, signaling, and carrier proteins and albumin, have also been found in exosomes. Also the histocompatibility complex (MHC)-I is ubiquitously expressed on all exosomes, whereas MHC-II expression is restricted to exosomes derived from antigen-presenting cells [211] (**Figure 7**).

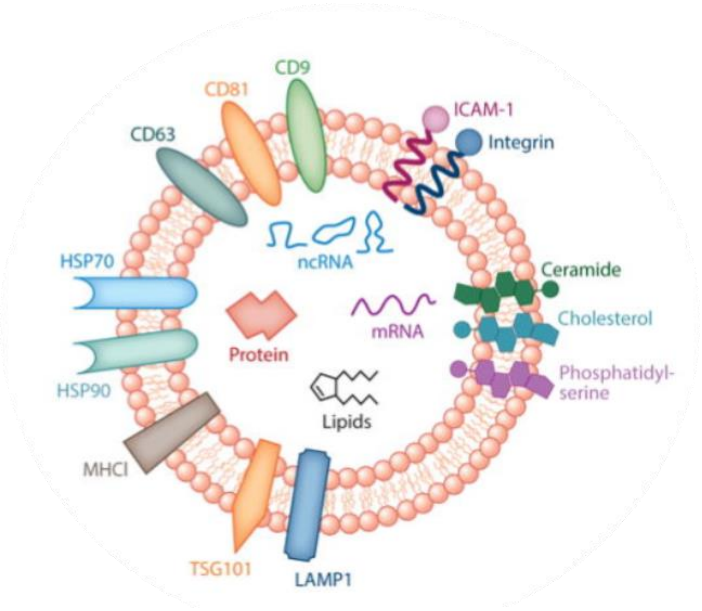

Figure 7. Exosomes membrane lipid content and molecular cargo. *Exosomes lipid bilayer has a lipid content different from that of the parent cell, enriched in cholesterol, ceramide, and phosphatidylserine. Markers ubiquitous in most exosomes include tetraspanins (CD9, CD63, and CD81); heat shock proteins; adhesion molecules; and markers of the ESCRT pathway, including LAMP1 and TSG101. Molecular cargo of exosomes have been characterized by proteins, lipids and RNA content, including non-coding RNAs. Image reproduced from Ibrahim et al. Annu Rev Physiol. 2016* [211].

By virtue of their biogenesis, the key feature of exosomes is to act as intercellular communication messengers. Once secreted, exosomes enter recipient cells via a variety of uptake pathways that differ according to the biological context. These mechanisms include receptor-ligand interaction; protease-mediated cleavage of exosomes; direct lipid membrane fusion; internalization by receptor mediated endocytosis and uptake by immune cells (through phagocytosis, pinocytosis, or micropinocytosis) [220], [221]. Due to their ability to transfer molecules from the parent to the recipient cells, a significant interest in characterizing their molecular cargo has emerged. As previously described, proteins and lipids vary greatly according to the different exosomes sources, so as expected, the payloads are even more diverse. According to the current version of the exosome content database, ExoCarta (http://www.exocarta.org/), 41,860 proteins, >7540 RNA (including 2,838 miRNAs) and 1116 lipid molecules have been identified from more than 286 exosomal annotated studies [222]. However, certain features are common among the majority of exosomes. Given their small size, generally they do not present neither organelles (such as ribosomes and mitochondria) nor DNA, unlike cancer-derived extracellular vesicles, which are larger than exosomes and contain double-stranded DNA [223]. Conversely, protein and lipids are largely present, including enzymes, transcription factors and structural proteins. Interestingly, the most important source of

signaling diversity is associated with the RNA content, including not only transcripts but also abundant non-coding RNA species such as miRNAs and long non-coding RNAs [224], [225]. It is known that this exosomal specific repertoire can alter the transcriptome of recipient cells, but the mechanisms underlying the selective packaging of signaling mediators still remains poorly understood. Unveiling these processes is key to clarifying the pathways of transduction as well as how cells alter their cargo under different conditions such as stress and disease.

3.3.2 EXOSOMES IN CARDIOVASCULAR PATHOPHYSIOLOGY

Exosomes and other extracellular vesicles have been described as mediators of disease. This role has been extensively studied in cancer cell signaling, related to tumor growth, recruitment of vascular progenitors, chemoresistance and metastasis [226]. Furthermore, different studies have shown that exosome secretion and their molecular cargo are sensitive to infection or stress stimuli. In the cardiac field, hypertrophic cardiac response, triggered by different stress stimuli (including e.g. hypertension, ischemia, arrhythmias, physical exertion…) has been shown to be mediated by vesicle-cellular cross-talk. Exosomes derived from stressed CMs have shown an enriched content in proinflammatory and apoptotic factors, such a HSP60 and TNFα, driving more inflammation and death to nearby CMs [227]. In the same way, Bang and colleagues demonstrated that fibroblasts secreted exosomes were enriched in miR-21 that was directly involved in hypertrophic effects [228]. At the same time, the release of the HSP70 protein, present in the surface of plasma exosomes, has been described in mouse CMs [229], stimulating different cardioprotective pathways [230].

It is well known that CMs interact with other cells via exosome-mediated transfer, but also endothelial cells, monocytes and vascular smooth muscle cells secrete exosomes, which have demonstrated to mediate angiogenesis and vascular healing, promoting migration, adhesion and proliferation [231]. In this way, some recent data has shown that exosomal HSP70 protein may be involved in the migration of monocytes [232]. Furthermore, exosomes derived from activated macrophages enriched in miR-223 or exosomes derived from atherosclerotic plaques which can transfer ICAM-1 and also miR-222 (ICAM-1 regulator), have been described to favor early atherosclerotic processes [233], [234]. Also vascular smooth muscle cells release exosomes, and their injection in apoE knock-out mice has demonstrated to reduce the development of atherosclerotic plaques in the aorta [235].

Another study has demonstrated that rodent serum exosomes from cardiomyopathies associated with type 2 diabetes, contain high levels of miR-320. This data correlates with *in vitro* studies where inhibition of endothelial cell proliferation and migration was observed after their

treatment with miR-320 enriched exosomes [236]. Furthermore, some cardiac-specific miRNAs have been found in the exosomes released after MI. Among these, the most characterized miRNAs are miR-133 with anti-apoptotic and anti-fibrotic effect; miR-1 with anti-oxidant role; and miR-499 with anti-apoptotic properties [237].

Definitely, exosomes could exert many different roles in CVD, with cardioprotective but also anti-inflammatory or anti-fibrotic properties among others.

3.3.3 STEM CELL-DERIVED EXOSOMAL miRNAs AS AN EMERGING TOOL FOR CARDIOVASCULAR REGENERATION

As previously mentioned, accumulating evidences suggest that the therapeutic effects of transplanted stem cells are predominantly mediated by secreted paracrine factors, including miRNAs. It has recently been found that stem cell-derived factors could be transferred via exosomes, regulating different pathological processes, like for example MSC-derived exosomes that depress oxidative stress [238] or exosomes derived from ESC, which have been shown to enhance the pluripotent markers, reduce caspase-3 and increase tube formation in endothelial cells *in vitro*, promoting endogenous cardiac repair [239]. CSC-derived exosomes have also demonstrated their potential after myocardial injection, decreasing infarct size and preserving LVEF in acute and chronic MI porcine models [240], [241]. Importantly, these CSC-derived exosomes can be also uptaken by fibroblasts, which modify their own secreted exosomes, decreasing collagen production and increasing collagen degradation by MMPs that promotes a reduced infarcted scar [242].

Importantly, several studies have recently shown that the cardioprotective effects of stem cell exosomes are predominantly achieved by these different miRNAs release. BMSC, MSC and CSC are the most representative stem cell populations where exosomal miRNAs have been found to enhance cardiac function by modulating different processes as described in detail below.

- **Cardiac exosomal miRNAs derived from BMSC**

As it has been already discussed, BMSC are a promising cell-based strategy for myocardial repair, and there has been growing evidence showing that BMSC exosomes carrying miRNAs, mediate the cardioprotective effect of these cells. Mayourian *et al*. found that exosomal miR-21-5p secreted from human BMSC could enhance cardiac tissue contractility in mature ischemic adult human CMs [243]. This was further confirmed by another study that demonstrated CMs protection in a mouse model of myocardial I/R [244]. Additionally, miR-22-

enriched exosomes secreted by BMSC after ischemic preconditioning, were found to exert anti-apoptotic effects, ameliorate fibrosis and improve cardiac function post-MI [245]. Further, Shao *et al*. demonstrated that BMSC derived exosomes contained high levels of miR-29 and miR-24 and low levels of miR-21, miR-15, miR-34, miR-130 and miR-378. These exosomes could repair the injured myocardium by suppressing cardiac fibrosis, inflammation and improving cardiac function in a rat model of MI [246]. On the other hand, hypoxic preconditioning of BMSC has been shown to improve their biological activities, and this effect was suggested to be mediated by affecting the exosomes cargo. Park *et al.* have also shown that systemic injection of hypoxic MSC-derived exosomes (that contained high levels of miR-26a) could attenuate the degree of infarct size and reduce arrhythmias after I/R in a rat model [247]. The expression of miR-210 has also been described to be increased in exosomes secreted from hypoxia-treated BMSC. Intramyocardial injection of these hypoxic cell derived exosomes, showed a strong induction of revascularization, reduced CMs apoptosis, decreased fibrosis and enhanced recruitment of CPC in the infarcted heart [248]. Also cardioprotective effects of miR-126-enriched exosomes was confirmed by *in vivo* studies that showed a decreased infarct size and reduced cardiac fibrosis in a rat model of MI [249]. Likewise, treatment with transplanted BMSC secreting exosomes containing high levels of miR-125b-5p demonstrated to improve cardiac function and tissue remodeling through modulation of the autophagic flux [250].

- **Cardiac exosomal miRNAs derived from MSC**

The angiogenic processes that occur in the post-MI heart are crucial for promoting tissue reperfusion and function recovery of the ischemic heart. Different studies have reported that tissue revascularization can be enhanced by MSC exosomes, suppling pro-angiogenic miRNAs. Luo *et al.* have reported the pro-angiogenic effects of miR-126-enriched exosomes isolated from adipose MSC, supported by *in vivo* studies that showed blood vessel formation in the infarct region of treated rats [249]. Interestingly, these miRNA-enriched exosomes were also found to decrease inflammation, determining decreased levels of inflammatory cytokines in hypoxic myocardial cells as well as in the serum of treated AMI rats [249]. Other studies in mice showed that intravenous injection of miR-210-enriched exosomes could also profoundly improve angiogenesis, limiting fibrosis and improving cardiac function after ischemia [251].

- **Cardiac exosomal miRNAs derived from CPC**

CPC derived exosomal miRNAs have been found to be the main cardioprotective mediators of CPC against heart damage after ischemia. In this context, Xiao *et al.* showed miR-21 upregulation in CPC-derived exosomes under oxidative stress conditions, protecting recipient CMs against related apoptosis [252]. Additionally, other study revealed that CPC-derived

exosomes contained high levels of miR-451 which also demonstrated to protect CMs from oxidative stress in a I/R cardiac injury model *in vivo* [253]. Therefore, the oxidative stress-treated CPC can secrete exosomes containing cardioprotective miRNAs that can preserve CMs against oxidative stress-induced apoptosis.

The knowledge of this exosomal therapeutic potential has allowed the development of new emerging tools where exosomes have been used not only as a therapy itself but also to improve the therapeutic potential of stem cells. Thus, pretreatment of CSC with MSC-derived exosomes stimulates proliferation, migration and tube formation capacity in CSC, improving their survival and angiogenic potency in a rat model of MI [254]. Interestingly, this and other studies have also demonstrated that treatment with exosomes significantly modifies the miRNA expression profile in recipient cells [255]. Thus, CSC pretreatment with exosomes showed upregulation of miR-147 and miR-503-3p and downregulation of miR-207, miR-326-5p and miR-702-5p leading to improved cardiac function and increased vessel density after their injection in the infarcted heart. On the other hand, other experimental techniques have employed $CD34^+$ stem cells engineered to secrete exosomes containing high levels of pro-angiogenic factors, and proved their efficacy to improve angiogenesis and decrease infarct size in ischemic mice [256] [257].

Furthermore, exosomes are able to incorporate and/or modify their molecular cargo under pathological conditions. Bioinformatic tools have defined the exosomes-miR profile under different pathological contexts, so exosomes have been considered as novel diagnostic biomarkers in CVD [258]. As a result, patients with coronary artery disease exhibit a subpopulation of circulating exosomes rich in miR-199a and miR-126 [259]. Exosomal-derived miR-1, miR-208 and miR-133 have also been shown to be elevated in patients with acute coronary syndromes. Thus, miR-133 present in exosomes can serve as a reliable biomarker for myocardial damage. In patients with AMI who developed heart failure, other specific molecules have been also described like the exosomal-derived miR-192, miR-194 and miR-34a [260]. Further research will be required to determine whether this combination of exosome-derived miRNAs could be an efficient strategy for clinical diagnostics.

4. GENE THERAPY

In the last two decades, many studies have focused on the development of stem cell therapy for the treatment of CVD. Nowadays, it is accepted the fact that the main contributors to the stem cells regenerative effects are their paracrine products. Importantly, among them, miRNAs and exosomes have emerged as new biological treatments for cardiac disease, among many others. Given the key role that some miRNAs play, it is necessary for future therapeutic applications, to develop systems that allow a robust overexpression of them. Also, taking into account the multitude of targets that miRNAs present, tissue and cell specific overexpression is also necessary, in order to avoid potential pathological effects in other organs. In that sense, gene therapy constitutes a great approach not only for gene but for small molecules overexpression *in vivo*.

It has been now 50 years since gene therapy was born, being actually an established reality that is advancing speedily. After many years of basic and pre-clinical research in different pathologies, gene therapy has been transferred from bench to bedside with more than 200 clinical trials already approved (http://www.abedia.com/wiley/years.php). The most common application of gene therapy has been the cancer treatment (66.6% of the trials), followed by monogenic disorders (11.5%) and by infectious and CVD (6.3 and 6.2 %, respectively) (**Figure 8A**). Although there has been an increase in the number of trials entering late phases, the overwhelming majority, are still in phase I and phase I/II (**Figure 8B**).

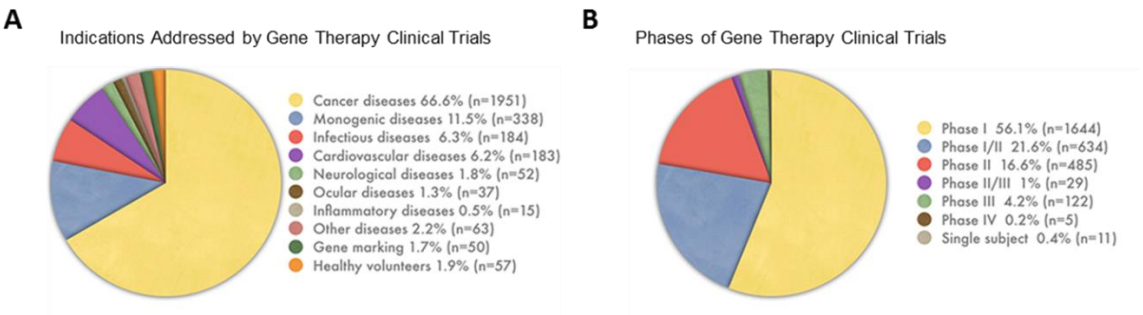

Figure 8. Gene therapy clinical trials. *Indications for the treatment with gene therapy in all the clinical trials performed until 2018* ***(A)*** *and clinical trials phases* ***(B)****. Data obtained from http://www.abedia.com/wiley/.*

The wide application of gene therapy has involved the development of an ideal carrier or vector. In general, vector systems are divided into viral vectors and no-viral vectors. Both

systems have been broadly used for delivery of therapeutic genes [261], [262], being viral vectors generally more efficient and cell-specific than non-viral vectors.

A variety of vectors have been studied including Adenoviral vectors, lentiviral vectors or Adeno-associated viral vectors (AAV). Adenoviral vectors have showed an efficient transduction of a wide range of dividing and non-dividing cells, including CMs [263]. However, their transient transgene expression and their high immunogenicity have compromised their efficacy and safety for clinical use. On the other hand, lentiviral vectors present the ability to integrate their genome and therefore achieve long-term transgene expression with absence of immunogenic or inflammatory response. The drawback of these vectors reside in their relatively poor transduction of myocardium *in vivo*, as well as their putative genome integration [264]. Finally, AAV have been broadly used due to their safety and low immunogenicity among other properties, becoming an ideal vector for therapeutic applications. AAV properties are described in detail below.

4.1 AAV VECTORS

4.1.1 AAV BIOLOGY, ORGANIZATION AND STRUCTURE

AAV vectors were accidentally discovered in 1965, when Atchinson and colleagues observed contaminant particles in their adenovirus preparations [265]. These small particles (18-25 nm of diameter) were shown to be non-autonomous, as particle production also required adenovirus co-infection, being named as adeno-associated virus (AAV).

AAV is a helper-dependent parvovirus from de Parvoviridae family. The AAV are composed of an icosahedric capsid and a small nonenveloped single-stranded DNA (ssDNA) virus of 4.7 Kb. The compacted genome of AAV is flanked by two inverted terminal repeats (ITRs) and hairpin structures of 145 nucleotides that contain the only regulatory cis sequences required to complete its life cycle: origin of replication, terminal resolution site and signals for packaging and integration. The genome contains three promoters that drive transcription of two genes, involved in virus replication (Rep) and synthesis of the capsid proteins (Cap) [266].

The first two promoters (P5 and P19) drive transcription of the large (Rep68, Rep78) and small (Rep52, Rep40) Rep proteins respectively. The two major Rep proteins are involved in viral genome excision, rescue, replication and integration and the minor Rep proteins, are involved in replicated ssDNA genome accumulation and packaging. The three AAV capsid proteins (VP-1, VP-2, and VP-3) are transcribed from the P40 promoter. VP-1 is initiated from the first cap transcript, and VP-2 and VP-3 are initiated at two different codon sites from the second

transcript (**Figure 9**). Finally, the assembly of these three proteins in a ratio 1:1:10 form the icosahedric capsid [266], [267]. Altenatively, an additional open reading frame (ORF) found in the Cap gene, codifies for the Assembly activating protein (AAP) which interacts with the capsid proteins acting also as an assembly scaffold [268], [269].

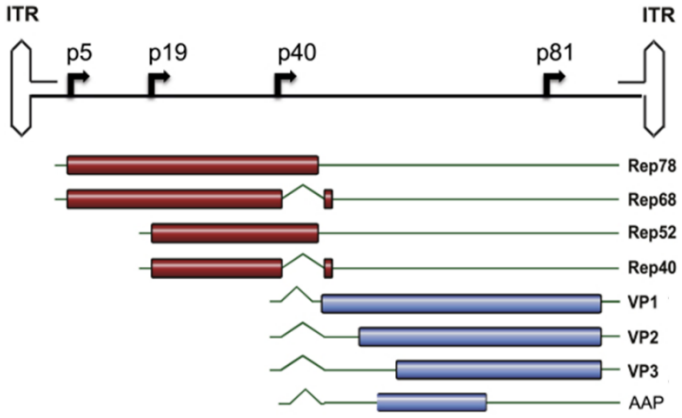

Figure 9. Structure of AAV genome and transcriptional variants. *General organization of the genome and genetic elements. T shaped black boxes indicate the ITRs. The horizontal arrows indicate the three transcriptional promoters. The solid lines indicate the transcripts. A polyadenylation signal is present. The first ORF encodes the four regulatory proteins (red boxes) arising from the promoter p5 and p19 and the alternative splicing. The second ORF (promoter p40) encodes the three capsid proteins (blue boxes) from two transcripts. VP-1 is initiated from the first cap transcript, and VP-2 and VP-3 are initiated at two different codon sites from the second cap transcript. An additional ORF found in the Cap gene codifies for the AAP. Image reproduced from Büning H et al. Mol Ther Methods Clin Dev. 2019* [270].

4.1.2 AAV AS GENE DELIVERY VECTORS

AAV has become one of the most actively investigated and used vehicle for gene therapy. For AAV production, the viral genes, Rep and Cap, are eliminated and substituted by the therapeutic expression cassete of interest downstream the selected promoter, while the ITRs sequences are maintained, generating a new plasmid called pAAV. Basically, all recombinant genomes are based on AAV2 ITRs, with a size limitation of 4.7 Kb for the insertion of transgenes. Furthermore, for AAV production the majority of studies use the pseudotyping strategy. The pAAV is combined with another plasmid that encodes the Rep and Cap proteins, which are supplied in trans together with the necessary genes from the helper-virus. ITR sequences are the only viral genomic sequence necessary to package the DNA of interest into the capsid, so the second plasmid which provides Rep and Cap proteins lacks ITRs, ensuring that this plasmid alone is not packaged into AAV capsid and does not replicate [271].

During the last years, different production methods based on transient transfection protocols in target/producer cells have been tested. Nowadays, the baculovirus infection of

insect cells (Baculovirus-SF9 cells system) and the transfection of mammalian cells (HEK293 cells primarily) are the two most common methods for AAV production [266]. For AAV purification, the most classical and easy way to purify them at laboratory scale, is by ultracentrifugation in iodixanol gradient [272]. This method is sufficient for fundamental *in vivo* preclinical evaluations. However, it is limited by the capacity of cell lysate volume that can be processed. Furthermore, the degree of purity is low, so for human clinical application, chromatographic techniques are used to allow high purity grade and up-scale productions [273], [274].

The transfection of the pAAV vector, with the specific transgene, can be combined with different serotype capsids. To date, 13 AAV serotypes and more than 100 AAV variants have been described. All the serotypes have been tested in several preclinical models, demonstrating tissue-specific tropism, which is dependent on the binding specificity of the vector to the cell surface receptors (**Figure 10**).

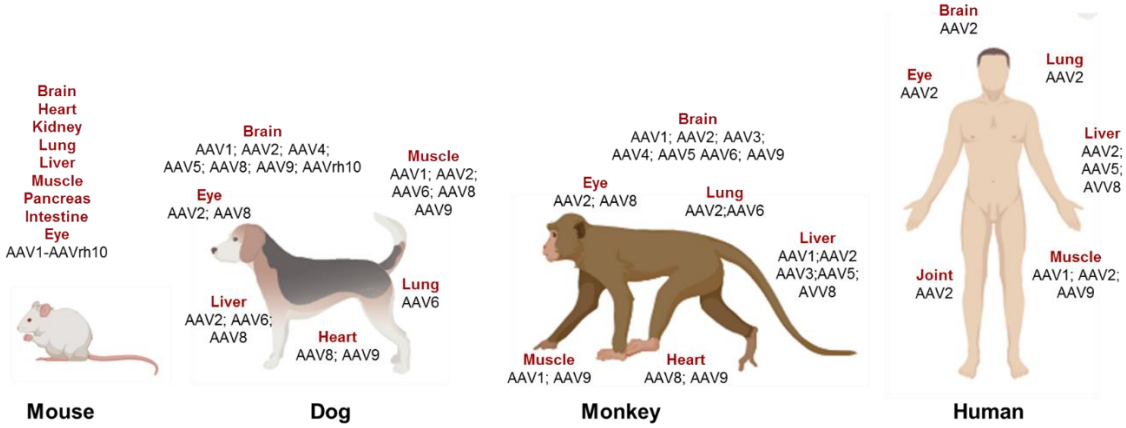

Figure 10. Summary of the AAV serotypes tested in several animal models and in humans to target different organs. *Image adapted from Srivastava. Curr Opin Virol. 2016* [275].

AAV exploit a broad range of cell surface receptors to mediate cellular uptake. Heparin sulfate proteoglycan, terminal galactose and several variants of sialic acid are currently identified as primary binding receptors for AAV. In addition to the primary carbohydrate interactions, secondary receptors also play an important role in viral transduction and together contribute to cell and tissue-specific tropism. For example, Bell *et al.* identified the unique amino acid differences in AAV9 capsid sequence necessary for binding to galactose [276], conferring AAV9 the ability to cross the blood-brain barrier and infect cells on the central nervous system [277], [278]. Secondary receptors like the epidermal growth factor or the platelet-derived growth factor receptor present in AAV6 and AAV5, respectively, play also an important role in viral transduction. Recently, a new type-I membrane protein, AAVR, has been identified as a

critical receptor for cell binding and internalization for all the serotypes [279]. This structural information has been used to alter the natural trafficking patterns of AAV. Furthermore, recombinant techniques involving direct evolution, capsid shuffling or random mutagenesis are being employed to modify AAV capsids [280], [281]. Employing these approaches, different studies have been able to identify novel AAV variants that preferentially transduce specific organs and tissues, as retinal cells [282] or some tumors [283].

Cell infection is initiated by capsid binding to cell-surface receptors and, in a second step, to a protein receptor that mediates endocytosis. The intracellular trafficking of the vector remains unclear, although the most accepted model has established that AAV traffics through the endosomal system and is able to escape from the endosomal compartment and enter the nucleus, via the nuclear pore complex. Once in the nucleus, the vector genome is uncoated from the capsid, the complementary DNA strand is synthesized and transcription is started. In absence of Rep proteins, ITR-flanked transgenes can form circular concatemers that persist as episomes in the nucleus of transduced cells [284].

One of the most interesting properties of AAV as gene delivery vectors is its low immunogenicity. Their ability to generate recombinant AAV particles lacking any viral genes but containing the DNA sequences of interest, makes them one of the safest strategies for gene therapy. In humans, only the wild-type AAV has the unique property of integration at a specific site into the human genome [285]. Nonetheless, because of viral genome manipulation, this propensity is not maintained in vectors. However, it has to be noted that despite the fact that AAV does not contain any viral genes to amplify the immune response, the humoral immune response against capsid proteins can produce elevated titers of neutralizing antibodies (NAbs), which results in a reduction of AAV-transduction rates. Moreover, CD8+ T cells directed to capsid antigens leads to rejection of AAV-transduced cells. This gains further complexity by the fact that most of the human population have already been exposed to AAV and have already developed an immune response against a particular variant. This pre-existing immunity to AAV, and the presence of circulating NAbs, can diminish the clinical efficacy of subsequent re-infections and the elimination of transduced cells, representing one of the greatest therapeutic challenges to the use of systemical delivery. Various strategies have been implemented to overcome this barrier, including the administration of immunosuppressants [286], plasmapheresis in patients with high NAb titers [287], delivery of empty capsids to adsorb Nabs [288], capsid mutagenesis altering NAb binding epitopes on AAV capsids [289], [290] or the use of direct evolution to generate mutant capsid libraries in order to select those that evade Nabs [291], [292]. More

recently, Liang *et al.* have also described the use of exosomes to envelope AAV to shield them from Nabs [293].

4.1.3 AAV FOR CARDIOVASCULAR GENE THERAPY

AAV possess an interesting biology that has encouraged their adoption as delivery vectors to target several organs in different diseases, including the cardiovascular ones. Many studies have been focused on improving AAV cardiac transduction efficiency and selectivity and minimizing undesirable gene delivery to other organs. Different strategies have been developed to this aim including the optimization of AAV vector selection and design, optimization of recombinant genome and administration route selection.

- **AAV vector selection and design.** As mentioned, to date, more than 100 AAV variants have been identified and isolated. AAV vector selection is key for an optimal and specific cardiac transduction. Comparison of effectiveness of the most studied AAV serotypes (1-9) by using a luciferase reporter gene in mice, revealed that AAV2, AAV6 and AAV9 were the most cardiotropic serotypes [294]. AAV6 and AAV9 have been largely used as the AAV serotypes of choice for cardiac-selective expression [295]. At the same time, recombinant AAV have also been developed to improve these individual serotypes. Muller *et al*. cross-packaged the genome of AAV2 consisting on cytomegalovirus (CMV) enhancer / myosin light chain (MLC) promoter into different serotype capsids and found rAAV2/6 for increase mice cardiac transduction [296]. Similar results were found using an AAV2/9 vector in non-human primates [297]. Other approaches have been based on the development of chimeric AAV vectors. For example, AAV2i8 has been created by replacing the hexapeptide sequence in a previously identified heparan sulfate receptor footprint on the AAV2 capsid surface with the homologous sequence from AAV8 [298], or by random mutagenesis of the capsid protein residues from AAV9 [299]. Yang *et al*. developed an AAVM41 cardiotropic chimera by shuffling the DNA of capsids from numerous serotypes and selecting for AAV variants that targeted the muscle [300]. Studies using these chimeras have demonstrated an improvement of transduction efficiency and cardiac tropism with a reduced affinity for liver amongst other organs.

- **Optimization of the recombinant genome.** To optimize specificity and efficiency of the recombinant genome, different approaches have been developed, being the inclusion of specific promoters the most broadly used. Also changes in ITR sequences, the use of synthetic target sequences or the use of self-complementary AAV vectors have been tested. Regarding specific promoters, different cardiac specific promoters have been assayed for heart expression. Some as the α-myosin heavy chain (αMHC) promoter has been shown to provide sufficient cardiac

specificity, but with significantly lower expression than the CMV promoter [301], [302]. Other studies have tested the combination of MLC and CMV promoters allowing a robust and specific cardiac protein expression [303], [304]. Cardiac troponin T (TnT) is another cardiac specific promoter that has been widely used with AAV6 and AAV9, in rodent as well as in swine models [305]–[307]. Use of disease-specific promoters is another strategy for temporal regulation, as the use of atrial natriuretic factor promoter, which is highly expressed in the failing myocardium in response to stretch [308]. Furthermore, other different strategies have also been developed to increase transgene expression. Insertion of mutations in the ITR sequence to specifically package AAV dsDNA have been designed [309], [310]. Also, the insertion of some synthetic miRNA target sequences into the 3' UTR of AAV-delivered genes has been engineered to make them susceptible to miR-122-driven suppression in the liver [311]. Finally, the use of self-complementary AAV vectors has been tested. In this strategy, the replication termination signal is eliminated in one of the ITRs, so during the production of double stranded DNA molecules, after replicating the first strand, instead of stopping in the second ITR, the complementary sequence of the newly synthesized strand is synthesized [312] allowing faster and higher transgene expression. However, this strategy involves the reduction of cloning capacity from 4.7 to 2.5 Kb.

- **Administration Route.** Importantly, the choice of AAV delivery pathway also impacts the efficiency and duration of transgene expression as well as the degree of systemic distribution and homogeneity within the tissue. The optimal delivery technique differs depending on the chosen vector and the treated tissue. Several methods have been tested with varying levels of success, being intravenous and intramyocardial delivery the most broadly tested for heart application in animal models. Intravenous delivery is a safe method that could trigger a relatively homogeneous expression in the tissue. Unfortunately, this is only useful in rodents but not in large animals, let alone in humans, where current vector technologies are not sufficient to transduce the myocardium by this route. The large doses needed would be prohibitory and minimal off-target expression may induce negative effects. On the other hand, intramyocardial injection, although with a more restricted transgene expression, allows high local concentration of virus, minimized off-target organ transduction and neutralized effect of pre-existing antibodies. For clinical application, less invasive techniques have been used. Antegrade intracoronary injection has been performed in several clinical trials, including the CUPID trial, although this procedure has not been the most efficient for AAV delivery into the CMs [313]–[315]. Furthermore, other methods like retrograde and intrapericardial injection have been reported. For retrograde injection the temporal occlusion of the left anterior descending

coronary artery increases the intravascular pressure. This effect enhances gene transfer but it also carries significant clinical risk [316]. On the other hand, when AAV are intrapericardially injected, only epicardial cells are transfected. In this case, pharmacological agents can be used to increase the cardiac permeability to vectors, but rising the risk to induce cardiac toxicity [317].

4.1.4 GENE THERAPY TO PROMOTE CARDIAC REGENERATION

Numerous studies have shown AAV gene therapy to be a feasible strategy for the treatment of heart failure in small animal models [318]. Efficient cardiac transduction and expression of gene products in large animal models was firstly considered as a challenge, but nowadays several studies have been performed with varying degrees of success. To date, genes related to beta-adrenergic signaling, calcium handling, angiogenesis, inflammation and metabolism have been the main ones expressed by AAVs. **Table 2** provides a summary of AAV gene therapy studies using pre-clinical models for the treatment of heart failure.

Table 2. AAV gene therapy studies for the treatment of CVD in large animal models. *(Adapted from Bass-Stringer et al. Heart. Lung. Cir. 2018)* [319].

AAV Vector + Molecular Target	Disease Model	Animal model	Delivery Method	Outcome	Ref
AAV6-VEGFA165	AMI	Dog	Intramyocardial injection	Enhanced arteriogenesis and CMs viability	[320]
AAV1-VEGFA165 +AAV1-Ang1	MI	Pig	Intramyocardial injection	Improved cardiac function and myocardial perfusion Higher cardiac vascular density, proliferating CMs and reduced apoptotic cells	[321]
AAV2/9-VEGF-A /PDGF-B	Chronic Ischaemia	Pig	Retroinfusion into lateral vein	Improved ejection fraction Increased myocardial blood flow reserve	[322]
AAV9-VEFG-B	Dilated cardiomyopathy	Dog	Intracoronary delivery	Preserved diastolic and contractile function Repressed ventricular chamber remodeling	[308]
AAV6-βARKct	Ischemic heart failure	Pig	Retrograde injection into coronary veins	Amelioration of LV haemodynamics and repressed LV remodelling Normalisation of neurohormones that are elevated during HF	[304]
AAV1-SERCA2a	Heart failure	Pig	Intracoronary injection	Preserved systolic function Favorable impact on ventricular remodeling	[323]
AAV1-SERCA2a	Congestive heart failure	Pig	Intracoronary injection	Increased Ca^{2+} storage capacity in cardiac tissue and restored coronary flow Increased eNOS and promoted activity in endothelial cells	[324]
AAV2/1-SERCA2a	Heart failure	Sheep	Cardiac recirculation delivery	Dose-dependent improvement in LV pressure and fractional shortening	[325]
AAV6-SERCA2a	MI	Sheep	Percutaneous delivery	Improved cardiac function and reduced remodeling	[326]
AAV2/1-SERCA2a	Heart failure	Sheep	Percutaneous reperfusion circuit	Improved LV function	[327]
AAV1-SERCA2a	Ischemic heart failure	Sheep	Cardiac surgery with recirculating delivery	Increased ejection fraction Decreased myocyte apoptosis and myocyte hypertrophy	[328]

AAV Vector + Molecular Target	Disease Model	Animal model	Delivery Method	Outcome	Ref
AAV1-SERCA2a	Ischemic cardiomyopathy	Sheep	Cardiac surgery with recirculating delivery	Improved end diastolic and systolic volumes Reduction of fibrosis	[329]
AAV9-SERCA2a	Ischemic cardiomyopathy	Sheep	Cardiac surgery with recirculating delivery	Improved LV function and reduced markers of oxidative stress Attenuated myocyte hypertrophy	[330]
AAV1-SERCA2a	Heart Failure	Dog	Intramyocardial injection	Improved heart function	[331]
AAV6-hSERCA2a	Heart Failure	Dog	Intramyocardial injection	Improved heart function Addition of immunosupression alleviated immune response	[332]
AAV1.SUMO1	Ischemic heart failure	Pig	Antegrade coronary infusion	Improved LV ejection fraction Prevented significant LV dilation	[333]
AAV9-S100A1	Heart failure	Pig	Retrograde coronary venous delivery	Normalized CMs calcium cycling, sarcoplasmic reticulum calcium handling and energy homeostasis	[303]
AAV6-S100A1	Post-ischemic heart failure	Pig	Retrograde delivery via anterior cardiac vein	Improved LV ejection fraction Favorable impact on cardiac remodeling	[334]
AAV9.I-1c	MI	Pig	Intracoronary delivery	Increased cardiac output and preserved cardiac function. Reduced fibrosis scar size	[335]
AAV2i8(BNP116.I-1c)	Ischemic heart failure	Pig	Intracoronary delivery	Higher stroke volume Improved heart contractility	[336]
AAV9.h HO-1	Ischemic heart failure	Pig	Retroinfusion	Decreased inflammation Increased ejection fraction	[337]
AAV6-shRNA-PLB	Healthy	Dog	Percutaneous	Effective knock-down expression but with some cardiac toxicity associated	[338]

Regarding to AAV clinical application, the CUPID clinical trial has been the first approach to treat CVD by gene therapy. In this study, the vector of choice was an AAV1 carrying the SERCA2a gene. The phase I trial established the safety of the vector in human application with potential therapeutic efficacy [339]. In the following phases IIa and IIb, 39 patients were randomized to receive either low, middle, high dose, or placebo, and demonstrated significant improvement in pre-specified endpoints in patients treated with the high dose 12 months after therapy [313]. Furthermore, long-term follow-up data showed a reduction in risk of adverse cardiovascular events in these patients *versus* the placebo group [314]. However, a larger phase IIb, multicenter, double-blind, placebo-controlled study failed to demonstrate a reduction in clinical events after AAV1.SERCA2a therapy compared to the placebo group [340]. Therefore, although AAV represent a thrilling tool in basic and preclinical research and are potentially able to succeed in clinical trials, continued efforts are essential for the successful clinical translation of this approach to the cardiac field.

An alternative AAV-strategy for cardiac therapy has also focused on the expression not only of key genes, but also miRNAs. Interestingly, many specific miRNAs capable of promoting CMs proliferation have been assessed as previously described in section 3.2.2. The most effective ones, miR-590 and miR-199 were delivered via AAV to mouse heart *in vivo*, inducing cardiac regeneration with a concomitant improvement of cardiac function after MI [166]. This study showed for the first time that post-infarct cardiac regeneration could be induced *in vivo* by delivering non-coding RNAs with a classical method of gene therapy. Another study described AAV9-mediated restoration of miR-1 expression in rats, modulating cardiac remodeling and pressure-induced hypertrophy [191]. Furthermore, miR-378, generally studied in the context of cancer and cell survival, was reported to be a regulator of CMs hypertrophy. Thus, injection of AAV-miR-378 recovered the physiological miRNA levels and modulated hypertrophy in a thoracic aortic constriction mice model [341]. Recently, another group has reported the benefit of using a doxycycline-inducible AAV9-miR-294 vector. In this work, this vector was delivered to mice and demonstrated that ectopic transient expression of miR-294 promoted CMs cell cycle reentry and improved cardiac function after MI [342]. Also directed to CMs, Gao *et al*. have recently reported the therapeutic potential of AAV9-miR-19a/19b in a mouse MI model. In their work, intra-cardiac injection of miR-19a/19b mimics or AAV encoding these miRNAs sequences demonstrated reduced cardiac damage and improved cardiac function [343]. Furthermore, in a transgenic mouse model of severe, chronic muscular dystrophy with an associated dilated cardiomyopathy, the long-term induction of miR-669a overexpression by AAV, improved animals' survival. Treated mice showed significant decrease in hypertrophic remodeling, fibrosis

and CMs apoptosis that correlated with an improved cardiac function [344]. On the other hand, miRNA down-regulation could be also a potential treatment. In this context, AAV9-antagomiR-25 demonstrated to increase the survival of CMs and prevented a decline in cardiac function [345].

Therefore, gene therapy has emerged as a promising approach in the cardiovascular field, not only for coding genes but also for non-coding molecules (like miRNAs) specific expression, suggesting a wide range of new therapeutic tools for heart regeneration.

Hypothesis and Objectives

Extensive data has already demonstrated the key role that miRNAs play in the homeostasis and pathology of the heart, suggesting the therapeutic benefit of their regulation. Importantly, CPC-exosomes have been described as main cardioprotective mediators against heart damage, giving a particular relevance to the miRNAs cargo present in them. Moreover, gene therapy has emerged as a promising approach for coding and non-coding molecules expression, being its use, clinically approved in different pathological disorders, including the cardiovascular ones.

Thus, the **hypothesis** of our study is that overexpression of specific exosomal-CPC miRNAs that positively regulate the homeostasis processes in the heart, could significantly contribute to regenerating and/or protecting the ischemic tissue. Moreover, the use of a gene therapy approach could greatly improve their action, allowing for a controlled, localized and sustained expression of specific miRNAs.

Based on these premises, this thesis attempts to fulfill the following **objectives**:

1. To develop and characterize Adeno-associated Viral Vectors serotype 9 (AAV9) designed with ubiquitous or cardiac-specific promoters, and analyze their *in vivo* biodistribution in mouse, taking into account critical aspects such as the different routes of delivery and the pathological context of the ischemic heart.
2. To define the specific miRNA repertoire of CPC-derived exosomes and identify key candidates with a potential role in the cardiac reparative processes after ischemia.
3. To evaluate the potential role of miR-935 against oxidative stress damage and the therapeutic efficacy of AAV9-TnT-miR-935 in a murine model of acute myocardial infarction.

Material and Methods

1. REPORTER VECTORS: VECTOR DESING AND CLONING

1.1 CLONING STRATEGY

AAV-vectors were generated from the AAV-TnT-pA plasmid with an expression cassette harboring a truncated 418 bp chicken TnT promoter, a multiple cloning site and a SV40 polyadenylation signal, flanked by the AAV inverted terminal repeats (ITR) (AAV-TnT-pA plasmid). This vector was kindly provided by Dr. Prasad [346] (**Figure 11A**).

First, an intermediary vector was generated by the amplification of the woodchuck hepatitis virus posttranscriptional regulatory element or WPRE sequence (element that increase mRNA stability) [347] by PCR from the pRRLSIN.cPPT.PGK-GFP.WPRE vector (Addgene, #16578). NotI and BamHI sites were included to facilitate cloning into pAAV-TnT-pA plasmid, generating the pAAV-TnT-WPRE-pA vector (**Figure 11B**). For biodistribution studies, reporter sequences were cloned into the multiple cloning site. cDNA encoding firefly luciferase sequence (Luc) was PCR amplified from the Luciferase-pcDNA3 vector (Addgene, #18964) and green fluorescent protein (GFP) was amplified from the pRRLSIN.cPPT.PGK-GFP.WPRE vector (Addgene, #16578) containing HindIII and NotI restriction sites, respectively. Reporter sequences were inserted downstream of the TnT promoter sequence, between HindIII and NotI sites of the pAAV-TnT-WPRE-pA vector, generating pAAV-TnT-LUC-WPRE-pA and pAAV-TnT-GFP-WPRE-pA final vectors (**Figure 11C**). Finally, TnT promoter sequence was replaced by the elongation factor -1 alpha (EF1α) promoter fragment. EF1α cDNA was amplified using primers flanked by XbaI and HindIII sites and the pSin-EF2-Nanog-Pur vector (Addgene #16578) as a template. Ubiquitous promoter sequence was subsequently subcloned to obtain the pAAV-EF1α-LUC-WPRE-pA and pAAV-EF1α-GFP-WPRE-pA final vectors (**Figure 11D**).

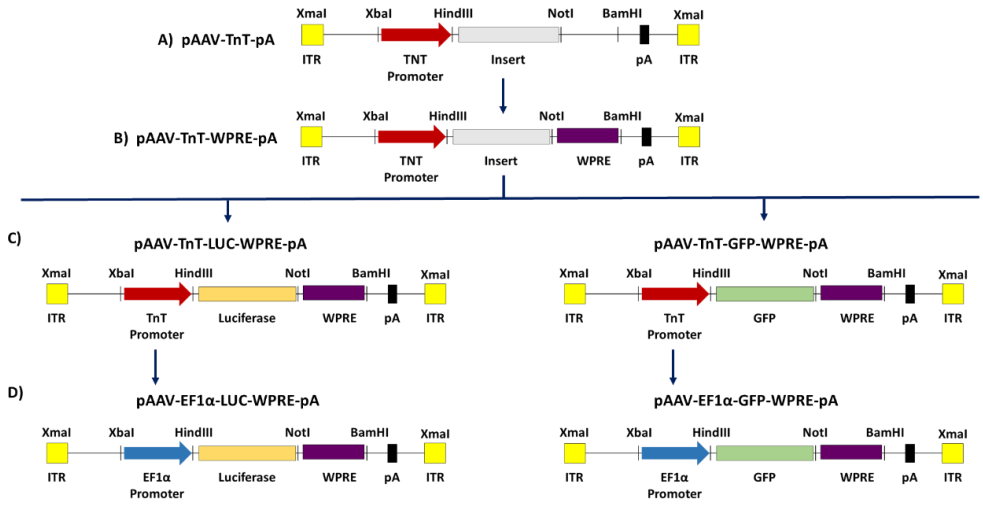

Figure 11. Schematic representation of cloning strategy for reporter vectors

1.2 CLONING PROTOCOL

The amplification PCR reactions were performed by mixing 50 ng of each template vector and 1 µl of the designed primers (10 µM stock) with the restriction sites sequences, and carried out with 0.2 µl Platinum Taq DNA Polymerase High Fidelity (Invitrogen) in a final volume of 50 µl, under the following conditions: 94 ºC for 2 minutes and 30 cycles of 94 ºC for 15 seconds, 58 ºC for 30 seconds and 68 ºC for around 30 seconds (depending on the PCR product, 1 minute/Kb), with no final extension (see **Table 3** for amplification primer sequences). PCR products were resolved in 1% agarose gels and amplified products bands were subsequently purified according to the manufacturer´s instructions (NucleoSpin Gel and PCR Clean-up, Macherey Nagel), eluting the resulting DNA in 30 µl of distilled water. Purified PCR products were cloned into pGEM-T Easy Vector (Promega). PCR products were ligated into pGEM-T using T4 DNA ligase (Promega) and incubated during 1-2 hours at room temperature (R/T). The ligation products were used to transform subcloning efficient DH5α chemically competent cells (Invitrogen) using heat-shock method. Briefly, 50 µl of DH5α were incubated with 2 µl of ligation product for 20 minutes on ice, followed by a heat shock treatment with an incubation for 45 seconds at 42ºC and 2 minutes on ice. Transformed cells were mixed with 300 µl of SOC Medium (ThermoFisher) and shaked for 2 hours at 37ºC. Then, transformed cells were seeded onto LB agar plates supplemented with 50 µg/ml ampicillin (Sigma), 0.5 mM IPTG (Sigma) and 80 µg/ml X-Gal (Sigma), and allowed to grow for 16-20 hours at 37ºC. Positive colonies were picked up and grown in 3 ml of LB broth with ampicillin (50 µg/ml) for 24 hours at 37ºC with shaking. Plasmid DNA was purified using NucleoSpin Plasmid Kit (Macherey-Nagel). Briefly, grown and harvested bacterial cells were centrifuged 11,000 x g during 30 seconds. After centrifugation, pellet was lysed and clarified by another centrifugation (11,000 x g for 10 minutes). Supernatants were loaded on a column with a collection tube and centrifuged (11,000 x g for 1 minute) for binding the DNA to the silica membrane of the column. Silica membrane was washed and dried by centrifugation (11,000 x g for 2 minutes). Finally, the resulting DNA was eluted in 50 µl of elution buffer.

Table 3. Amplification primer sequences

Vector Template	*Primer Name*	*Sequence (5´-3´)*
pRRLSIN.cPPT.PGK-GFP.WPRE	*WPRE-NotI-FW*	*aattGCGGCCGCtagttcaggtgtattg*
	WPRE-BamHI-REV	*aattcatatGGATCCatggttcgcaattc*
Luciferase-pcDNA3 vector	*Luc-HindIII-FW*	*aattAAGCTTCCACCatggaagacgccaaa*
	Luc-NotI-REV	*aattGCGGCCGCttacacggcgatctttccgc*
pRRLSIN.cPPT.PGK-GFP.WPRE	*GFP-HindIII-FW*	*ttAAGCTTCCACCatggtgagcaagggc*
	GFP-NotI-REV	*ttGCGGCCGCttacttgtacagctcgtc*
pSin-EF2-Nanog-Pur	*EF1α-XbaI-FW*	*aattTCTAGAgtgcccgtcagtgggcagag*
	EF1α-HindIII-REV	*aattAAGCTTtcacgacacctgaaatggaa*

**Restriction sites in the primer sequences are indicated in uppercase.*

For final vector's cloning, plasmid digestions were performed with NotI and BamHI in 1XNEB 3.1 buffer for WPRE insertion, HindIII and NotI in 1XNEB 3.1 buffer for reporter insertions and XbaI and HindIII in 1XNEB 2.1 buffer for promoter exchange. Each digestion was performed in 50 µl of final volume at 37ºC overnight. After digestion, vector products were dephosphorylated at 5'-termini using Shrimp Alkaline Phosphatase (SAP, USB Affymetrix) for 1 hour at 37ºC. All digestion products were run in a 1% agarose gel and the amplicon bands were purified using NucleoSpin Gel and PCR Clean-up (Macherey Nagel), eluting the resulting DNA in 30 µl distilled water. Then, a ligation reaction was performed with the purified vector, the insert and 1 µl of T4 DNA Ligase (New England Biolabs) and incubated overnight at 16 °C. Ligation product was transformed into 50 µl of DH5α competent cells as described above. After adding 300 µl of SOC medium and incubating at 37ºC for 2 hours with shaking, transformed cells were plated onto LB agar plates supplemented with ampicillin (50 µg/ml) and incubated overnight at 37ºC. Discrete colonies were picked up and grown in 3 ml of LB Broth with ampicillin (50 µg/ml) for 24 hours at 37ºC with shaking. DNA was purified using NucleoSpin Plasmid Kit (Macherey-Nagel) as described above and eluted in 50 µl of elution buffer. DNA was tested by digestion and Sanger sequencing to verify the constructs. Once the complete sequence was verified, selected DNA plasmids were transformed into competent DH5α cells and growth in 400 ml of LB Broth with ampicillin (50 µg/ml) for 24 hours at 37ºC with shaking. High copy plasmids were purified using NucleoBlond® Xtra Maxi kit (Macherey-Nagel) and eluted in 200 µl of elution buffer.

2. PLASMID EXPRESSION ANALYSIS

2.1 CELL CULTURE

The murine embryonic fibroblast cell line NIH/3T3 (ATCC) and the cardiac muscle cell line HL-1 (kindly donated by Dr. Claycomb, Louisiana State University) were cultured for *in vitro* studies. NIH/3T3 were cultured in Dulbecco's modified Eagle's medium (DMEM) (Gibco) supplemented with 10% fetal bovine serum (FBS) (Hyclone), 1% Penicillin / Streptomycin (Lonza) and 1% Glutamine (Gibco). The HL-1 cell line was maintained in culture flasks coated with 0.1% gelatin and cultured in Claycomb medium (Sigma-Aldrich), also supplemented with 10% FBS, 1% Penicillin / Streptomycin and 1% Glutamine. Both cell lines were maintained at 37 ºC and 5% CO_2 and 95% humidity.

2.2 *IN VITRO* PLASMID TRANSFECTION

For the plasmid transfection assay, NIH/3T3 were plated at a density of 84,000 cells/cm^2 in a 24-well plates and HL-1 cells were plated in 24-well plates coated with 0.1% gelatin at a density of 48,000 cells/cm^2. After 24 hours, cells were transfected with Xtreme-Gene according to the manufacturer's instructions. Briefly, the transfection reagent (2.5 µl) and the plasmid (1 µg) were diluted each in 200 µl of Opti-MEM reduced serum medium (Invitrogen). After 5 minutes, diluted plasmid was mixed gently with the diluted reagent and incubated for 5 minutes at R/T. Finally, 400 µl of the complex was added to the cells.

2.3 LUCIFERASE ASSAY

Plasmid luciferase activity was measured with a Dual Luciferase Reporter Assay (Promega) 48 hours after transfection. Briefly, cells were incubated with passive lysis buffer shaking for 15 minutes at R/T. Cell lysates were collected and after three freeze-thaw cycles, transferred to a luminometer plate. Luciferase assay reagent and Stop and Glo® reagent were dispensed into the appropriated luminometer tubes, on a conventional luminometer (Oriol L. Berthold Detection System) and luciferase activity was measured according to the manufacturer´s instructions. For this assay, *Renilla* luciferase vector (p-RL-CMV) was included for correction of transfection efficiency.

3. AAV PRODUCTION, PURIFICATION AND TITRATION

3.1 AAV PRODUCTION

AAV vectors were produced using HEK293T as packaging cells. HEK-293T cells were maintained in DMEM with high glucose and pyruvate (Gibco), supplemented with 10% FBS (Hyclone), 1% Penicillin/Streptomicyn (Lonza) and 1% Non-essential amino acids (Lonza) and grown in a humidified atmosphere at 37 ºC and 5% CO_2. For AAV production, culture media was exchanged by DMEM supplemented with 2% FBS and the transfection was carried out using poly-ethylene imine (PEI, Sigma-Aldrich) (10mM and pH 7-7.5). For each production, a mixture of 55 µg of the helper plasmid pDP9 (kindly provided by Dr. Muller (DKFZ, Germany)), that provides the viral genes required for the replication and encapsidation of AAV, and 20 µg of the specific construct containing the recombinant AAV genomes, were transfected. After 72 hours cells were collected, debris were eliminated by centrifugation and the pellet was resuspended in 7 ml of Lysis Buffer (50 mM Tris, 150 mM NaCl, 2 mM MgCl2, 0.1% Triton X-100) and kept at -80ºC. The supernatant of the cells was collected and treated with 8% poly-ethylene glycol solution (PEG-800, Sigma-Aldrich) for 48-72 hours at 4ºC to precipitate the particles. Then, the supernatant was centrifuged at 3000 rpm for 15 minutes and the pellet resuspended in 7 ml of Lysis Buffer. Cell lysate and precipitated pellet from the supernatant were frozen and thawed in three rounds to release the viral particles. Both lysates were mixed and treated with Dnase-I and Rnase-A (Roche) 0.1mg/plate for 1 hour at 37ºC.

3.2 AAV PURIFICATION

The viral purification was performed by ultracentrifugation in iodioxanol gradient (OPTIPREP, Atom). Different iodioxanol concentrations (consisting of 57%, 40%, 25%, and 15%) were prepared (**Table 4**) and added to an ultracentrifuge tube (Beckman) (from 57% to 15%) to make an iodioxanol gradient. Phenol red was included in the 57% and 25% concentrations to facilitate the localization of the vector band. After sealing, the tubes were centrifuged in a Ti70 rotor (Beckman) at 69,000 rpm for 2.5 hours at 16ºC. After centrifugation, the viral particles are distributed through the 40% density step as shown in **Figure 12**. The virus was recovered by inserting a 19-18G gauge needle into the tube and collected in Amicon 100K columns (MERK Millipore) to determine viral concentration. Three cycles of 15 ml of 5% sucrose in PBS were added to columns with viral particles and centrifuged to eliminate the iodioxanol and concentrate the vector.

Table 4. Iodioxanol gradient composition

ml/tube	*%*	*Iodioxanol (ml)*	**PBSMK 7.4 (ml)*	*NaCl 5M (ml)*	*H_2O MiliQ (ml)*	*Total (ml)*
9 ml	*15*	*6.00*	*3.23*	*4.80*	*9.97*	*24*
6 ml	*25*	*5.82*	*1.91*	*-*	*6.21*	*14*
5 ml	*40*	*9.32*	*1.91*	*-*	*2.80*	*14*
5 ml	*57*	*11.40*	*0.60*	*-*	*-*	*12*

* PBSMK 7.4 (PBS 12.8 ml + $MgCl_2$ 1M 1.1 ml + KCl 2.5M 1.12 ml)

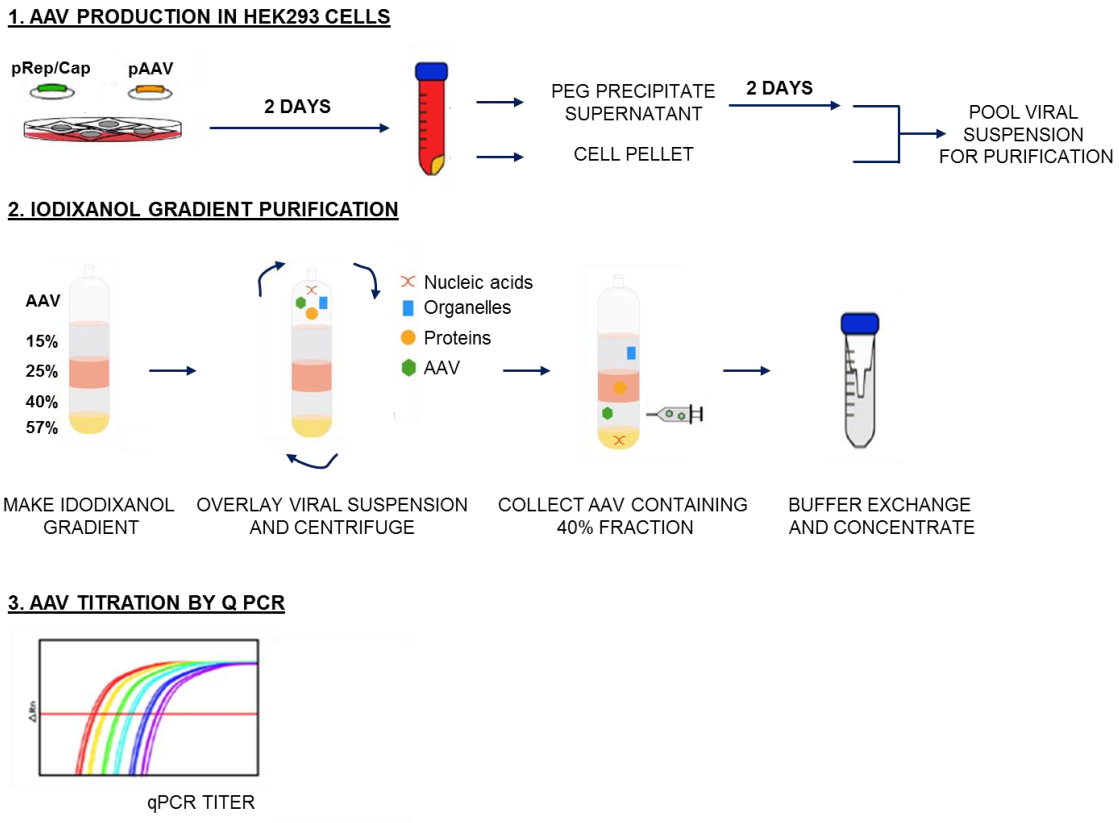

Figure 12. AAV production, purification and titration methods

3.3 AAV TITRATION

Viral titers (viral genomes (vg)/ml) were determined by qPCR. Viral DNA was extracted using the High Pure Viral Nucleic Acid Kit (Roche) following the manufacturer´s instructions. qPCR was performed in triplicate with sequence specific primers (**Table 5**) and titers were calculated using a standard curve of the plasmid employed for each production.

Table 5. Titration primer sequences

Viral Vectors	*Primer Name*	*Sequence (5´-3´)*
TnT- Viral Vectors	*WPRE-TnT-FW*	*ACGCAACCCCCACTGGTT*
	WPRE-TnT-REV	*AAAGCGAAAGTCCCGGAAAG*
EF1α- Viral Vectors	*EF1α-FW*	*GGTGAGTCACCCACAAAGG*
	EF1α-REV	*CGTGGAGTCACATGAAGCGA*

4. ANIMAL MODELS

All animal experiments were performed in accordance with the "Principles of Laboratory Animal Care" formulated by the National Society for Medical Research and the "Guide for the Care and Use of Laboratory Animals" prepared by the Institute of Laboratory Animal Resources (Commission on Life Science, National Research Council). All animal procedures were approved by the University of Navarra Institutional Committee on Care and Use of Laboratory Animals, and performed in strict accordance with the Animal Ethical Committee guidelines (ethical protocol #091-15). Male 8-10-week old C57BL/6 mice were purchased from Harlam Laboratories and maintained according to the institution´s guidelines.

4.1 INDUCTION OF MYOCARDIAL INFARCTION AND VIRAL VECTOR ADMINISTRATION

For MI model, the left anterior descendent (LAD) coronary artery was permanently ligated [348]. For surgical procedure, animals were anesthetized with 2% isoflurane (Isoflo®, ABBOTT S.A) and placed on a heating table, in a supine position, endotracheally intubated for mechanical ventilation with supplementary oxygen.

Anesthesia was maintained with a combination of 3% isofluorane and 0.01 mg/kg fentanyl (Fentanest, Ken Pharma) during all the surgery. Then, a thoracotomy was performed at the left three intercostal space, the pericardium was opened and the LAD coronary artery ligated with a 7.0 absorbable suture. Fifteen minutes after artery ligation, myocardial ischemia was confirmed by color change of the left ventricular wall. The intercostal incision was closed with a 6.0 absorbable suture. The endotracheal tube was removed and spontaneous breathing restored. Animals were kept in a cage with a heating blanket for several hours and supervised until recovered. For analgesia, 24 and 48 hours after surgery 20 µl of Ketoprofen (Ketofen®, Jesús Guerrero) was subcutaneously injected and to prevent infections, 2 ml of enrofloxacin (5 mg/ml) (Alsir®, Esteve veterinaria) was added in 1L of the drinking water during 7 days.

For AAV biodistribution studies, mice received the virus either by intravenous retro-orbital injection or by intramyocardial injection, 15 minutes after artery ligation. Intramyocardial injection at two points of the peri-infarcted area by using a Hamilton syringe (Hamilton, 701N, 10 µl) was performed.

5. BIODISTRIBUTION STUDIES

5.1 BIOLUMINISCENCE IMAGING

Bioluminescence imaging was performed using an IVIS chamber coupled device camera system (Xenogen, Alameda, CA). For *in vivo* images, mice were anesthetized with 40 µl of a mixture of Ketamine (Imalgéne 500, merial) and Xilacine (Rompun, Bayer) solution (ratio 9:1) and intraperitoneally injected with 100µl of a solution of the substrate d-luciferin (150µg/kg dissolved in PBS). After 5 minutes of exposure, animals were sacrificed and organs (heart, liver, spleen, intestine, testes, lung, kidney, brain, quadriceps and gastrocnemius muscles) were quickly excised and placed on a dish for *ex vivo* imaging. Next, organs were frozen in liquid nitrogen and stored at -80ºC until assayed. All bioluminescence images were processed using Living Image 2.20 software package (Xenogen).

5.2 QUANTITATIVE LUCIFERASE ACTIVITY ASSAY

Frozen tissue samples were disrupted using a T10 basic ULTRA-TURRAX (IKA) in Luciferase Lysis Reagent (Promega). After three cycles of freezing and thawing, samples were centrifuged 2 minutes at 16000 g and supernatants were collected. Luciferase activity was measured in a mixture of 10 µl of tissue lysate and 50 µl of Luciferase Assay Reagent with a conventional luminometer according to the manufacturer´s instructions. The amount of total protein present in each tissue homogenate was quantified by BCA assay (Thermo Scientific) using bovine serum albumin as a standard. The data is represented as the levels of luciferase activity (relative light units, RLUs) normalized to protein content (RLU/mg).

5.3 QUANTIFICATION OF AAV GENOME COPIES

Total genomic DNA was extracted from mouse tissues using the QIAamp DNA Mini Kit (Qiagen). qPCR was conducted for detection of vector genome copies, using 50 ng of genomic DNA from each sample and primers for amplifying Luciferase sequence (FW 5'-TCTGAGGAGCCTTCAGGATT-3' and REV 5'-TTTTGGCGAAGAAGGAGAAT-3'). Standard curve was prepared with known copy numbers of corresponding plasmid (calculated from its concentration and base pairs) and DNA samples were assayed in duplicate. The results were represented as vector genome copy/µg genomic DNA.

5.4 TISSUE PROCESSING, IMMUNOFLUORESCENCE AND HEMATOXILIN-EOSIN STAINING

Animals were sacrificed 60 days after vector administration and hearts excised for histological analysis. Mice were anesthetized and perfused with PBS wash for 5 minutes or until heart and liver were cleared of blood. Then, organs were excised and fixed in 4% paraformaldehyde for 4 hours at 4ºC. After washing in PBS (three times, 5 minutes each), samples were equilibrated with 15% sucrose in PBS for 4 hours at 4ºC and then 30% sucrose in PBS overnight. Hearts and livers were mounted in OCT for subsequent frozen sectioning.

For immunofluorescence (IF) analysis, 8 µm serial sections were performed. The presence of GFP positive cells was analyzed without amplification, and then IF was performed for specific cell type detection. Immunolabeling was performed with antibodies against sarcomeric alpha-actin (Sigma-Aldrich) for CMs detection and argininosuccinate synthase 1 (ASS-1) (Abcam) for hepatocyte detection (**Table 6**). Primary antibodies at 1/200 and 1/100 dilution respectively, were incubated at 4ºC overnight. Next, after rinsing with PBS-Tween 0.1%, Alexa Fluor 647 donkey anti-mouse IgG and Alexa Fluor 594 donkey anti-goat IgG (Invitrogen) were added as secondary antibodies (**Table 6**), diluted 1/100 and 1/500 respectively, and incubated for 1 hour at RT. Nuclei were stained with Hoechst previously diluted 1:1000 in PBS/Glycerol (1:1) solution. Images were captured digitally by LSM 510 META (Carl Zeiss, Germany) confocal microscope.

Table 6. Antibodies used for immunofluorescence assay

Type	*Antibody Name*	*Host*	*Dilution*	*Manufacturer*	*Catalog No.*
Primary	*Anti-α-Actinin (Sarcomeric)*	*Mouse*	*1/200*	*Sigma-aldrich*	*A7811*
Primary	*ASS-1*	*Goat*	*1/100*	*Abcam*	*ab77590*
Secondary	*Alexa Fluor 647 anti-mouse IgG*	*Donkey*	*1/100*	*Invitrogen*	*A31571*
Secondary	*Alexa Fluor 594 anti-goat IgG*	*Donkey*	*1/150*	*Invitrogen*	*A11058*

Hematoxilin-Eosin staining was performed to evaluate the presence of inflammatory cells or relevant anatomophatological alterations in tissues. Briefly, samples were stained with Hematoxilin (Erlich) for 10 minutes. After rinsing in distilled water, samples were immersed in water with chlorhydric acid at 37% until tissue turned purple. Then, samples were immersed in lithium carbonate solution and rinsed in distilled water again. Eosin solution at 0.5%, pH 5, was

added for 5 minutes. Finally, samples were rinsed, dehydrated and mounted in DPX. Images were scanned with Aperio CS2 (Leica Biosystems).

5.5 SERUM METABOLITE ANALYSIS

Blood samples were drawn by heart bleeding at the sacrifice time-points. Serum samples were obtained by centrifugation of blood samples at 600g for 15 minutes at 4ºC and then stored at -80ºC. Commercial kits (Roche) were used to measure plasma levels of lactate dehydrogenase (LDH) and creatine kinase (CK), valuing cardiac toxicity, and alkaline phosphatase (ALP) and alanine aminotransferase (ALT) for determination of liver toxicity.

6. TRANSCRIPTION ANALYSIS

The specific miRNA repertoire of adult human cardiac progenitor cells (CPC) was analyzed by the group of Dr. Bernad (CNB-CSIC). Aiming to define the specific CPC miRNA repertoire, a comparative analysis was conducted by RNAseq of the whole cell fraction and the exosomal compartment of these cells. In this analysis, three independent human isolate CPC (CPC1-CPC3) cell populations were compared with two independent human isolate bone marrow-derived mesenchymal stem cells (MSC1 and MSC2), as the gold standard in cell therapy with adult stem cells, and two independent human isolate primary dermal fibroblasts (HDF1 and HDF2) as a distant reference lineage.

6.1 HUMAN CELLS AND CULTURE CONDITIONS

Human cardiac progenitor cells (CPC) were purified from three human myocardial samples by c-kit immunoselection. CPC were maintained and expanded essentially in the same growth conditions used for the CAREMI clinical trial (EudraCT 2013-001358-81). Briefly, human cardiac biopsies were obtained from patients suffering from an open-chest surgery. Tissue samples were obtained from the right atria appendage and minced into small pieces. Enzymatic digestion was carried out treating the tissue with collagenase type 2 (Worthington Biochemical Corporation) for 3 times of 30 minutes each to obtain a cellular suspension. CMs were removed by centrifugation and filtration through 40 µm cell strainers. CPC were purified from the human myocardial samples after immunodepletion of CD45-positive cells by c-kit immunoselection [349]. Cells were maintained in DMEM/F12 and neurobasal medium (1:1) (Invitrogen) supplemented with 10% fetal bovine serum embryonic stem cell-qualified (FBS ESCq, Invitrogen), 2 mM L-glutamine (Lonza), 100 U/mL penicillin and 1000 U/mL streptomycin (Lonza), 0.5X B27 supplement, 0.5X N2 supplement, 10 ng/mL bFGF and 0.5X ITS (all from Invitrogen), 30 ng/mL IGF-II and 20 ng/mL EGF (Peprotech). Human bone marrow-derived MSC

and HDF were obtained from the Inbiobank Stem Cell Bank (www.inbiobank.org). MSC and HDF were maintained in Dulbecco's Modified Eagle Medium-low glucose (DMEM-low glucose; Sigma) supplemented with 10% FBS (Sigma), 2 mM glutamine (Lonza), 100 U/mL penicillin and 1000 U/mL streptomycin (Lonza). All the cultures were maintained in a 3% O2 and 5% CO2 atmosphere. CPC population was characterized by flow cytometry following standard protocols. A selected FACS expression profile for the CPC markers stage-specific embryonic antigen 1 (SSEA1), activated leukocyte cell adhesion molecule (CD166), Thy-1 cell surface antigen (CD90) and endoglin (CD105), and negative for the hematopoietic markers, protein tyrosine phosphatase, receptor type C (PTPRC; CD45) and the progenitor cell antigen CD34 was analyzed, as previously described [349].

6.2 EXOSOMAL ISOLATION

Exosomal fractions were obtained from cell supernatants by standard serial centrifugation method [350]. Briefly, culture supernatant was centrifuged (320 x g for 5 minutes) to discard cells, dead cells and cell debris, and the supernatant was filtered through 0.22 µm membranes and kept for the next step. After two rounds of ultracentrifugation 100,000 x g during 70 minutes 4ºC (Beckman Coulter Optima L-100XP), pellets (exosomes) were kept and supernatants discarded. For exosomes' characterization, purified particles were analysed by transmission electron microscopy and nanoparticle tracking analysis. Exosome markers were detected by western-blot using the ExoAb Antibody Kit (CD9, CD63, CD81 and HSP70 antibodies, rabbit anti-human, with goat anti-rabbit HRP secondary antibody, following standard protocols.

6.3 RNA-seq ANALYSIS

RNA was isolated from CPC (CPC1–3), MSC (MSC1 and MSC2) and HDF (HDF1 and HDF2) and their derived exosomes by miRNeasy kit (Qiagen). RNAseq libraries were constructed with the SMALL RNA Sample Preparation Kit (Illumina). Libraries were sequenced in single-end mode and 75 bp lengths. Fastq files were demultiplexed using the Casava v1.8.2 pipeline. Sequenced reads were quality-controlled and pre-processed using cutadapt v1.6 to remove adaptor contaminants. Resulting reads were aligned and gene expression quantified using RSEM v.1.2.3, over hg19 human reference and Ensembl gene build 65. Only miRNAs with at least 10 counts per sample were considered for statistical analysis. Data were then normalized and differential expression tested using the bioconductor package EdgeR v3.0.8. It was considered as differentially expressed those genes with a Benjamini-Hochberg adjusted p-value ≤0.05. PCA analysis was generated using the prcomp function in R from scaled expression data.

6.4 ISOLATION OF MOUSE CARDIAC CELLS

Hearts were collected from transgenic Bmi1$^{(Cre/+)}$/*Rosa*26$^{(tomato/+)}$ mice that were generated by crossing the Bmi1$^{(creER/+)}$ strain [351] with the *Rosa*26$^{(tomato/+)}$ reporter mice (Ai9 Jackson Laboratory). Double heterozygous mice received tamoxifen dissolved in corn oil (Sigma), intraperitoneally injected with a dose of 7.5 µg/g body weight. At 5-days post-tamoxifen induction, animals were anesthetized, the chest was open and the heart was cannulated for standard Langendorff retrograde perfusion closing the aortic valve. Cannulated heart was removed rapidly and retrograde-perfused under constant pressure (60 mmHg; 37ºC during 8 min) in $Ca2^{+}$ free Stock Perfusion Buffer (see **Table 7** for buffers composition). For enzymatic tissue digestion, a mixture of 0.2 mg/ml Liberase (Roche) and 0.14 mg/ml trypsin (Invitrogen) and $Ca2^{+}$ (12.5 µM) was added to the perfusion buffer. The heart was perfused with the Digestion Buffer until become pale (10 min), then it was removed and gently minced into small pieces by mechanical digestion. Digestion was neutralized with Stopping Buffer 1, and CMs were pelleted by gravity (around 20 min). Supernatant was aspirated and collected and pellet cells resuspended in Stopping Buffer 2. After CMs sedimentation by gravity, supernatant was collected again and serial sedimentation rounds were carried out (for CMs pellet). Calcium concentration was increased from 60 µM to 1 mM final concentration in five steps (60 µM, 112 µM, 212 µM, 500 µM and 1 mM). Final pellet was described as myocyte fraction and resuspended in TRIzol™ for RNA extraction. Supernatant aspirated described as Non-myocyte fraction was processed for cell sorting. A similar procedure was followed in infarcted animals.

Table 7. Buffer composition for Langendorff retrograde perfusion

Buffer	*Reagent*	*Final Concentration*
Ca^{2+} free Stock Perfusion Buffer	*NaCl*	*113 mM*
	KCl	*4.7 mM*
	$MgSO_4$	*1.2 mM*
	Glucose	*5.5 mM*
	KH_2PO_4	*0.6 mM*
	Na_2HPO_4	*0.6 mM*
	$NaHCO_3$	*12 mM*
	$KHCO_3$	*10 mM*
	HEPES Buffer Solution	*10 mM*
	2,3-Butanedione monoxime	*10 mM*
	Taurine	*30 mM*
Digestion Buffer	*Ca^{2+} free Stock Perfusion Buffer*	
	Liberase	*0.2 mg/ml*
	Trypsin	*0.14 mg/ml*
	$CaCl_2$	*12.5 µM*
Stopping Buffer 1	*Ca^{2+} free Stock Perfusion Buffer*	
	Fetal Bovine Serum	*10%*
	$CaCl_2$	*12.5 µM*
Stopping Buffer 2	*Ca^{2+} free Stock Perfusion Buffer*	
	Fetal Bovine Serum	*5%*
	$CaCl_2$	*12.5 µM*

Non-myocyte fraction was incubated with CD45 Monoclonal Antibody (30-F11) eFluor 450 (eBioscience) and Ly-6A/E (Sca-1) Monoclonal Antibody (D7) APC, (eBioscience). Three different populations were separated from Non-myocyte fraction with a BD FacsAria II Special Order System cell sorter. Final pellets were described as Bmi1+ (selected from tomato expression), Sca1+Bmi1- (negative tomato fraction and positive APC fraction) and Non-myocytes (negative tomato and APC fraction) (**Figure 13**).

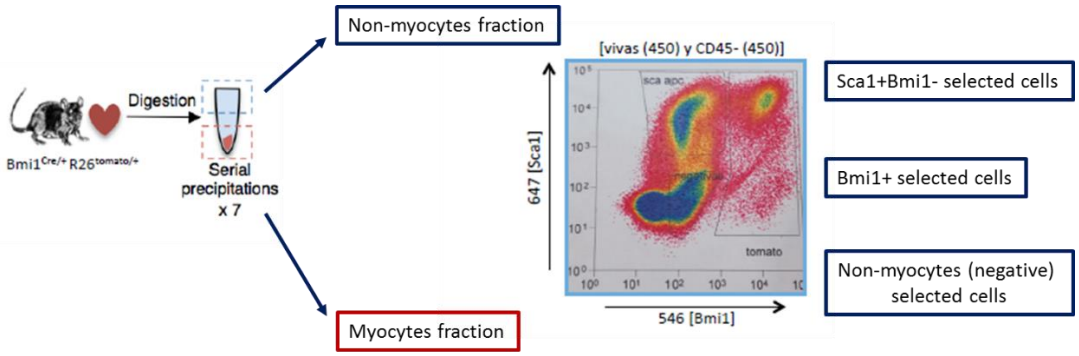

Figure 13. Isolated Cell Mouse Populations. *After serial precipitations final pellet was described as myocyte fraction. Non-myocyte fraction was sorted and divided into Sca1+Bmi1- selected cells, Bmi1- selected cells and non-myocyte (negative) selected cells.*

6.5 RNA ISOLATION, REVERSE TRANSCRIPTION AND QUANTITATIVE PCR ANALYSIS

Total RNA from cells and digested tissue pellet was extracted using the TRIzol™ Reagent (ThermoFisher). Pellet were homogenized with 800 µl of TRIzol, incubated 5 minutes to permit complete dissociation of the nucleoproteins complex, and mixed with 200 µl of chloroform. After incubation for 2-3 minutes, the mix was centrifuged for 15 minutes at 12.000 g at 4ºC and the aqueous phase containing the RNA was transferred to a new tube. For RNA precipitation, 500 µl of isopropanol and 5-10 µg of RNase-free glycogen (Sigma-Aldrich) was added and incubated overnight at -80ºC. Next, RNA was centrifuged for 10 minutes at 12.000 g at 4ºC, and the pellet was washed in 1 ml of 70% ethanol and dissolved in DEPC-treated water. RNA yield was measured using a NanoDrop spectrophotometer (Thermo Scientific).

6.6 miRNA DETECTION AND QUANTIFICATION BY TAQMAN ASSAY

In the reverse transcription step, target-specific stem-loop reverse transcription primers were used. These primers provide exclusive specificity for the mature miRNA target and form an RT primer/mature miRNA chimera that extend the 3´ end of the miRNA to produce a template that can be used in standard TaqMan real-time PCR.

In the first step, cDNA is reverse transcribed from 5 ng of RNA samples incubated with the RT reaction mix (Thermo Fisher) prepared with 0.75 µl of 10X RT Buffer, 0.5 µl of MultiScribe Reverse Transcriptase, 0.075 µl of dNTPs (100 mM), 0.094 µl RNase Inhibitor, 2.081 µl nuclease-free water and 1.5 µl of specific reverse transcription primer (Thermo Fisher). The reaction was incubated in a 2720 Thermal Cycler (Applied Biosystems) 16ºC for 30 minutes, 42ºC for 30 minutes and 85ºC for 5 minutes (**Figure 14A**).

In a second step, 1.5 µl of cDNA was carried out in each qPCR with 5 µl of TaqMan Universal PCR Master Mix 2x No AmpErase UNG (Thermo Fisher), 1 µl of a specific pre-formulated TaqMan Assay (the TaqMan probe and PCR primer set) (Thermo Fisher) and 3.3 µl of nuclease-free water. The real-time PCR amplification was carried out in a QuantStudio Real Time PCR System (Thermo Fisher Scientific) under the following conditions: 95ºC for 10 minutes and then 95ºC for 15 seconds and 60ºC for 60 seconds for up to 40 cycles (**Figure 14B**). miRNA expression was considered as the ΔCt values of the specific miRNAs after normalizing with the different miRNA endogenous expression. TaqMan™ MicroRNA Assays (Thermo Fisher) used to detect and quantify the specific microRNA are detailed in **Figure 14.**

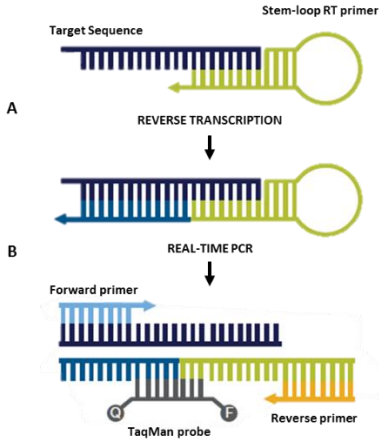

Assay Name	*Assay ID*	*Employed*
U6 snRNA	*001973*	*Mouse miRNA normalizer*
mmu-miR-935	*470972*	*Mouse specific miR-935*
hsa-miR-935	*002178*	*Human specific miR-935*
RNU48	*001006*	*Human miRNA normalizer*
hsa-miR30a-5p	*000417*	*Exosomal miRNA normalizer*

Figure 14. TaqMan MicroRNA Assay approach. *A simple two-step process which employs an innovative target-specific stem-loop reverse transcription primer. The primer extends the 3' end of the target to produce a template* ***(A)*** *that can be used in standard TaqMan real-time PCR* ***(B)*** [352]. ***Table.*** *TaqMan™ MicroRNA Assays (Thermo Fisher).*

7. GENE ONTOLOGY ANALYSIS

For gene enrichment analysis, hsa-miR-935 and mmu-miR-935 putative target genes were selected from TargetScan (http://www.targetscan.org/vert_72/) database. Gene Ontology (GO) enrichment was performed using enrichGO function from clusterProfiler R package [353]. Selecting those categories with an enrichment p value < 0.05.

8. *IN VITRO* APOPTOSIS ASSAYS

8.1 miRNA TRANSFECTION AND OXIDATIVE STRESS INDUCTION

HL-1 cells and cardiac fibroblasts were plated in gelatinized 24-well tissue culture plates at a density of 48,000 cells/cm^2 and 84,000 cells/cm^2, respectively. After 24 hours, medium was removed and cells were transfected with Lipofectamine 2000 according to the manufacturer's instructions. Briefly, the transfection reagent (0.5-1 µl) and the RNA (25nM final concentration) were diluted each in Opti-MEM reduced serum medium (Invitrogen) and incubated for 10 minutes. Diluted RNA was mixed with the diluted reagent and incubated for 5 minutes at R/T. Finally, the complex was added to the cells in a dropwise manner. Cell culture was transfected with mmu-miR-935 (mirVana® miRNA-935 mimic) as well as its respective inhibitor (mirVana® miRNA-935 inhibitor) and their respective controls (mirVana® miRNA Mimic Negative Control #1 and mirVana® miRNA Inhibitor Negative Control #1) (ThermoFisher) and maintained in Opti-MEM reduced serum medium during the experiment.

For oxidative stress induction, 24 hours after transfection, medium was replaced by fresh media and cells treated with Hydrogen Peroxide (H_20_2) (Panreac) at a final concentration of 900 and 100 µM for CMs and cardiac fibroblast, respectively. Apoptosis assays were performed at 5 hours after oxidative stress induction.

8.2 ANNEXIN-V DETECTION

Cells were harvested and stained with FITC Annexin-V Apoptosis Detection Kit I (BD Biosciences) for 15 minutes at R/T following the manufacturer's protocol at indicated time points. The percentage of Annexin V^+ / PI^+ cells was analyzed using FACS Canto II (BD Biosciences) and FlowJo flow cytometry analysis software.

9. miRNA-VECTOR EXPRESSION

9.1 miRNA-VECTOR CLONING

For RNAs overexpression, one of the most common method is the use of synthetic targeting sequences inserted in endogenous miRNA backbones. Previous reports have observed toxicity when short RNAs were overexpressed with an AAV-vector. This toxicity was avoided by addition of the RNA sequence in a backbone of miRNA instead of a shRNA [354], [355]. The miRNA backbone is the hairpin structure of the natural miRNA where the specific duplex sequence is replaced by the mature miRNA of interest, also known as artificial miRNA. This structure reduces steady-state levels of the mature miRNA and prevents the RNAi machinery saturation. Furthermore, these artificial miRNAs have demonstrated effective gene silencing and safety both *in vitro* and *in vivo* [356], [357]. Functional backbones have been tested from a number of natural miRNAs [358]–[361]. Among them, scaffolds derived from miR-30 or the synthetic inhibitory BIC/miR-155 RNA (SIBR) are the two most used [362], [363]. Zeng and colleagues utilized for the first time miR-30 backbone to produce functional artificial miRNAs and suppress the expression of endogenous human genes [362], and other studies have already used AAV containing miR-30 backbone for miRNA overexpression [364].

In this work, we have employed the scaffold of miR-30 to generate our designed miRNA for *in vivo* overexpression with AAV. For that aim, the constructs were created by re-designing the human miR-30. The stem of the primary miR-30 transcript was replaced with specific duplex sequence of miR-935 (**A**) or a scramble sequence (obtained from Sh Scramble hairpin plKO viral vector Addgene #1864) (**B**). This design does not affect normal miRNA maturation and processing. In fact, this design harnesses endogenous enzymatic processing by the RNase III Drosha, which increases subsequent Dicer recognition and specificity, leading to more miRNAs

produced in the cell that are available for incorporation into the RISC complex for target mRNA degradation. These sequences are preceded by HindIII sequence and finished by NotI sequence and were designed to be cloned into pUC57 (Genscript). The two different plasmids (pUC57-miR935 and pUC57-Scramble) were digested and purified sequences were cloned into digested AAV-TnT-LUC-WPRE-pA to replace the luciferase gene by miR-935 or Scramble miRNA sequences (**C**). Cloning protocol was performed as described above in section 1.2.

A)

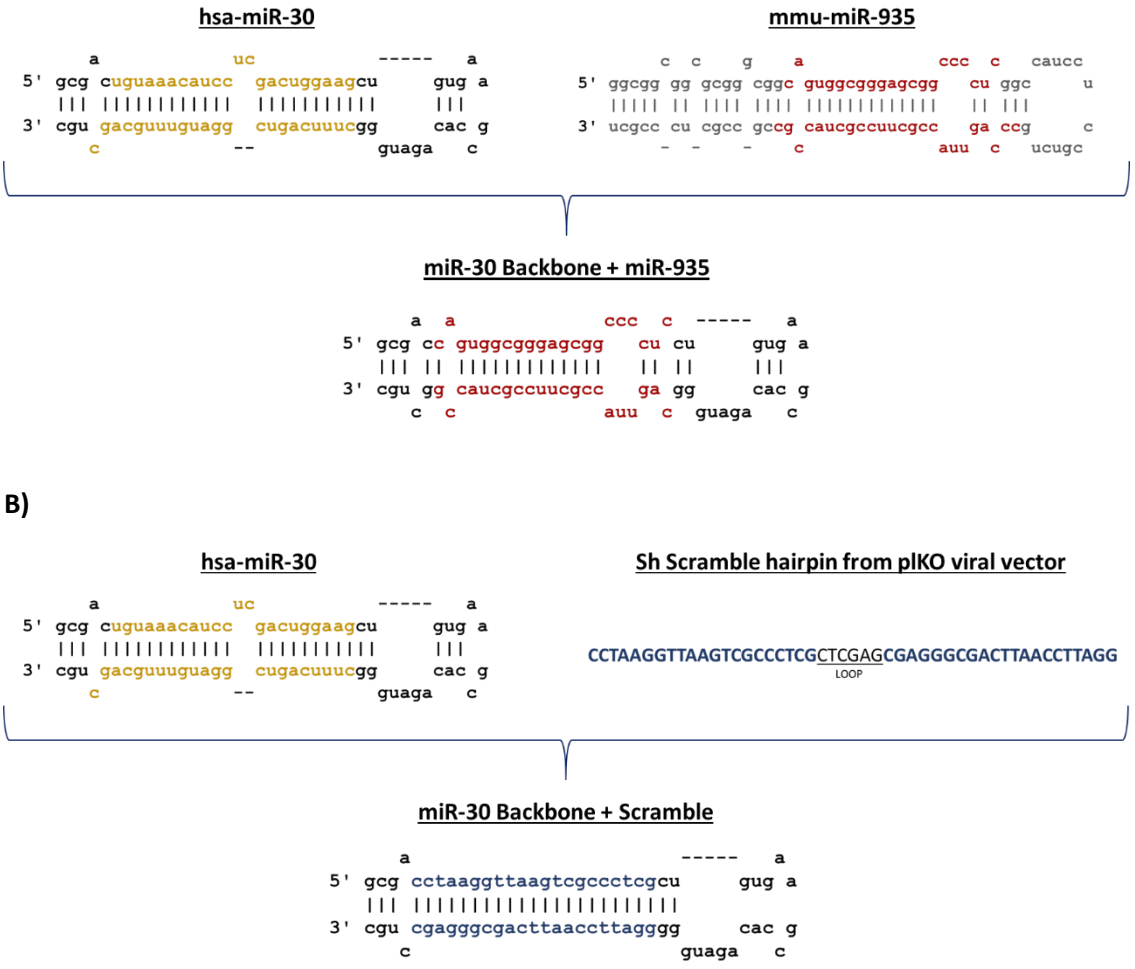

B)

C)

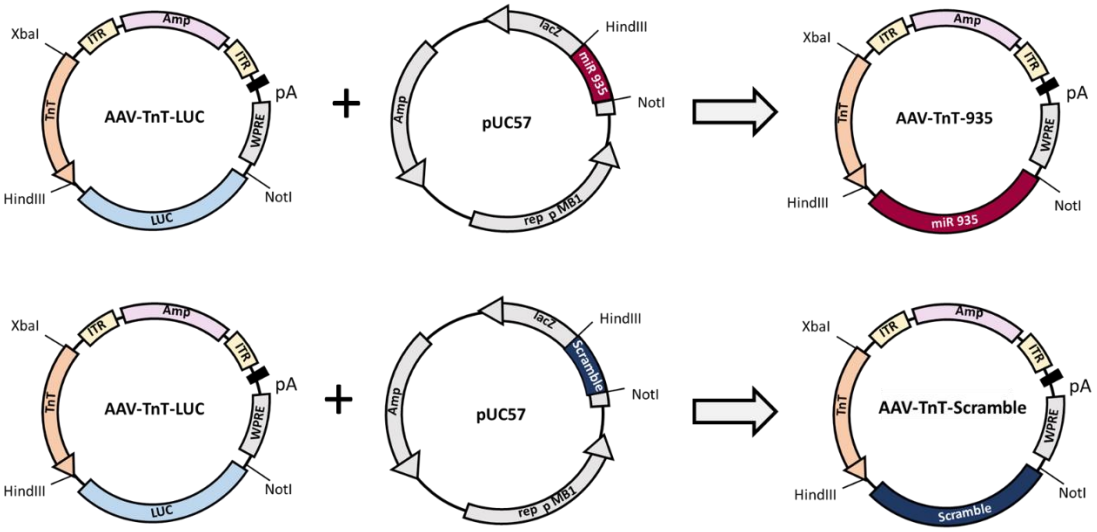

Figure 15. Strategy of miRNA expression. *Diagram of the hsa-miR-30 cassette (mature sequence is labelled in yellow), diagram of the mmu-miR-935 (mature sequence is labelled in red) and design of the miR-30 backbone with miR-935 mature sequence cassette* ***(A).*** *Diagram of the hsa-miR-30 cassette (mature sequence is labelled in yellow), sequence of sh-scramble hairpin from plKO viral vector and design of the miR-30 backbone with Scramble sequence cassette (mature sequence of Scramble is labelled in blue)* ***(B).*** *Schematic representation of cloning strategy for AAV-TnT-miR-935/Scramble vectors* ***(C)****.*

9.2 miRNA-VECTOR EXPRESSION ANALYSIS

Plasmid expression analysis was corroborated in the cardiac muscle cell line HL-1. Cells were cultured and plasmid transfection was performed as described above in section 2. Detection of miR-935 overexpression was analyzed by RT-qPCR as described in section 6.5.2.

10. *IN VIVO* FUNCTIONAL AND HISTOLOGICAL ANALYSIS

10.1 ECHOCARDIOGRAPHIC STUDIES

The therapeutic potential of AAV-TnT-miR-935 was analyzed in a mouse model of MI. LAD ligation and AAV intramyocardial administration were performed as described above in section 4. For echocardiographic studies, animals were anesthetized with isoflurane (Isoflo®, Abbott S.A) at 4% for induction and 1.5% for manintenance and 100% of oxygen. Each mouse was placed on a heating table in a supine position with the extremities fixed and the chest was shaved using a chemical hair remover (Veet, Reckitt Benckiser). To improve the visibility of the cardiac chambers, warmed ultrasound gel (Quick Eco-Gel, Lessa) was applied to the thorax. Heart rate was recorded before the echocardiography study.

Echocardiography (ethical protocol #091-15 approved by the University of Navarra) was performed 2, 30 and 60 days after LAD artery ligation in AAV-TnT-miR-935 and AAV-TnT-miR-Scramble treated groups. Vevo 770 ultrasound system (Visualsonics) was performed in mice as previously described by our group [365].

Left ventricular (LV) remodeling was quantified according to the guidelines and standards of American Society of Echocardiology, and the Guide to echocardiography study using the Vevo 770 and the Vevo 770® Protocol-Based Measurement and Calculations guide. For structural analysis, first volume in diastole (VD) and volume in systole (VS) were calculated using the Simpson´s rule from a long-axis view and four different short-axis views, from the aortic annulus to the endocardial border at the apex level, in diastole and systole. Once VD and VS were calculated, Stroke volume (SV), fractional shortening (FS%) and ejection fraction (EF%) were calculated through the following equations:

$$SV=VD-VS$$

$$FS\%=[(VD-VS)/VD] \times 100$$

$$EF\%= (SV/VD) \times 100$$

The apical location of the infarction in our model involve the poor definition of the endocardial border on the short-axis view, especially at mid-ventricular and apical levels, so the fractional area change (FAC%) was calculated in one parasternal long-axis (FAC% long) in systole (Areas) and diastole (Aread). The long-axis views were acquired using gain settings that optimized the visualization of the endocardial and epicardial walls. The following equation were used to FAC% calculation.

$$FAC\%= [(Endocardial\ Aread – Endocardial\ Areas)/Endocardial\ Aread] \times 100.$$

10.2 MORPHOMETRIC ANALYSIS

For histological assessment, animals were sacrificed at 60 days post-myocardial infarction. First, mice were anesthetized by injection of 40 µl of a mixture of Ketamine (Imalgene 500, Merial) and Xilacine (Rompun, Bayer) solution (ratio 9:1) and perfusion-fixed with PBS for 5 min and Zn-Formalin (Thermo Scientific) for 15 minutes under physiological pressure. After perfusion, hearts were excised and fixed overnight in Zn-Formalin at 4ºC overnight. A mouse heart slicer matrix (Zivic instruments) was used to cut the heart in 4 equally sized blocks (Apical-Infarcted zone, peri-infarcted zone, medium and basal). Hearts blocks were dehydrated

overnight in ethanol 70% at 4ºC and embedded in paraffin. For histological analysis, 5 µm serial sections were performed.

Quantification of heart tissue vascular density was performed by IF analysis for Caveolin-1. Serial sections were deparaffinized and rehydrated by immersion through xylene for 30 minutes and then 100% ethanol, 90% ethanol, 70% ethanol, 50% ethanol, and deionized water (5 minutes each). Heat-induced antigen retrieval was performed using a pressure cooker and Tris-EDTA pH=9 buffer. Then, sections were washed in distilled water for 5 minutes. To permeabilize the tissue, sections were washed for 5 minutes in 0.1% PBS-Tween, and to block non-specific bindings sections were incubated with 10% bovine serum albumin (BSA) for 30 minutes. Primary antibody anti-Caveolin-1 (Cell signaling #3238S) diluted 1/100 in PBS and 1% BSA was incubated overnight at 4ºC. After rinsing sections with 0.1% PBS-Tween samples were incubated with secondary antibody Alexa Fluor 488 donkey anti-rabbit IgG (Invitrogen #A21206) diluted 1/100 for 1 hour at R/T. Finally, slides were rinsed in 0.1% PBS-Tween. Nuclei were stained with Hoechst, previously diluted 1:1000 in PBS/Glycerol (1:1) solution, and images were captured digitally by Axio Imager.M1 (Zeiss) microscope. Twelve images from serial heart sections were captured and analyzed with Image J 1.48v software.

Tissue remodeling was analyzed by Sirius Red staining. Serial sections were deparaffinized and immersed for 30 minutes in Sirius Red solution. This solution contains Sirius Red (Direct Red 80, Sigma) in 0.1% aqueous solution of picric acid. Then, samples were washed, dehydrated in three changes of ethanol, cleared in xylene and mounted in DPX. Cardiac hypertrophy was analyzed by H-E following the protocol described in section 5.4. For quantification, 12 images of peri-infarcted zone were scanned (Aperio CS2, Leica) from serial heart sections and analyzed with Image J 1.48v software.

11. STATISTICAL ANALYSIS

Normal distribution was assessed using the Shapiro-Wilk test and D'agostino-Pearson test. Comparisons among groups were performed using one-way ANOVA or mixed factorial ANOVA (with within- and between-subjects factors) tests followed by simple comparisons (contrasts). Comparisons between two groups were performed using Student's t test followed by Mann-Whitney test. Graphic representations were performed using Prism GraphPad 6.01 software and statistical analyses were performed using Stata 12 for Windows software (College Station, TX: StataCorp LP.). Differences were considered statistically significant when $P < 0.05$ *(*) or* $P < 0.01$ *(**).*

Results

1. BIODISTRIBUTION AND TRANSDUCTION EFFICIENCY STUDY OF AAV9 VECTORS

The general objective of this study has been to develop an optimal delivery system for miRNAs overexpression in heart. Gene therapy, and specifically AAV, was considered as an optimal approach to allow a controlled, localized and sustained transgene expression. In this context, the biodistribution of AAV9 vector under different experimental conditions was first analyzed. AAV9 efficacy and specificity was assessed, taking into account key considerations such as the use of different promoters, different routes of delivery and animal models, comparing healthy and ischemic heart mice. Thus, their use as a cardiac delivery vector for therapeutic applications was carefully evaluated.

1.1 AAV-PLASMID GENERATION AND CHARACTERIZATION

First, specific plasmids for following AAV production were generated by standard molecular biology techniques as previously described. These vectors were designed with a ubiquitous (EF1α) or a specific promoter for CMs (TnT). For biodistribution studies, these vectors were generated expressing the Luciferase gene under these promoters. In order to validate their expression and specificity, plasmids were tested *in vitro* in 3T3 fibroblast and HL1 cardiac cell lines and their tissue-specific expression was evaluated by luminometry. Luciferase expression was detected in both cell lines when the ubiquitous promoter was used. Furthermore, cardiac cells showed high luciferase expression levels when transfected with the vector having the TnT promoter (**Figure 16A**), whereas almost no expression was detected in the fibroblast cell line (**Figure 16B**). This data validates the plasmid constructions and confirms the cell-specific expression of pAAV-TnT- plasmid for future *in vivo* studies.

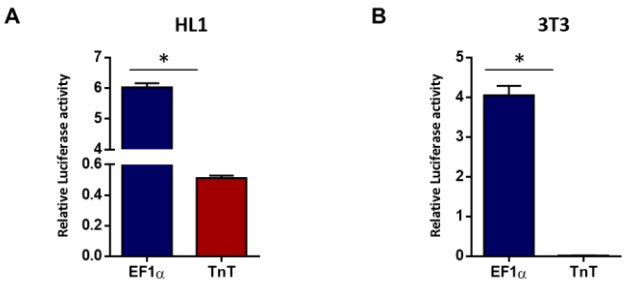

Figure 16. Luciferase activity in HL1 (A) and 3T3 cells (B) transfected with AAV-plasmids carrying ubiquitous or cardiac-specific promoters. *Relative activity of firefly luciferase expression was standardized to a transfection control, using Renilla luciferase plasmid. Data are represented as average ± SD values. Significant differences are indicated as *P < 0.05.*

1.2 HEART SPECIFIC EXPRESSION OF AAV SEROTYPE 9 IN MOUSE

AAV9 has been described as the most cardiotropic serotype, and therefore the most efficient vector for myocardial transduction [366]–[368], so it was selected as the delivery vector to perform our study. AAV9 vectors expressing luciferase reporter gene under the control of EF1α or TnT promoters were generated. Both vectors AAV9-EF1α-Luc and AAV9-TnT-Luc were delivered to mice by two different administration routes and evaluated in healthy as well as in a pathological context. For that aim, healthy (Co) and acutely infarcted (MI) mice received the AAV9-EF1α -Luc or AAV9-TnT-Luc by intravenous (IV) or intramyocardial (Imyo) injections and luciferase expression was analyzed at day 14 post-injection (**Figure 17**).

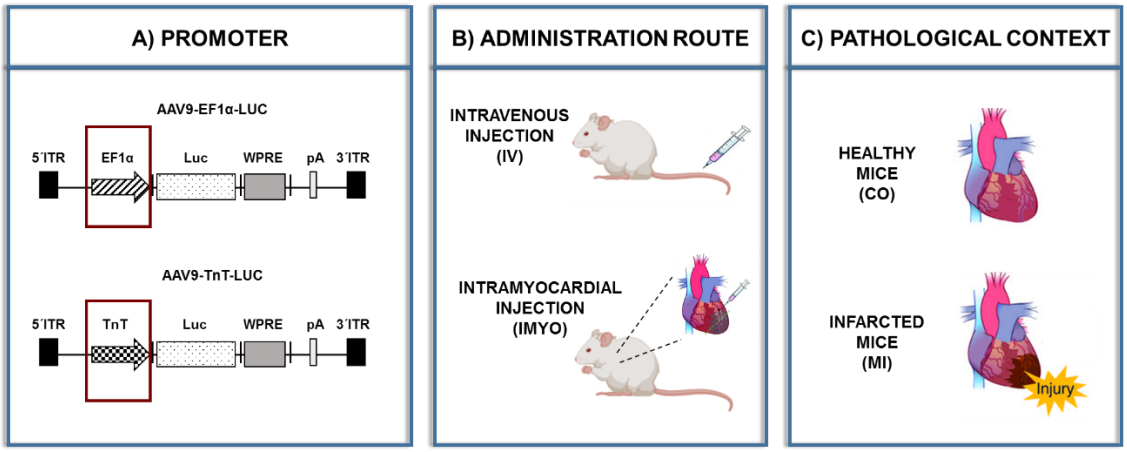

Figure 17. Schematic representation of AAV9-EF1α-Luc and AAV9-TnT-Luc vectors expressing luciferase (Luc) from EF1α or TnT promoters, the WPRE and the SV40 late poly(A) signal (pA), flanked by the AAV ITRs (A). AAVs were assessed in healthy (CO) and acutely infarcted (MI) mice (B). AAVs were intravenously (IV) or intramyocardially (Imyo) delivered (C).

Luciferase expression was analyzed in heart and compared with liver, which is considered the main target organ for AAV vectors. Significant differences were found in organ transduction efficiency, depending on the promoter and the administration route. A modest luciferase expression was found in heart (**Figure 18A**) when the ubiquitous EF1α promoter was used. This expression was significantly higher after intramyocardial delivery than after intravenous delivery in both healthy and infarcted mice. However, when the luciferase gene was driven under the control of the TnT promoter, cardiac expression was greatly increased in comparison to the construct with the EF1α promoter. Also, in this context, intramyocardial injection significantly increased the transduction efficiency of the vector in comparison to the systemic administration and no differences were observed between control and infarcted

animals. Interestingly, these analyses revealed that independently of the promoter, MI significantly increased luciferase expression levels (~5-10 fold higher) after intravenous administration in comparison to the healthy animals.

When the livers of these mice were analyzed, as expected, high luciferase expression levels were observed when the ubiquitous promoter was used (**Figure 18B**). In this case, intramyocardial injection slightly reduced hepatic luciferase expression in comparison with the intravenous delivery. Tissue specific expression of TnT promoter was confirmed whereas minimal liver expression was found when this vector was used, being the expression levels more than 100 fold lower.

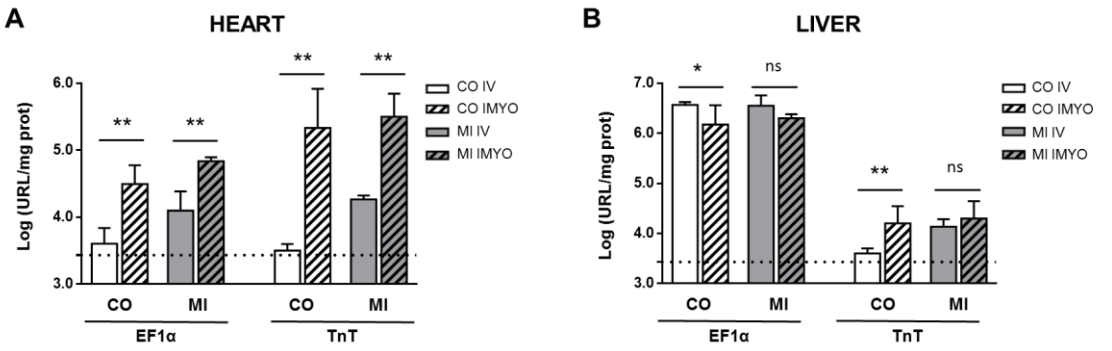

Figure 18. Heart specific expression of AAV serotype 9 in mouse. *Luciferase activities in protein extracts of Hearts* ***(A)*** *and Livers* ***(B)*** *from mice that received 1.0x10^{10} vg of AAV9-EF1α-Luc (EF1α) or AAV9-TnT-Luc (TnT) by intravenous (IV) or intramyocardial injection (Imyo), in healthy (CO) or myocardial infarcted (MI) mice (n=3-4 mice per group). Luciferase activity is expressed as log of relative light units (RLU) per mg of tissue. The dashed line shows the luciferase expression in non-AAV injected-mice (control). All data are* represented *as mean ± SD. Significant differences are indicated as *P < 0.05; ** P < 0.01.*

1.3 BIODISTRIBUTION AND TIME-COURSE EXPRESSION OF AAV9-EF1α

Since we confirmed in our animal model the intramyocardial administration as the most efficient for AAV-heart transduction, independently of the promoter and the pathological context, we selected this method for the following studies.

In order to evaluate the stability and transgene expression, a single dose of 1.0x10^{10} vg of AAV9-EF1α-Luc was intramyocardially administered in healthy and infarcted animals. Luciferase expression was determined by bioluminiscence *in vivo* and *ex vivo* and then quantified in organ extracts at different time points, starting at day 1 and finishing 60 days after vector injection. In healthy and infarcted mice, luciferase expression increased in a time-dependent manner, both in the liver and in the heart, being detectable at day 1, and reaching maximum

levels between day 3 to 7, levels that were maintained for up to 60 days (**Figure 19A, B**). Furthermore, we observed that MI did not affect the sustainability of transgene expression, but as previously described, MI slightly reduced transgene expression in the liver and greatly increased transgene expression in the heart (**Figure 19A, B**).

In vivo bioluminescence images in the whole body of mice corroborated that when the EF1α-promoter was used, luciferase expression was significantly higher in the liver. Furthermore, *ex vivo* imaging in different organs including heart, liver, spleen, intestine, testis, kidney, brain, lung, quadriceps and gastrocnemius muscles, confirmed that luciferase expression was accumulated in the liver, whereas no expression was found in other major organs when it was analyzed by bioluminescence imaging (**Figure 19C, D**).

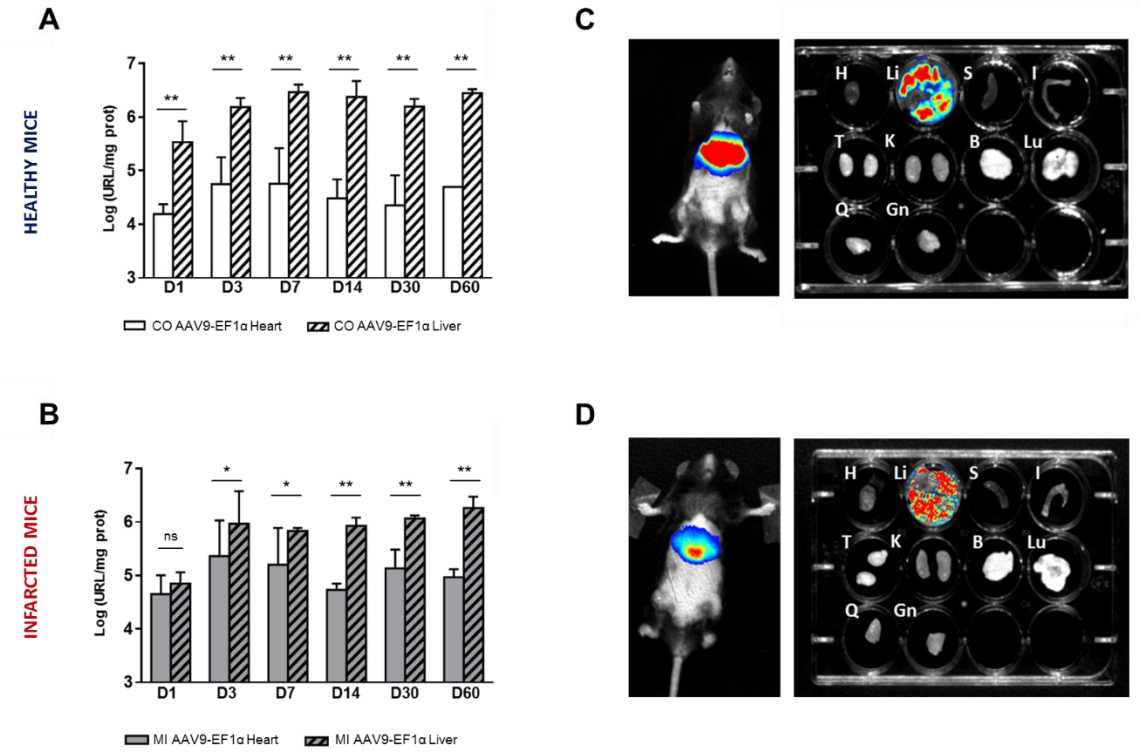

Figure 19. Biodistribution and time-course expression of AAV9-EF1α-Luc. *Luciferase activity in healthy* ***(A)*** *and myocardial-infarcted mice* ***(B)*** *intramyocardially injected with 1.0x10^{10} vg of AAV9-EF1α-Luc (n=2-3 mice per group). Heart and liver organs were collected at different time points for ex vivo luciferase assay. Luciferase activity is expressed as log of relative light units (RLU) per mg tissue. Representative in vivo and ex vivo bioluminescence images from healthy and infarcted mice, respectively at day 60 after vector administration* ***(C, D).*** *((H): Heart, (Li): Liver, (S): Spleen, (I): Intestine, (T): Testis, (K): Kidney, (B): Brain, (Lu): Lung, (Q): Quadriceps, (Gn): Gastrocnemius). All data are represented as mean ± SD. Significant differences are indicated as *P < 0.05; ** P < 0.01.*

Next, we examined the copy numbers of AAV genomes in these organs by quantitative PCR analysis. In healthy animals, the AAV-EF1α vector robustly transduced the liver, showing significant higher viral genome copies of this vector in liver than in hearts (**Figure 20A**). Importantly, similar results were found in the infarcted animals (**Figure 20B**). Moreover, the number of genomes were stabilized at day 7 in both liver and heart. In the liver of healthy animals, AAV genome copies were higher than in the infarcted mice, in clear correlation with luciferase expression levels. However, the heart showed that in contrast with the luciferase expression values, vector genomes were lower in the infarcted than in the healthy mice (**Figure 20A, B**). Thus, the lower expression levels detected in the liver after MI can be explained by a reduction of vector genomes. However, the higher expression levels observed in the heart are not associated with a higher retention of vector genomes, indicating that the transcription of AAV genomes in the infarcted heart is higher than in a healthy organ. When vector genome copies were quantified in the other major organs, minimal number of genomes were found (**Figure 20C, D**).

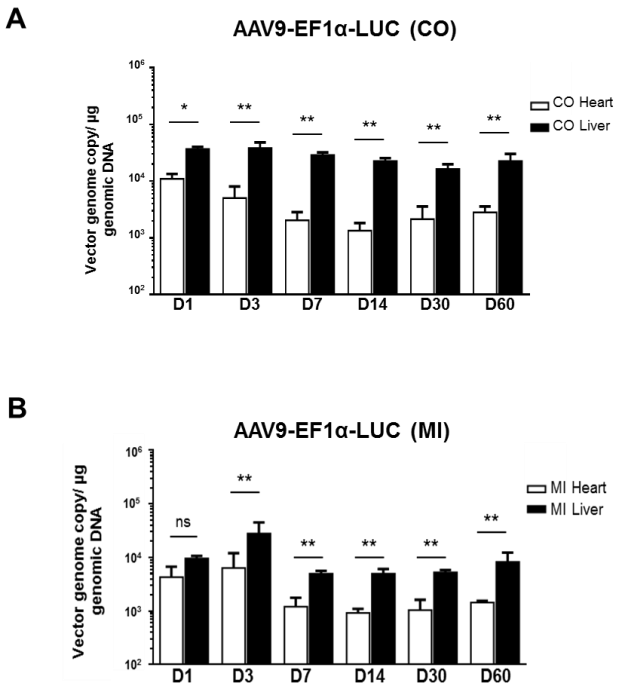

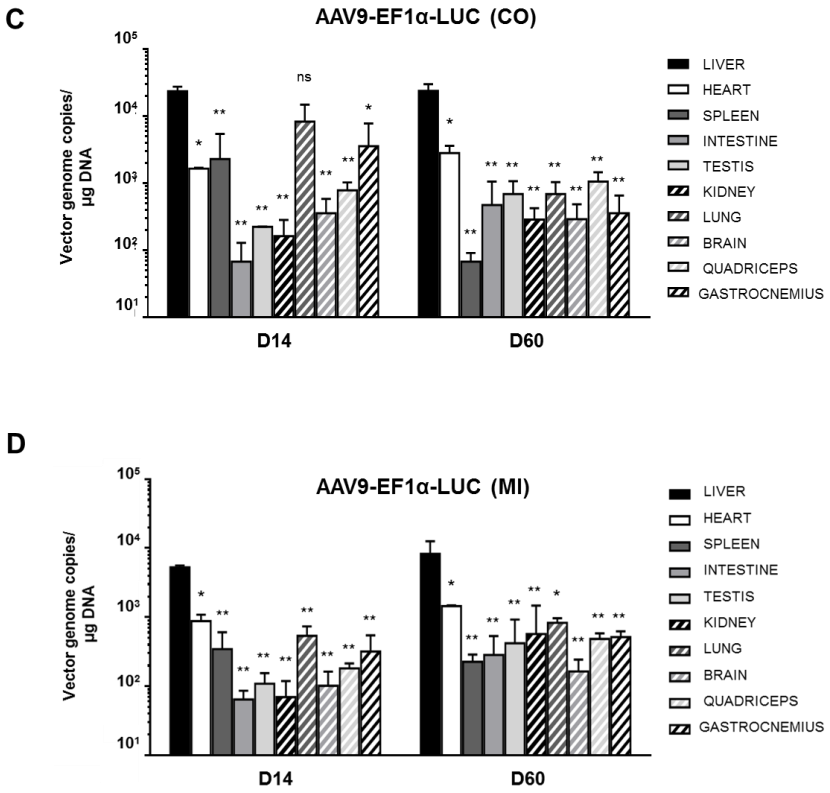

Figure 20. Genomic Biodistribution of AAV9-EF1α-Luc. *Quantification of viral genome copies by qPCR in hearts and livers from healthy* ***(A)*** *or infarcted* ***(B)*** *mice, at different time-points. Quantification of vector genome copies by qPCR in other major organs from healthy* ***(C)*** *or infarcted* ***(D)*** *mice, 14 and 60 days after intramyocardial injection (n=2-3 per group). All data are represented as mean ± SD. Significant differences compared to liver are indicated as *P < 0.05; ** P < 0.01.*

1.4 BIODISTRIBUTION AND TIME-COURSE EXPRESSION OF AAV9-TnT

As previously reported for AAV9-EF1α–Luc, AAV9-TnT-Luc sustained expression and biodistribution was assessed. In a similar way, AAV9-TnT-Luc (one dose of $1.0x10^{11}$ vg) was intramyocardially injected in healthy and infarcted mice and the time-course expression was evaluated. A similar time-course expression was observed since viral expression was detectable by day 1 and reached a peak by day 3-7 that was stable for at least 60 days. Furthermore, luciferase expression was clearly detected in the heart by using the cardiac promoter (**Figure 21A**) although in this case heart luciferase levels were moderately reduced by heart damage (**Figure 21B**). TnT-derived luciferase expression was also detected in the liver but with a minor intensity in comparison with the ubiquitous promoter. Regarding *in vivo* bioluminescence analysis, the expression of luciferase was found confined to the left side of the thoracic cavity. Furthermore, when different organs were analyzed, luciferase expression was clearly detected in the heart, with minimal expression in the liver, and no expression found in other major organs (**Figure 21C, D**).

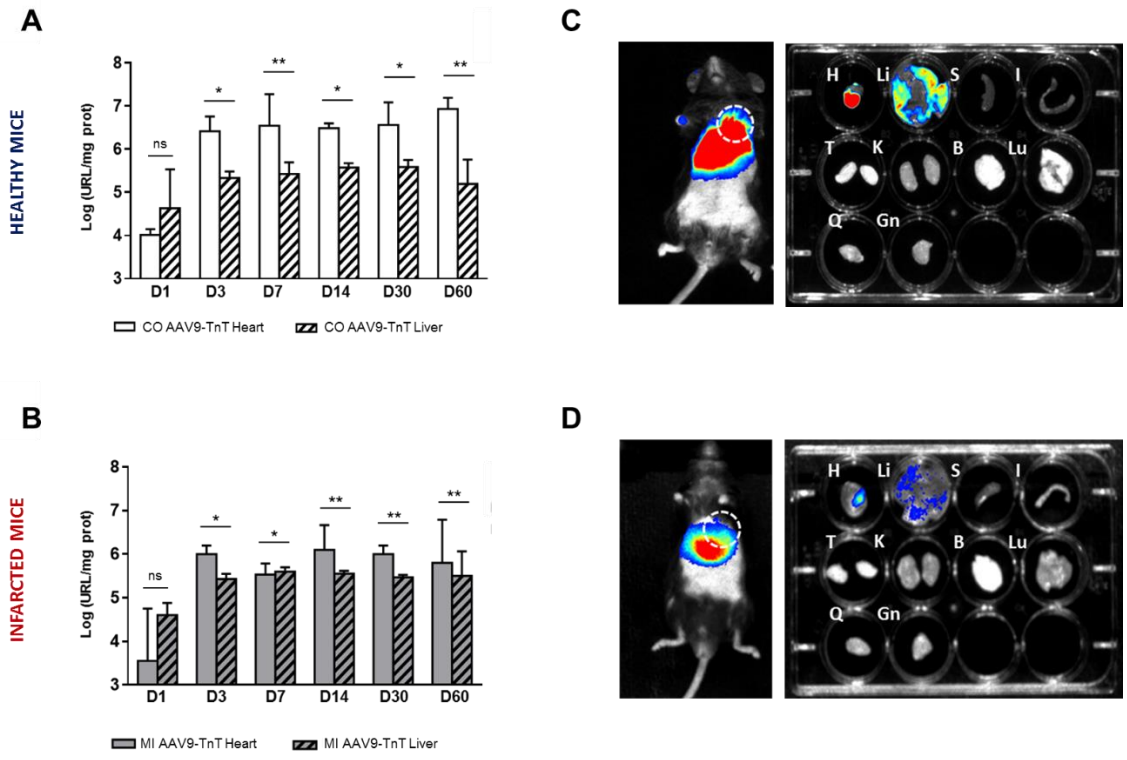

Figure 21. Biodistribution and time-course expression of AAV9-TnT-Luc. *Time course of luciferase activities in protein extracts from heart and liver from healthy* ***(A)*** *and myocardial-infarcted mice* ***(B)*** *intramyocardially injected with 1.0x10^{11} vg of AAV9-TnT-Luc (n=2-3 mice per group). Luciferase activity is expressed as log of relative light units (RLU) per mg of tissue. In vivo and ex vivo representative bioluminiscence images from various tissues from healthy and infarcted mice, respectively* ***(C, D).*** *((H): Heart, (Li): Liver, (S): Spleen, (I): Intestine, (T): Testis, (K): Kidney, (B): Brain, (Lu): Lung, (Q): Quadriceps, (Gn): Gastrocnemius) 60 days after vector administration. Intensity images have been modified to put in evidence the localized expression. Circles indicate heart located expression. All data are represented as mean ± SD. Significant differences are indicated as *P < 0.05; ** P < 0.01.*

Not only the expression but also the AAV9 genome copy numbers were analyzed in the selected organs by qPCR. Like mice injected with AAV9-EF1α –Luc, mice injected with the AAV9-TnT-Luc vector showed significant higher transduction in the liver than in the heart. Importantly, and primarily in infarcted animals, the copy number of AAV9 genome present in heart was lower over time (**Figure 22A, B**). Similar to AAV9-EF1α-Luc, minimal viral genome copies were found when other major organs were analyzed (**Figure 22C, D**).

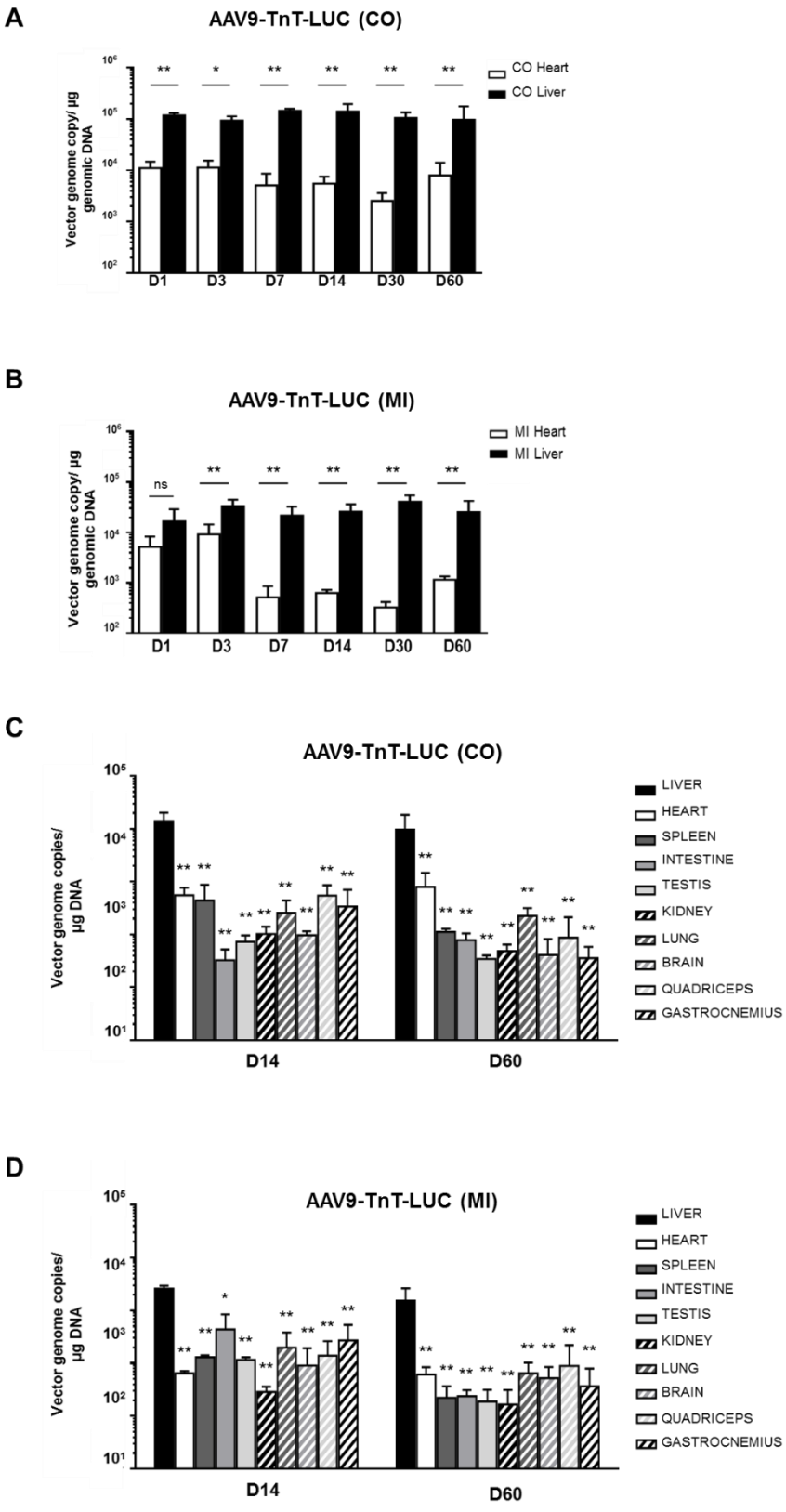

Figure 22. Genomic Biodistribution of AAV9-TnT-Luc. *Quantification of viral genome copies by qPCR in hearts and livers from healthy* ***(A)*** *or infarcted* ***(B)*** *mice, at different time-points. Quantification of vector genome copies by qPCR in other major organs from healthy* ***(C)*** *or infarcted* ***(D)*** *mice, 14 and 60 days after intramyocardial injection (n=2-3 per group). All data are represented as mean ± SD. Significant differences compared to liver are indicated as *P < 0.05; ** P < 0.01.*

This data clearly shows that despite the reported serotype 9 cardiotropism, AAV9 mainly transduces the liver. The highest viral genome accumulation was observed in liver and, as expected, independently of the promoter used. Furthermore, we observed that MI increased transgene expression in the heart independently of the promoter and the route of administration. Interestingly, once again, this increase was not associated with a major retention of AAV genomes in the heart but with a higher production rate of protein per AAV genome (**Figure 23**).

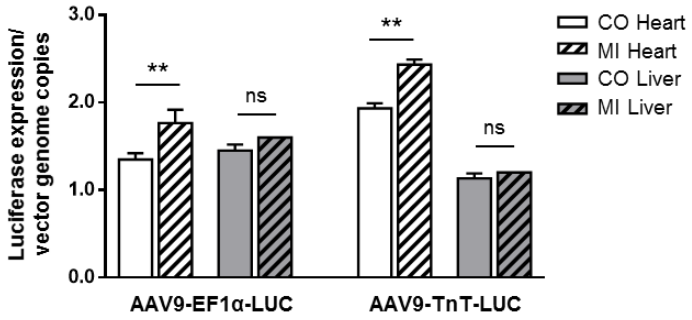

Figure 23. Biodistribution of AAV9-TnT. *Rate of luciferase expression per AAV genome copies 30 days after injection.All data are represented as mean ± SD. Significant differences are indicated as *P < 0.05; ** P < 0.01.*

1.5 AAV9-TnT CELL SPECIFIC-EXPRESSION

In order to confirm AAV9 tissue distribution, specificity and long-term expression, the luciferase reporter gene was replaced by the green-fluorescence-protein (GFP) reporter gene. Tissues fluorescence transgene expression was analyzed 60 days after intramyocardial vector injection in healthy mice. A weak GFP expression was observed in hearts when the AAV9-EF1α was used. By contrast, robust GFP expression was found in the heart of mice that received the AAV9-TnT vector. Thus, only a few positive CMs were found when the ubiquitous promoter was used, whereas an extensive GFP+ area was detected in the heart when the cardiac promoter was used. Moreover, GFP specific expression in cardiac cells was confirmed by GFP and cardiac α-actin co-expression (**Figure 24A**). On the other hand, high GFP expression was found in the liver tissue when mice were injected with AAV9-EF1α vector. These mice showed most of the hepatocytes positive for GFP, while in the mice injected with the vector carrying the TnT promoter, no GFP+ hepatocytes were found (**Figure 24B**).

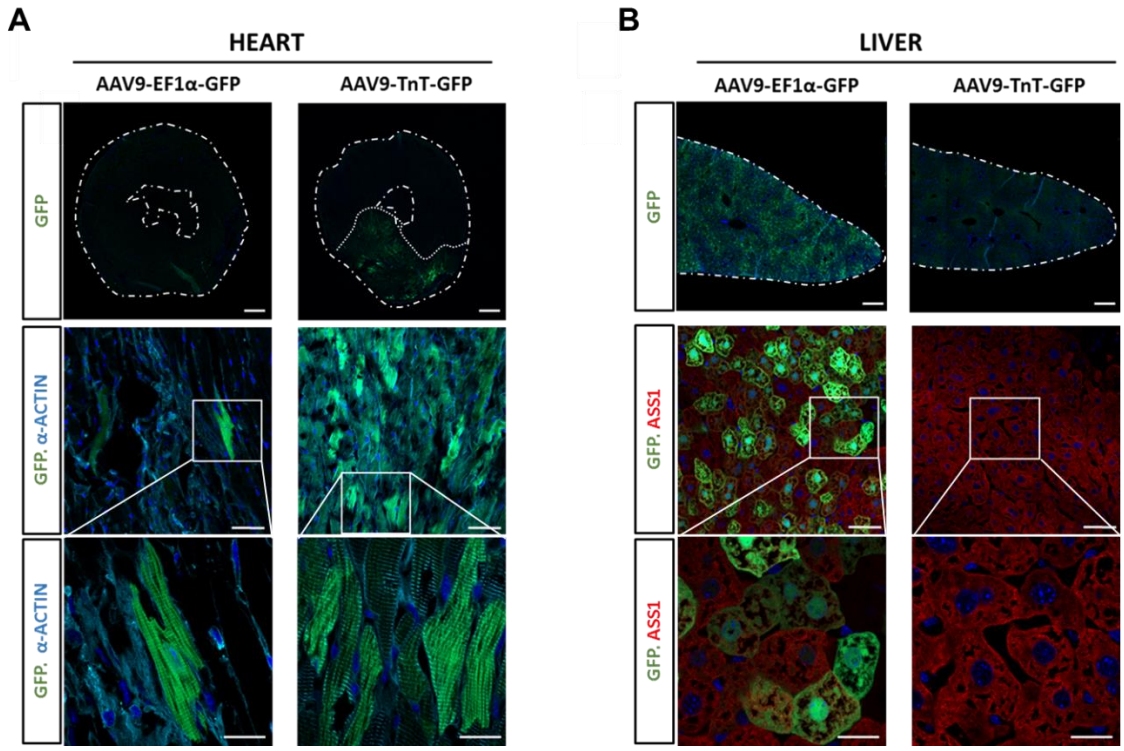

Figure 24. Cell specific-expression. *Histological analysis in hearts* ***(A)*** *and livers* ***(B)****, 60 days after AAV intramyocardial injection (1.0 x 10^{10} vg) (n=2 per group). CMs were labeled for cardiac alpha-actin (light blue), and hepatocytes for argininosuccinate synthetase (ASS-1) (red). Nuclei were stained with Hoechst (dark blue). Limits of the organs and GFP^+ area are delimited by dashed lines. Scale bars: 500 µm (top); 50 µm (middle); 20 µm (below).*

1.6 SAFETY AND TOXICITY EVALUATION AFTER AAV9 ADMINISTRATION

During the biodistribution studies, several biochemical parameters were measured in blood in order to evaluate potential AAV toxicity in liver and heart. Hepatic and cardiac function were determined at 3, 14, 30 and 60 days after virus administration. No significant increase in the plasma levels of the markers for heart toxicity, lactate dehydrogenase (LDH) and creatine kinase (CKMB) together with the markers for liver toxicity, alkaline phosphatase (ALP) and alanine aminotransferase (ALT) were detected at any time-point in the biodistribution experimental groups, confirming that AAV9 transgene expression did not cause any tissue damage (**Table 8**).

Table 8. Safety and toxicity evaluation after AAV9 administration

Post-Injection DAY	GROUP	ENZYME			
		LDH (U/L)	CK (U/L)	ALP (U/L)	ALT (U/L)
3d	(CO) AAV-EF1a-Luc	622 ± 111	257 ± 21	38 ± 0	13 ± 1
	(MI) AAV-EF1a-Luc	389 ± 46	270 ± 86	48 ± 4	15 ± 3
	(CO) AAV-TnT-Luc	321 ± 83	287 ± 29	33 ± 1	12 ± 1
	(MI) AAV-TnT-Luc	520 ± 344	495 ± 40	40 ± 9	38 ± 22
14d	(CO) AAV-EF1a-Luc	285 ± 37	234 ± 125	75 ± 18	11 ± 3
	(MI) AAV-EF1a-Luc	357 ± 91	237 ± 24	85 ± 15	14 ± 7
	(CO) AAV-TnT-Luc	312 ± 68	470 ± 72	96 ± 20	13 ± 4
	(MI) AAV-TnT-Luc	497 ± 122	259 ± 91	80 ± 2	34 ± 27
30d	(CO) AAV-EF1a-Luc	425 ± 191	233 ± 112	59 ± 5	23 ± 6
	(MI) AAV-EF1a-Luc	435 ± 216	187 ± 57	72 ± 14	16 ± 10
	(CO) AAV-TnT-Luc	389 ± 184	274 ± 128	62 ± 15	14 ± 3
	(MI) AAV-TnT-Luc	375 ± 69	198 ± 8	68 ± 8	35 ± 14
60d	(CO) AAV-EF1a-Luc	421 ± 165	217 ± 27	49 ± 12	23 ± 9
	(MI) AAV-EF1a-Luc	334 ± 49	215 ± 42	49 ± 6	19 ± 3
	(CO) AAV-TnT-Luc	452 ± 159	170 ± 47	75 ± 38	22 ± 17
	(MI) AAV-TnT-Luc	253 ± 65	132 ± 37	56 ± 8	26 ± 3
	Control (No AAV)	405 ± 32	453 ± 49	100 ± 23	27 ± 16

** Mean values of the enzymes Lactate Dehydrogenase (LDH), Creatine Kinase (CK), Alkaline Phosphatase (ALP), Aspartate Aminotransferase (AST) and Alanine Aminotransferase (ALT) from the different intramyocardial administration groups 3, 14, 30 and 60 days post-injection. All data are represented as mean ± SD. Non-significant increase were found in the experimental groups in comparison with the control group (n=2-3) (P > 0.05).*

Histologically, vector administration did not provoke any obvious alteration in neither heart nor liver. H&E staining did not show any obvious presence of inflammatory cells, and no noticeable anatomopathological alterations neither in heart nor in liver (**Figure 25**).

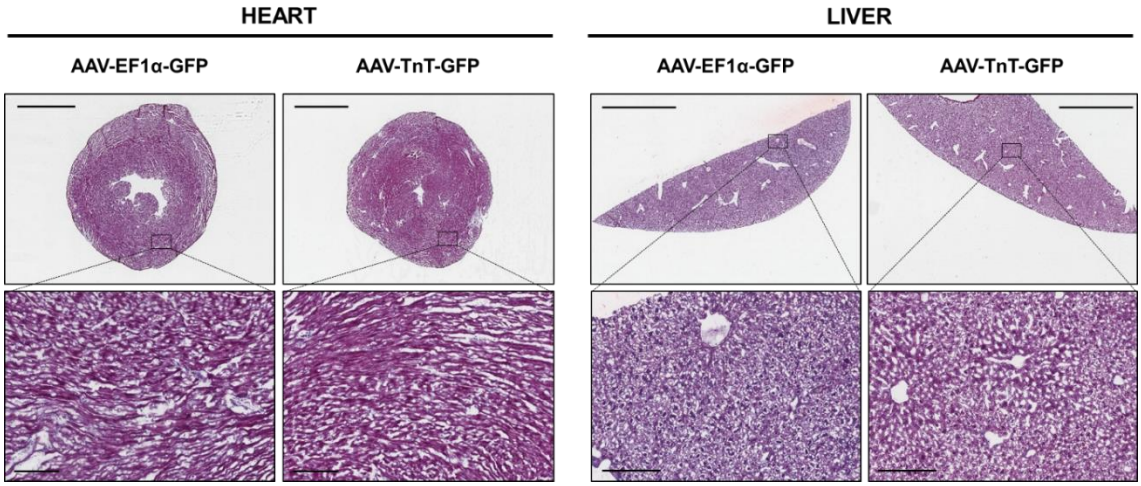

Figure 25. H&E histological analysis of Heart and Liver tissues. *Infiltration of inflammatory cells and/or morphological changes of Heart* ***(A)*** *and Liver* ***(B)*** *were not observed 60 days after intramyocardial injection of AAV9-EF1α-GFP and AAV9-TnT-GFP (n=2 per group). Scale bars: 2 mm (top); 200 µm (below).*

2. SPECIFIC miRNA REPERTOIRE OF CARDIAC EXOSOMAL COMPARTMENT

Aiming to define the specific CPC miRNA repertoire, an RNA-seq was conducted as a first approach to compare the whole miRNA expression profile of the CPC with their derived exosomes.

2.1 CPC EXOSOMES CHARACTERIZATION

CPC were purified and maintained following the protocol described for the CAREMI clinical trial and characterized by flow cytometry for positive expression of SSEA1, CD166, CD90 and CD105, and negative expression of protein tyrosine phosphatase, CD45 and CD34 [349]. Exosomes were isolated by a series of ultracentrifugation steps [350], and their identity was analyzed. Purified particles were studied by transmission electron microscopy where a typical ultrastructure was found (**Figure 26A**). Furthermore, nanoparticle tracking analysis of the purified exosomes revealed high levels of purity with a mean diameter of 90-125nm (**Figure 26B**). Additionally, purified exosomes demonstrated to express typical exosomal markers such as CD63, CD9, HSP70 and CD81, when analyzed by western blot (**Figure 26C**).

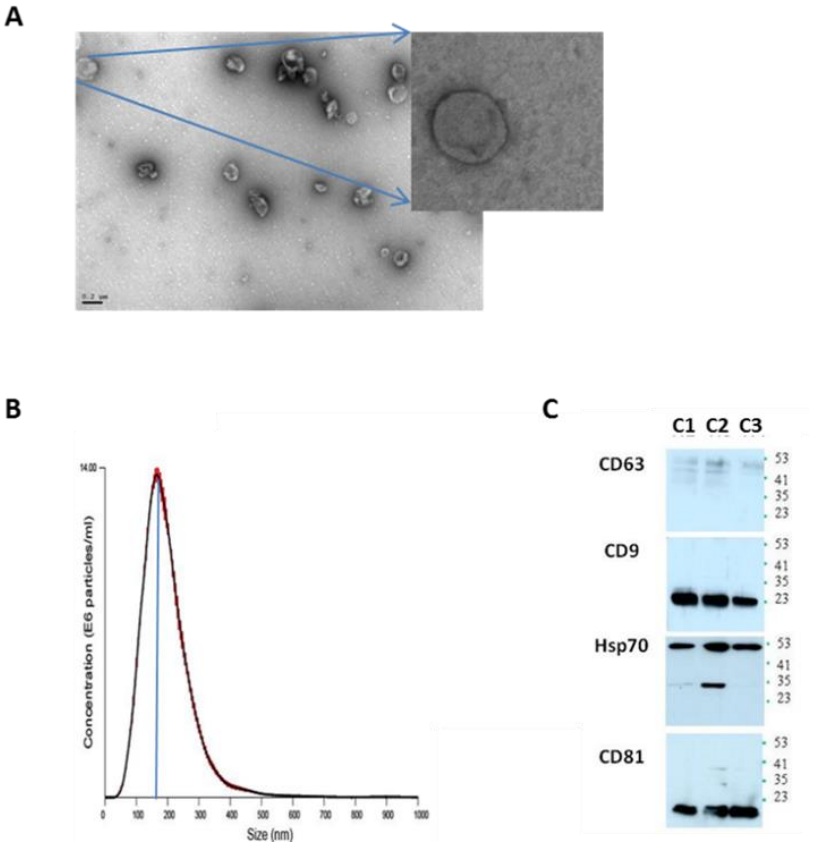

***Figure 26. Exosome purified fraction characterization**. Exosomes were isolated by serial ultracentrifugations from supernatants of three independent CPC human donors (C1, C2 and C3). Transmission electron micrographs showing exosomes secreted by human CPC in culture. Scale bar: 0.2 µm **(A)**. Nanoparticle Tracking Analysis (NTA) of purified exosomes **(B)**. CD63, CD9, Hsp70 and CD81 western-blot for CPC purified exosomes **(C)**.*

2.2 COMPARATIVE ANALYSIS OF CPC EXOSOMAL COMPARTMENT BY RNA-seq

In order to study the miRNA repertoire of CPC and their exosomal compartment, a comparative analysis by RNA-seq was conducted. Initially, the expression of 391 miRNAs was detected in the whole miRNA transcription profile of CPC. On the other hand, when the analysis was focused on the CPC exosomal fraction, a total of 350 different miRNAs were detected. When overlapping both miRNA repertoires, 292 miRNAs were common to both cellular and exosomal CPC compartments, whereas 99 miRNAs were preferentially found in the whole cell fraction and 58 in the exosomal compartment (**Figure 27A, B**). The differential exosomal/cellular expression profile was further evaluated for the most representative exosomal-miRNAs. miR-2110, miR-1911-3p, miR-199a-3p and miR-411-5p were found in high amounts in CPC-exosomes, showing miR-2110 and miR-1911-3p the ones with higher exosomal/cellular ratio (25.5 x 10^3 and 24.0 x 10^3, respectively). Both miRNAs were nearly specific for the exosome compartment (**Figure 27C**).

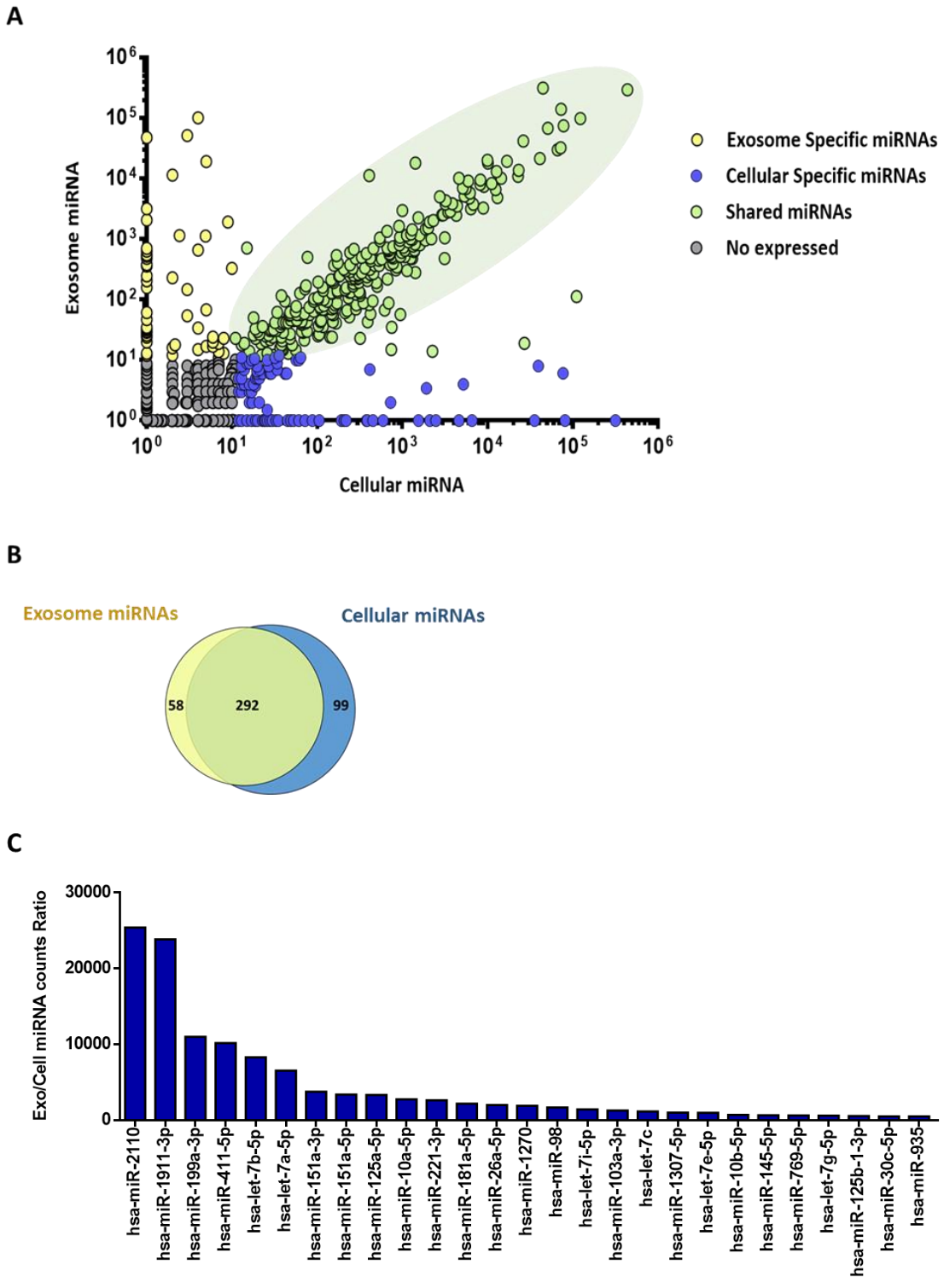

***Figure 27*. Comparative analysis of miRNA repertoire in the cellular and exosomal compartments of CPC by RNA-seq.** Correlation plot showing a positive correlation between miRNAs found in the cell and exosomal compartment. miRNAs expression was considered for ≥ 10 counts/sample **(B)**. Venn Diagram highlighting the number of miRNAs preferentially found in the cell fraction (blue), in the exosomal compartment (yellow) and in both (green) **(B).** Differential exosomal/cellular expression profile for the most representative miRNAs detected in the CPC exosomal compartment **(C).**

To gain specificity in the association of CPC exosomal miRNAs with a cellular type (CPC) or cell derived compartment (exosomes), exosomal CPC miRNA repertoire was challenged with mesenchymal stem cell (MSC) and human dermal fibroblast (HDF) exosomes. miRNA transcriptome analysis through RNA-seq rendered a total of 481 expressed miRNAs in these cell types-derived exosomes. Both unsupervised hierarchical clustering (**Figure 28A**) and the Principal Component Analysis (PCA) (**Figure 28B**) neatly distinguished the three cell populations, confirming that the miRNA transcriptome of CPC, MSC and HDF cell lineages-exosomes clearly differs from each other. The comparative analysis of the miRNA exosomal compartment for the three populations defined 80 miRNAs that were differentially expressed between CPC and MSC and 88 exosomal miRNAs differentially expressed between CSC and HDF. Interestingly, 40 exosomal miRNAs were commonly differentially expressed between CPC and both MSC/HDF (**Figure 28C**).

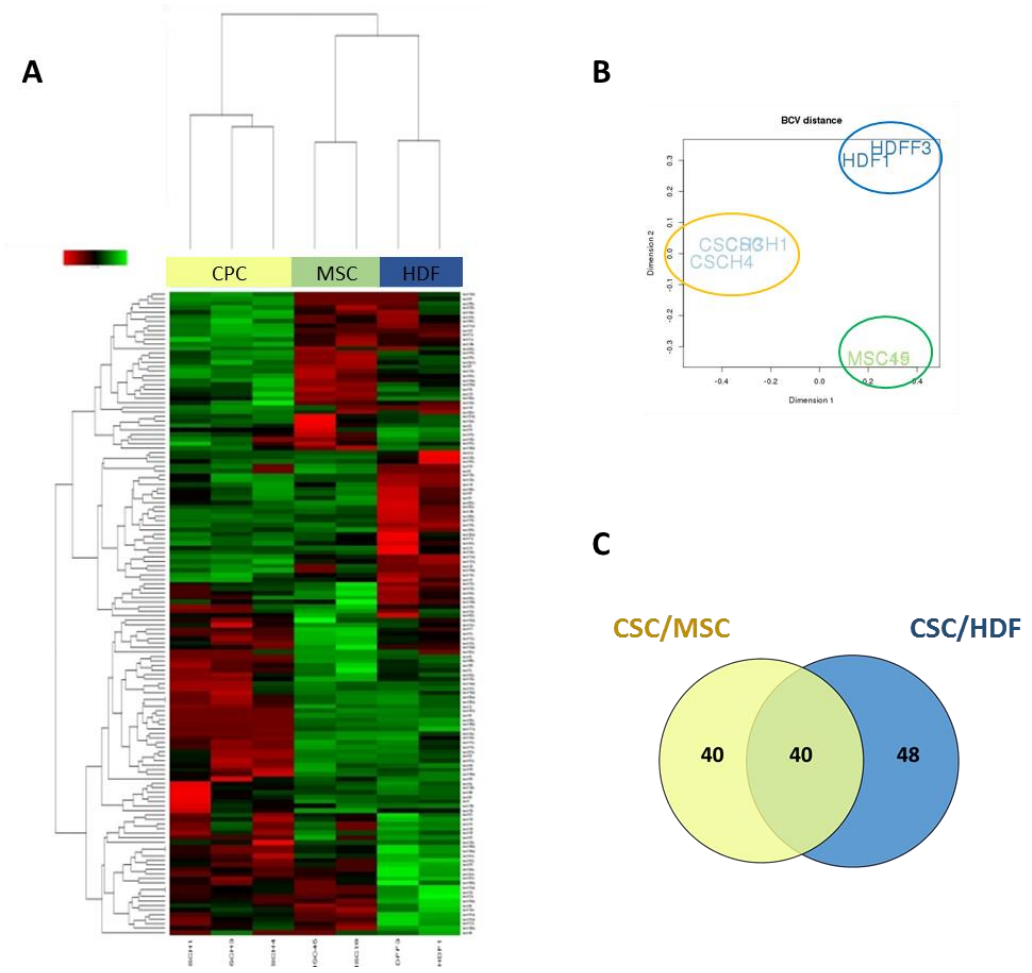

***Figure 28*. CPC exosomal fraction compared with MSC and HDF exosomes by RNA-seq.** Normalized heat map analysis of miRNA sequences **(A)** and clustering analysis **(B)** confirms that CPC, MSC and HDF exosomal compartments are distant and clearly represent differentiated clusters. Venn diagram shows the number of miRNAs differentially expressed in CPC *vs.* MSC (yellow), in CPC *vs.* HDF (blue) and commonly differentially expressed between CPC and both MSC/HDF (green) **(C)**.

Furthermore, among these 40 exosomal miRNAs, 35% (14 miRNAs) were found up-regulated in CPC exosomes (**Figure 29A**), whereas 65% (26 miRNAs) were found down-regulated in CPC exosomes in comparison with both MSC/HDF exosomes (**Figure 29B**). miR-935 was found as the most significantly up-regulated molecule with a ratio between CPC and MSC/HDF of 10.2 and 7.1 log2FC, respectively. The most down-regulated miRNAs were miR-196b-5p, miR-10b-3p and miR-303 with a ratio between CPC and MSC/HDF of -9.8/-11.5, -9.4/-8.6 and -8.7/-6 log2FC, respectively.

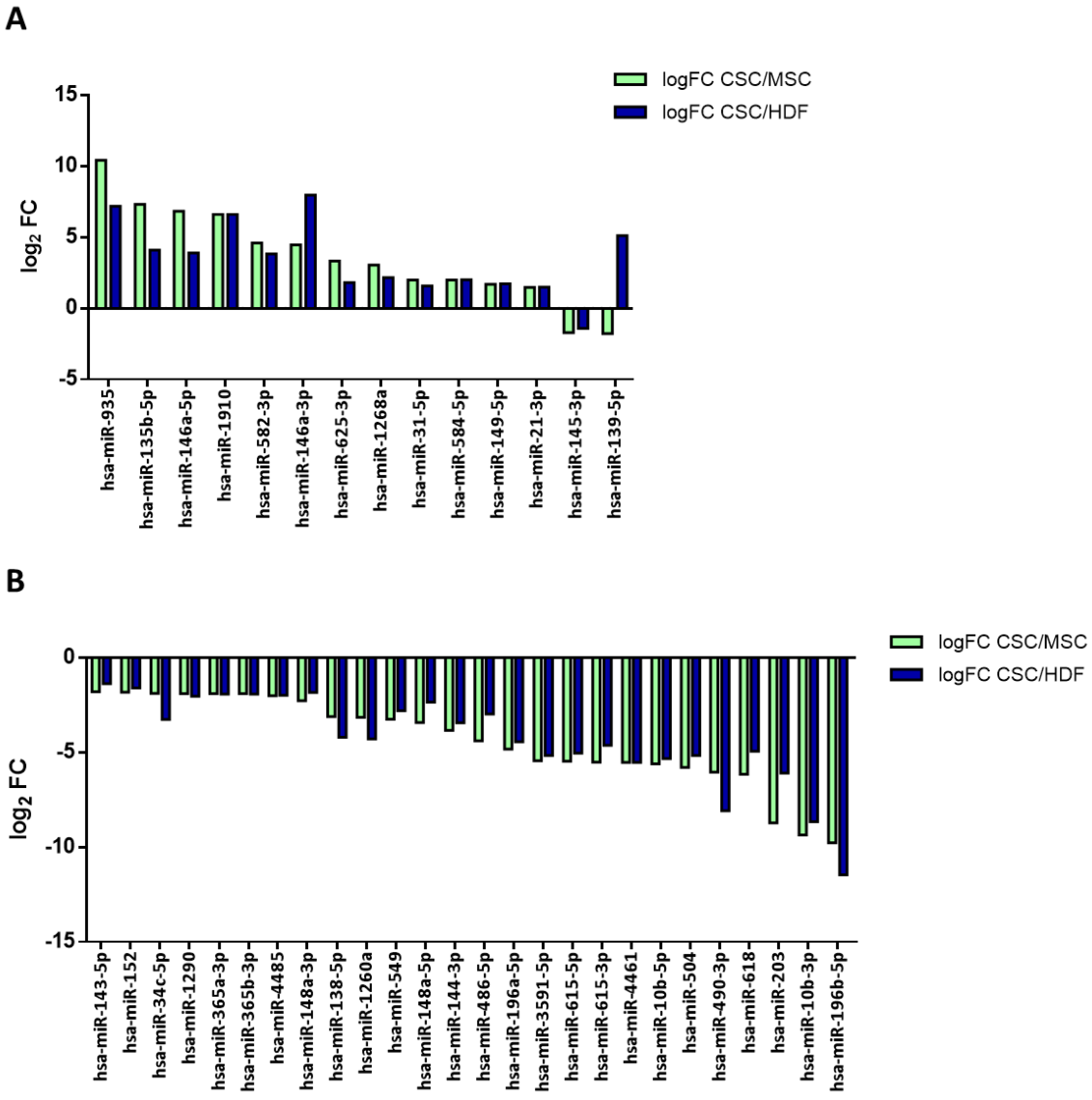

***Figure 29*. Differential expression of specific CPC-miRNAs *vs.* MSC- and HDF-miRNAs.** Plot (log_2 FC) of miRNAs up-regulated **(A)** or down-regulated **(B)** in CPC *vs.* MSC (green bars) and CPC *vs.* HDF (blue bars).

The expression and localization of the most up-regulated miRNAs in CPC *vs.* MSC/HDF exosomes (**Figure 29A**) were further studied. Regarding to their expression in the whole transcriptome of CPC, miR-146a-5p and miR-31-5p presented high expression levels followed by far by miR-935, miR-584-5p and miR-625-3p. miR-135b-5p was at the lowest level expression in the whole cell. On the other hand, their preferential localization was assessed by analyzing the level of expression in the exosomal compartment compared with the whole cell (Δ exo/cell). miR-135b-5p, miR-146a-3p and miR-625-3p were preferentially found in the exosomal compartment with a ratio of 2.0, 3.4 and 7.7, respectively. miR-935 and miR-584 were found expressed in a similar proportion and by contrast, miR-31-5p showed higher expression in the whole cell. Interestingly, miR-1268 was only found in the exosomal compartment (**Figure 30**).

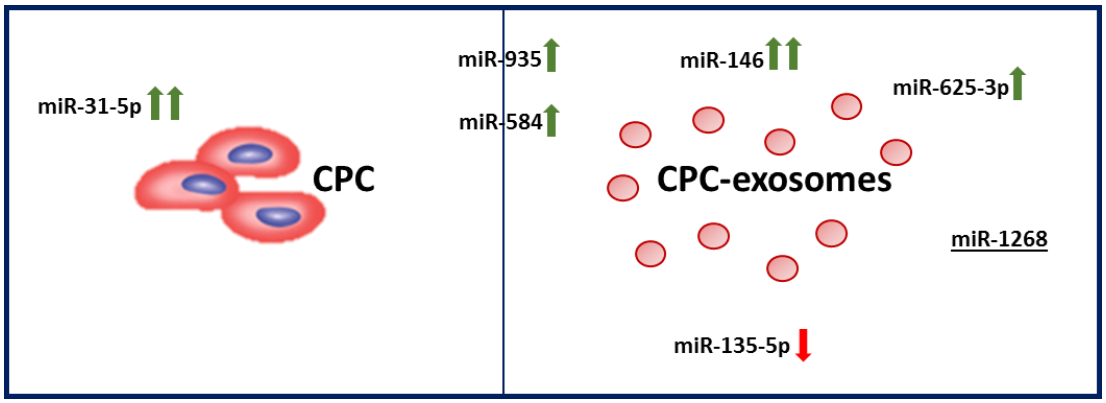

Figure 30. **Schematic representation of the expression and localization of the most representative CPC-derived exosomal enriched miRNAs.** Arrows represent the expression miRNAs levels in the whole CPC cell. Underline miRNA is considered specific for this compartment.

3. FUNCTIONAL ANALYSIS OF miR-935

miR-935 was found as the most differentially expressed miRNA in CPC derived exosomes when compared with both MSC and HDF exosomes, so it was the selected miRNA for further functional analysis. Firstly, as a preliminary validation of RNA-seq data, miR-935 expression was measured by qPCR in CPC as well as in their derived exosome preparations. miR-935 showed a significant overexpression in three independent CPC isolates in comparison with two independent MSC and two independent HDF isolate cell populations (**Figure 31A**). Furthermore, a clear overexpression was also evident in exosome CPC preparations (**Figure 31B**) in comparison with equivalent preparations of MSC and HDF exosomes. This data corroborates RNA-seq results and suggests that miR-935 exosomal expression profile correlates with its expression in the whole cell, with substantially higher expression in CPC in comparison with MSC and HDF.

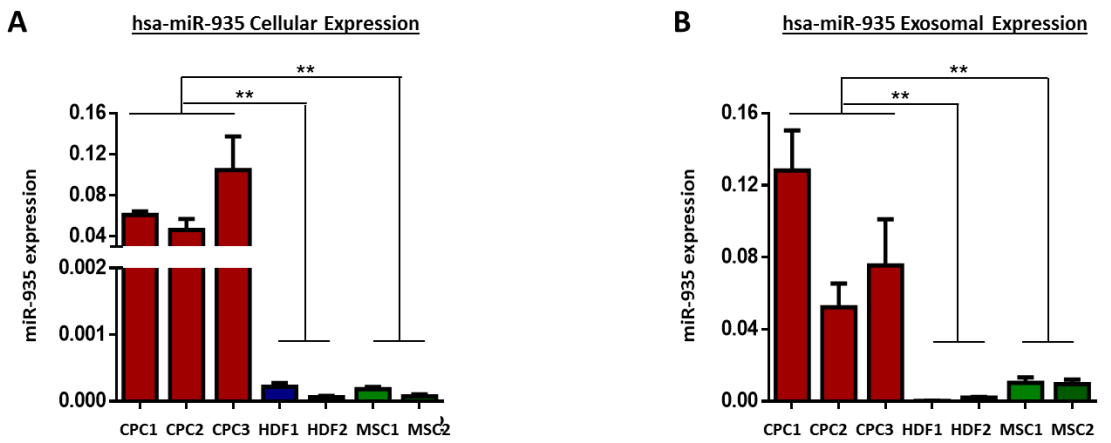

Figure 31. Validation of miR-935 expression in CPC cellular and exosomal compartments. *qPCR analysis of miR-935 expression in cellular* ***(A)*** *and exosomal compartments* ***(B)*** *of three isolate CPC (red), two isolate HDF (blue) and two isolate MSC (green) cell populations. Relative miRNA expression is represented as* $2^{-\Delta Ct}$ *value in comparison with the normalizers miRU48 (for cellular expression) and miR-30a-5p (for exosomal expression). All data are represented as mean ± SD. Significant differences among CPC, HDF and MSC mean values are indicated as ** P < 0.01.*

The role of miR-935 has not been well elucidated yet. Few experimental evidences have shown its involvement in different types of cancer, but its association with stem cells and specifically with CPC has not been previously reported.

In order to determine miR-935 biological function and its action at the cardiovascular level, a miRNA target prediction analysis was carried out using public databases. Global predicted analysis of the functional categories of target genes associated with this miRNA was explored in human as well as in its mouse orthologous. Selected functions included general cardiac processes such a cardiovascular development and angiogenesis, followed by other processes related to cell proliferation and apoptotic signaling. Interestingly, some categories related with cell death in response to oxidative stress or cellular response to hypoxia were also annotated (**Figure 32A, B**).

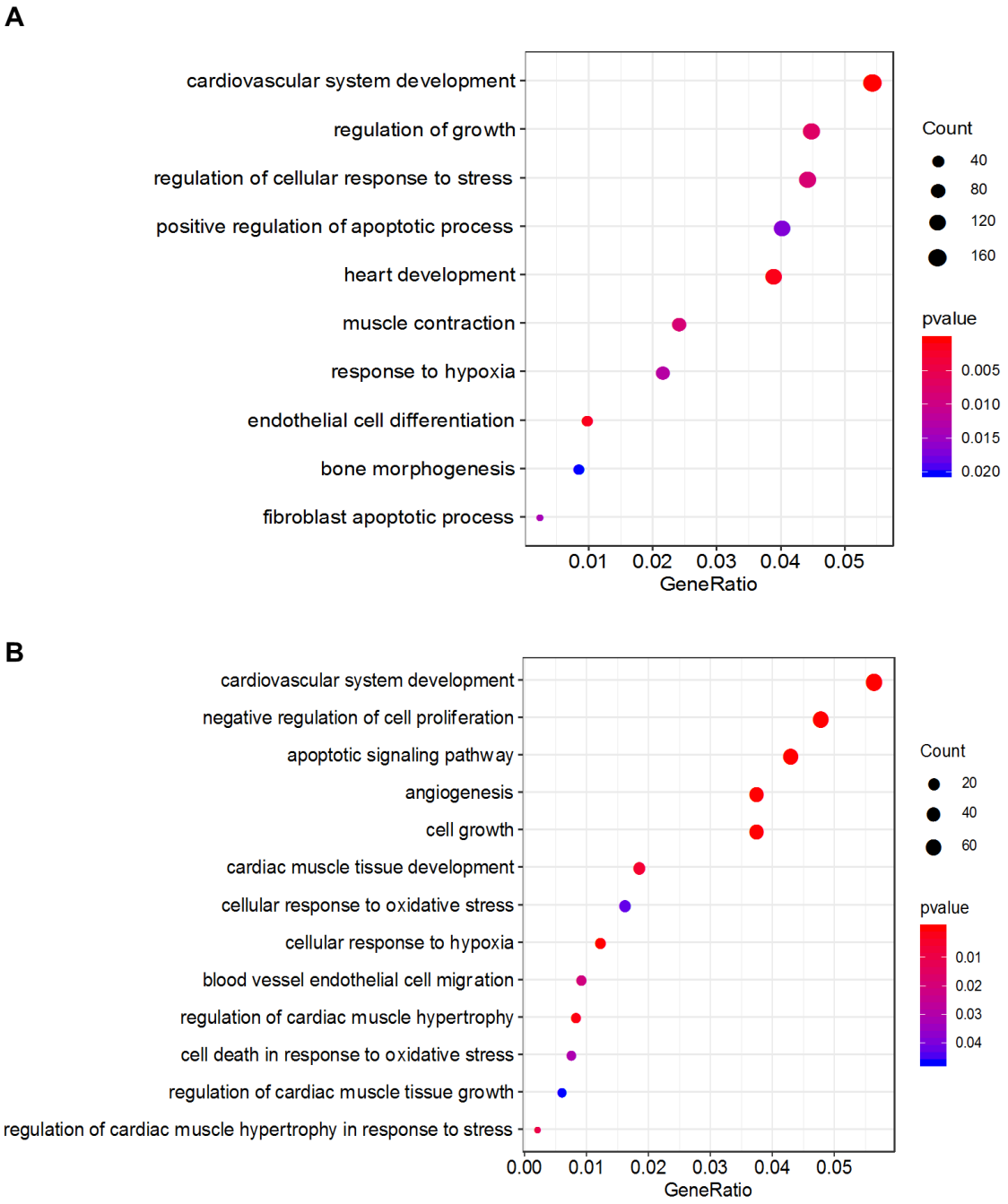

Figure 32. Gene Ontology (GO) analysis of the functional categories of target genes associated with the human (A) and mouse (B) miR-935. *Categories were selected with an enrichment P value < 0.05.*

In view of miR-935 potential biological activities, including apoptosis regulation and oxidative-stress response, and taking into account that other CPC-derived exosomal miRNAs have already been described for their cardioprotective effect, the potential role of miR-935 in this context was tested *in vitro*.

miR-935 was overexpressed and inhibited in CMs as well as in cardiac fibroblast cells and cellular response to oxidative stress induced by H_2O_2 was evaluated. Five hours after stimulus, the miR-935 mimic transfection showed a positive trend to increment CMs survival while, on the contrary, the transfection with miR-935 inhibitor diminished its protective effect (**Figure 33A**). No representative changes were observed in cardiac fibroblasts (**Figure 33B**). These results suggested that miR-935 could be participating in pathways involved in CMs anti-oxidant stress protective mechanisms.

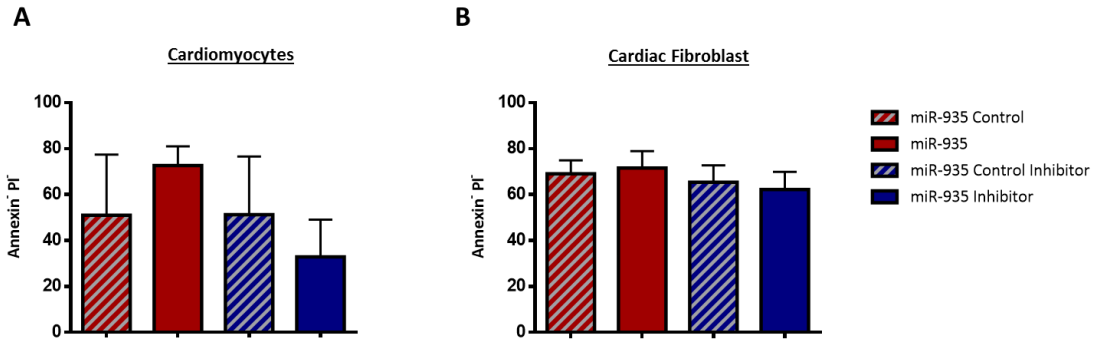

***Figure 33*. Evaluation of cardioprotective miR-935 effect against oxidative stress.** Effect of miR-935 mimic and miR-935 Inhibitor in cell apoptosis determined by Annexin-V and PI flow cytometry analysis in CMs **(A)** and Cardiac Fibroblast cells **(B)** 5 hours after H_2O_2 treatment (900 and 100 µM, respectively). Percentage of surviving cells are quantified as Annexin V^- - PI^- . Results are represented as mean ± SEM.

4. ANALYSIS OF THERAPEUTIC POTENTIAL OF AAV9-TnT-miR-935 IN A MOUSE MODEL OF MYOCARDIAL INFARCTION

In view of the putative protective role of miR-935, its action in a pathological model of MI model was assessed.

Firstly, miR-935 expression was analyzed in different cardiac progenitor cell populations characterized by Bmi1 or Sca1 expression, CM and non-CM cells isolated from healthy hearts. Interestingly, it was found that miR-935 expression was highly expressed in the more primitive cardiac progenitor compartment ($Bmi1^+Sca1^+$) [73], in good agreement with previous results in human CPC. This high miRNA expression was followed by $Bmi1^-Sca1^+$ and non-CM cells, all of them higher (>20 fold) than in the CMs population (**Figure 34**).

Next, we evaluated the impact of MI in miR-935 expression profile. The different cardiac populations were isolated from ischemic hearts, 5 days post-infarct. Results showed that MI provokes a reduction in miR-935 expression in all populations. Thus, miR-935 expression practically disappeared in $Bmi1^{-}Sca1^{+}$, non-myocyte and CM cells, being only detectable, although at low level, in $Bmi1^{+}Sca1^{+}$ cells (less than 125-fold in comparison with its physiological levels) (**Figure 34**). These results demonstrated that the expression level of the miR-935 is severely affected by myocardial damage.

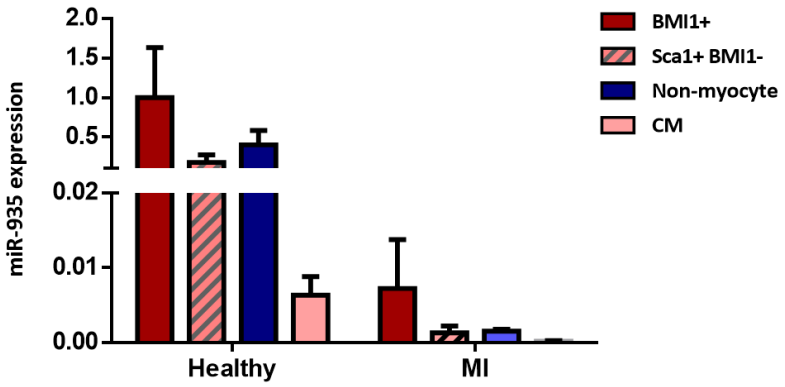

Figure 34. Analysis of the effect of MI in miR-935 expression. *qPCR analysis of miR-935 expression in different mouse heart subpopulations including cardiac progenitors-like populations ($Sca1^{+}Bmi1^{+}$; $Sca1^{+}Bmi1^{-}$), CMs and the Non-myocyte fraction, in healthy and ischemic mice 5 days post-infarction. Relative miRNA expression is represented as $2^{-\Delta\Delta Ct}$ value (miRNA expression was normalized with miRU6 and sample values referred to Sca1+Bmi1+ population). Results are represented as mean ± SD.*

Therefore, in view that *in vitro* miR-935 mimic overexpression enhanced CMs survival in response to oxidative stress and that the expression levels of miR-935 were decreased in the ischemic heart, the putative therapeutic effect of miR-935 overexpression was assessed in a mouse model of MI.

Thereby, miR-935 was cloned in the AAV9-TnT-vector for its specific cardiac overexpression. A miRNA with a scramble sequence was also cloned into the AAV9-TnT- vector and used as control for *in vivo* experiments. Specific plasmids for AAVs production were generated by following the protocols previously described.

miR-935 expression was *in vitro* tested by transfection of the AAV plasmids in the HL1 cardiac cell line. High miR-935 expression levels were detected after AAV9-TnT-935 plasmid transfection whereas no expression was found when the scramble plasmid was used (**Figure 35**).

Once the plasmid constructions were validated, AAV-TnT-935 and AAV-TnT-Scramble viral vectors were produced for the treatment of infarcted mice.

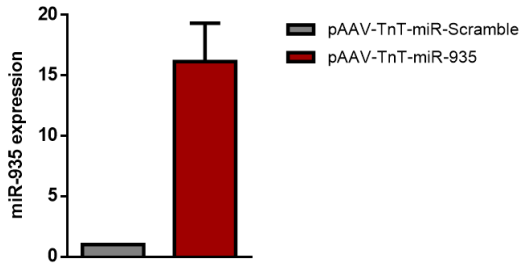

Figure 35. Analysis of miR-935 expression in HL1 cell line after plasmid transfection. *qPCR analysis of miR-935 expression after AAV-TnT-miR-935 and AAV-TnT-miR-Scramble plasmid transfection. Relative miRNA expression is represented as $2^{-\Delta\Delta Ct}$ value (miRU6 was used for normalization of miRNA expression and values are referred to pAAV-TnT-miR-Scramble). Data are represented as average ± SD values.*

AAV9 viral vectors encoding miR-935 or miR-Scramble were injected in the peri-infarct area of adult male C57BL/6 mice 15 minutes after the induction of permanent LAD occlusion (n=9/group). Cardiac function was assessed by echocardiography 2, 30 and 60 days after MI (**Figure 36**).

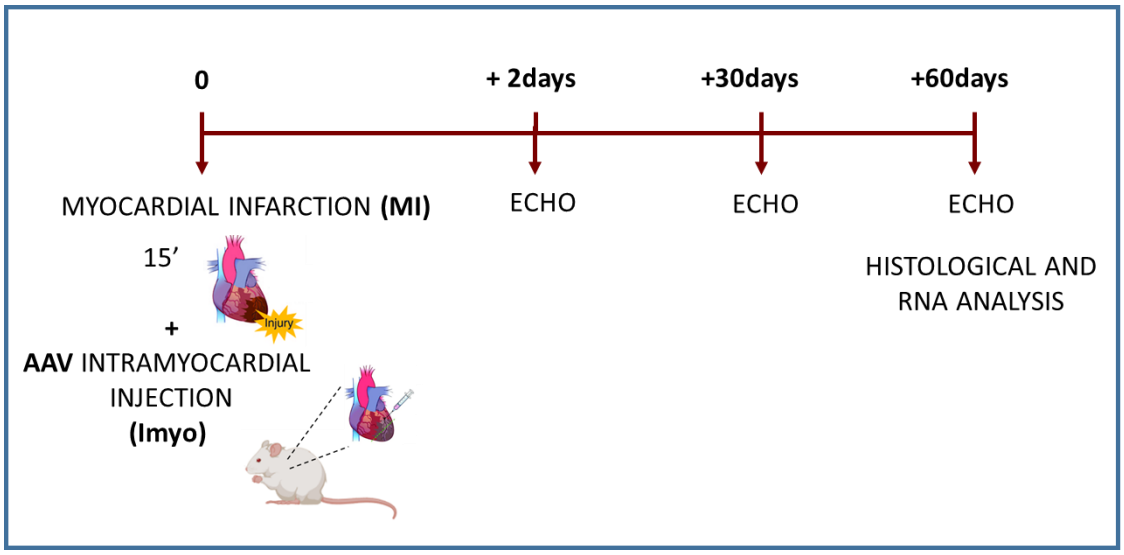

Figure 36. Schematic representation of the experimental design for the in vivo study

A significant functional improvement was not detected after miR-935 treatment despite that a slight positive trend in Δ ejection fraction (ΔEF%; EF% day 60 – EF% day 2) was observed after 2 months of miR-935-AAV treatment in comparison with the control group. A similar observation was evidenced for the Δ fractional area change (ΔFAC%; FAC% day 60 – FAC% day 2) when AAV9-TnT-miR-935 treated group and Scramble group were compared (**Figure 38A, B**).

Volume in diastole (VD) and volume in systole (VS) were also analyzed (**Table 9**) but not significant differences were found between both groups.

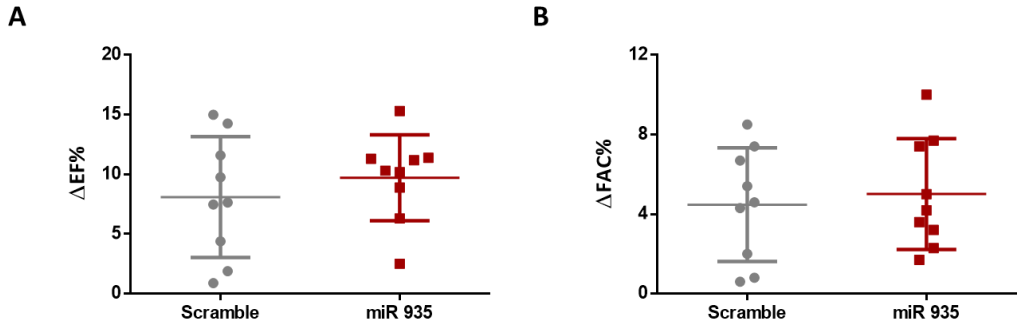

Figure 38. Effect of AAV9-TnT-miR-935 administration on cardiac function. *Percentage of ΔEF (EF% d60 – EF% d2)* **(A)** and ΔFAC *(FAC% d60 – FAC% d2)* **(B)** *assessed by echocardiography in mice treated with AAV-miR-935 and control group.*

Table 9. Echocardiographic studies

	AAV9-TnT-miR-Scramble	***AAV9-TnT-miR-935***
EF%		
2d	*27.1 ± 3.8*	*26.0 ± 5.9*
30d	*32.8 ± 5.6***	*32.6 ± 5.5****
60d	*35.2 ± 6.0***	*35.7 ±5.8****
FAC%		
2d	*16.8 ± 2.8*	*16.5 ± 4.6*
30d	*20.0 ± 3.7***	*18.1 ± 4.2*
60d	*21.2 ± 4.4 ***	*21.5 ± 4.2 ****
VS (ul)		
2d	*48.1 ± 6.1*	*46.8 ± 9.4*
30d	*61.0 ± 12.7**	*63.4 ± 16.1***
60d	*69.1 ± 15.6***	*68.5 ± 15.0***
VD (ul)		
2d	*65.1 ± 7.7*	*62.8 ± 9.4*
30d	*90.2 ± 14.7***	*93.0 ± 17.1****
60d	*105.9 ± 18.7****	*99.4 ± 25.8****

**Values of EF%, FAC%, VS and VD, 2, 30 and 60 days after MI and AAV administration. Results represent the mean ± SD. *p<0.05; **p<0.01 and ***p<0.001 between 2 days and 30 or 60 days after treatment.*

To evaluate if viral vector administration could induce positive tissue remodeling in infarcted hearts, animals were sacrificed 60 days after infarction and processed for histological assessment (n=7 animals per group) and miRNA expression analysis (n=2 animals per group).

First, infarct wall thickness was measured in hearts from both experimental groups. miR-935 treatment group showed a trend of greater thickness in the infarct wall in comparison with the scramble group, although it did not reach statistical significance (**Figure 39A-C**). In the same way, a tendency was observed in cardiac hypertrophy, showing a lower degree but no significant in miR-935 treatment group 2 months post-infarction (**Figure 39D-F**), suggesting a trend for a positive tissue remodeling. Furthermore, in order to determine if miR-935 expression could affect tissue vascularization of the peri-infarct zone, vascular density was determined (small caliber caveolin-1-positive vessels) (**Figure 39G-I**) but no differences were found.

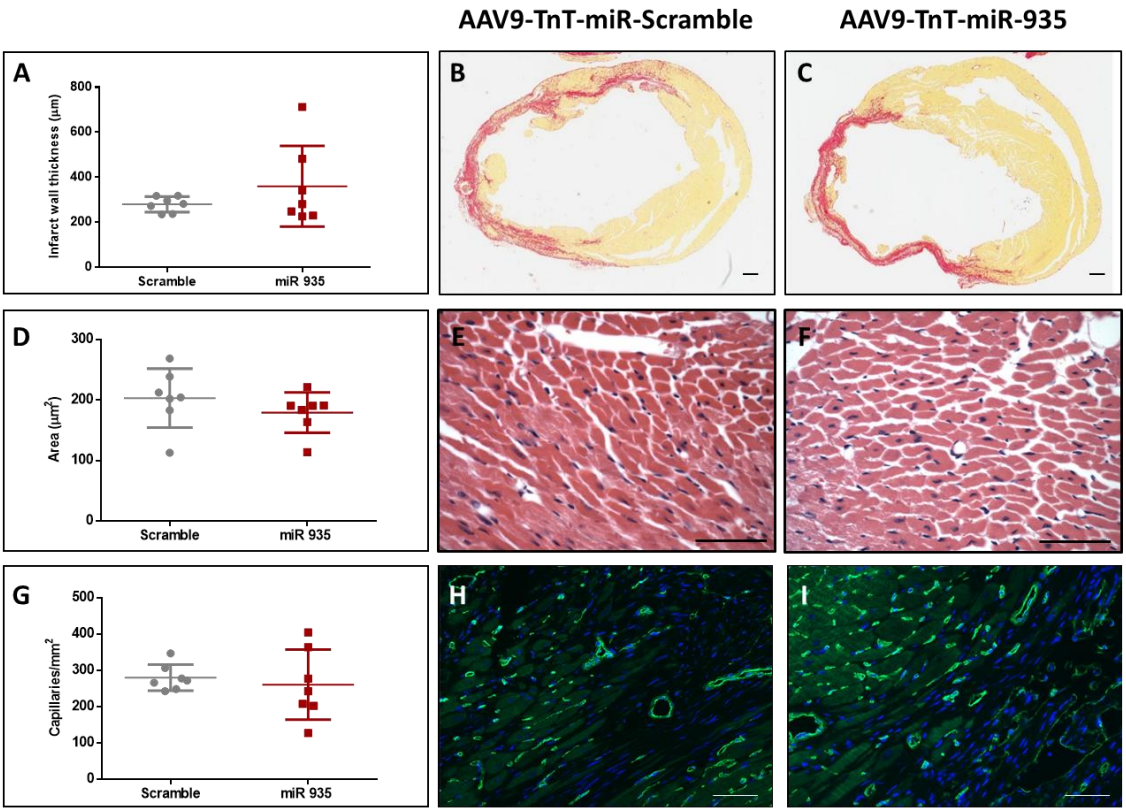

Figure 39. Effect of AAV9-TnT-miR-935 administration on cardiac tissue remodeling and revascularization. *Infarct wall thickness (µm) determined in Sirius Red serial stained sections in Scramble treated animals in comparison with miR-935 treated group* ***(A-C).*** *Hypertrophy determined by quantification of CMs size (µm²) in H&E immunostained serial sections in Scramble compared with miR-935 group* ***(D-F).*** *Capillary density determined by quantification of caveolin-1-positive capillaries (4-10 µm diameter) represented as capillaries/mm² in Scramble compared with miR-935 group* ***(G-I).*** *Representative images from remote (E-F) and peri-infarct (H-I) areas are included.* Scale bars: 50 *µm.*

Finally, miR-935 expression was confirmed in hearts 2 months post-infarction. High levels of miR-935 expresion were detected in the treated group (not in the scramble group) at the infarct zone, confirming the correct expression of our AAV vector (**Figure 37**).

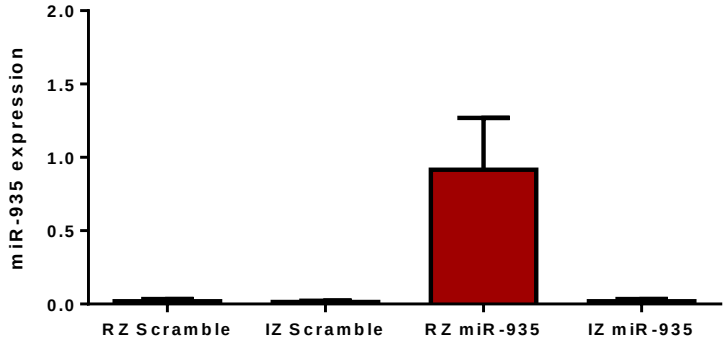

Figure 37. Analysis of miR-935 expression in the remote zone (RZ) and infarct zone (IZ) of treated hearts. *qPCR analysis of miR-935 expression after AAV9-TnT-miR-935 and AAV9-TnT-miR-Scramble treatment in infarcted mice, 60 days post-injection. Relative miRNA expression is represented as $2^{-\Delta Ct}$ (x 10^3) values. miRU6 was used for normalization of miRNA expression. Results are represented as mean ± SD.*

Discussion

Heart regeneration has been a leading topic of research in the cardiac field. The main strategies proposed to date have been based on transplantation of different sources of stem cells. Other alternative approaches have aimed to stimulate the cardiac regeneration process by different genes overexpression. In this context, gene therapy, and specifically AAV, are considered a promising alternative to express therapeutic genes in the heart. Thus, AAV transgene expression of different proteins and growth factors have already been tested for the treatment of CVD in different animal models [369]. Furthermore, in the last years, research has also focused on the role of non-coding molecules involved in the reparative processes. The possibility that miRNAs, important modulators of mRNA translation, can be regulated to induce cardiac regeneration and/or protection has emerged as an interesting approach. Thus, the development of an optimal delivery vector that allows a controlled, localized and sustained expression in the heart could represent an interesting tool that could help to deeper understanding different miRNA functions in the heart.

With the aim of using AAV as delivery vector for future studies or therapeutic applications, we studied its efficacy and specificity, taking into account key considerations such as the use of different promoters (ubiquitous or cardiac specific promoters), different routes of delivery (intravenous or intramyocardial administration) and animal models of healthy and myocardial infarcted mice. AAV9 was selected as the delivery vehicle to perform the study as it has been shown to be the most efficient AAV serotype for cardiac transduction [297], [368], [370]. It has been described that systemic administration of recombinant AAV vectors in healthy mice results in predominant liver transduction independently of the serotype. Despite this fact, a greater number of viral genomes is detected in the heart when injecting serotype 9 in comparison with the other serotypes, showing a greater affinity for the heart [371]. As important as the viral serotype is the vector delivery route, which has already been broadly tested in rodents. In our biodistribution study, we have found that intramyocardial injection of AAV9 with an ubiquitous promoter slightly reduces AAV9-mediated transgene expression in the liver in comparison with the intravenous injection, but significantly increases the expression in the heart. Similarly, when a cardiac specific promoter is used, we also observe that intramyocardial injection broadly favors a higher cardiac expression in comparison with the intravenous delivery, whereas slight variations are found in the liver. Our data is consistent with the results obtained by other groups that compared different delivery methods, even though the promoter they used was different and the vector dose varied among studies. Similarly to us, Fang *et al.* compared the efficiency of AAV9, intravenously or intracoronary injected in healthy animals, finding that the intravenous delivery was less effective for AAV9 cardiac gene transfer [372]. Another study

also evaluated AAV9 transduction efficiency after intramyocardial administration, showing that this route was more efficient and also safer in comparison with the intravenous one [373].

As previously mentioned, we have shown that when an ubiquitous promoter is used, vector transduction and transgene expression are mainly detected in the liver. This hepatic expression is independent of the administration route (intravenous or intramyocardial) and independent of heart damage. Although higher cardiac transduction levels can be obtained with AAV9 than with other serotypes [370], specific cardiac tropism cannot be recognized for this vector. Other groups have shown that AAV9 liver transduction levels can be minimized by using lower vector doses. In a dose-escalation study, it was reported that doses of $3.0x10^{10}$ vg infected around 32% CMs but only 3.2% of hepatocytes [368]. In another study, Bär *et al.* defined $5.0x10^{11}$ vg to transduce 60% heart cells but only 1.2% of liver cells [374]. In contrast, in our study and in the study performed by Fang *et al.,* we showed that despite using low AAV doses ($1.0x10^{10}$ vg) high transduction is achieved in the liver [372]. This aspect should be carefully considered in additional studies, especially for future clinical applications of this vector.

Despite the demonstrated effectiveness of the intramyocardial administration in the different animal models, the intravenous delivery continues to be studied, mainly due to the low morbidity associated with AAV infusion and the homogeneous expression of the therapeutic molecule. However, its diffuse distribution to non-cardiac tissues can exert undesirable secondary effects, also requiring higher doses to attain a given level of cardiac transgene expression. Furthermore, the intramyocardial administration route has also the advantages that it diminishes the neutralization effect of preexisting antibodies and also solves the limitation of the endothelial barrier, a hurdle for efficient gene transfer [375]. The only limitation of this delivery route might be the restricted expression area, although vector diffusion in the cardiac tissue has been evidenced by others and also by us in our histological studies. In any case, since AAV9 transduction is not restricted to the myocardium and liver can be transduced at high levels, new strategies are needed in order to reach cardiac specific expression. Appropriate tissue specific expression is key for the delivery of therapeutic genes, since off-target expression might lead to deleterious side effects. In this context, some specific strategies such as the incorporation of miRNA-regulated cassette [376], [377], random mutagenesis of AAV9 protein capsid [299] or the use of cell-specific promoters, have been described to selectively restrict gene expression in non-cardiac tissues. For this last strategy, the best considered promoters include the α-myosin heavy chain and the cardiac troponin genes. The MHC-2 promoter has been used for specific cardiac expression, reported in a rat and in a pig model of heart failure [303], [378]. In our study, a 418 bp fragment from the chicken cardiac Troponin-T promoter has

been included in our construction. This promoter was first described by the group of Dr. French [379], which showed robust luciferase and GFP expression in heart after systemic administration of AAV9 to 1-week-old mice. Similarly, another group has recently reported an efficient transduction of CMs following intravenous injection of 5.0x 10^{11} vg of AAV9-TnT-GFP in healthy animals [380]. In our study, after intravenous administration of a low AAV9 dose (1.0x10^{10} vg), limited heart transduction was found although, transduction efficiency, was greatly increased when AAV were intramyocardially delivered.

AAV expressing transgenes under the control of TnT promoter have been already used in different studies of MI [381], [382]. However, here we have analyzed for the first time the transduction efficacy of this vector considering at the same time the administration route and importantly, the heart damage. It is essential to consider the pathological context where the AAV are going to be used, and study how this environment could modify the biodistribution and transgene expression. In this work, we have found that MI improves transgene expression in the heart, independently of the promoter or route of delivery. After ischemia, the loss of CMs could explain a decrease of AAV genomes in heart and therefore a lower transgene expression. However, the rate of protein per AAV genome was found increased after damage, suggesting a greater AAV genome expression in the ischemic conditions. DNA-double-strand-break repair pathways are involved in AAV genome processing [383]. Furthermore, more than a decade ago it was reported that inflammatory cytokines such as IL-1β, IL-6 and TNF-α are able to significantly increase AAV-mediated transgene expression [384] and these three cytokines have been shown to be released during MI [5]. Thus, it could be hypothesized that the heart injury and DNA damaging agents could increase the vector genome processing and remain stable as transcriptionally-active molecules, thereby significantly increasing transgene expression. This is a very important point to take into account for future clinical applications since toxicology studies of gene therapy vectors are performed in healthy animals that do not reflect patient situation in terms of transduction efficiency and transgene expression levels.

In summary, we have shown striking differences in organ specific vector expression when different promoters and administration routes are used. We have demonstrated that, on the contrary to previous reports, serotype 9, although still better than other serotypes for cardiac application, is not cardiotropic, as we find the highest viral genomic DNA levels in the liver. Interestingly, when we used a cardiac specific promoter, we confined the expression of these vectors to the heart, avoiding gene expression in the liver. This expression is detected early and is stable over time when delivered intramyocardially and, importantly, it is also confirmed in the ischemic heart, the pathological context where these vectors might be applied

for therapeutic purposes. Therefore, our cardiac specific vector AAV9-TnT represents, in particular when injected intramyocardially, an effective tool for gene or small molecules overexpression, which could represent the development of new gene therapy approaches for MI.

In this context, not only genes but non-coding molecules overexpression open new perspectives for novel treatment modalities in many pathologies, including CVD [261], [385]. Among others, miRNAs have demonstrated to play a key role in the development and function of the heart, with an especial relevance shown for those derived from the exosomes. Therefore, the identification of the exosome molecular cargo could greatly help to elucidate new potential therapeutic molecules with a key role in the reparative processes after cardiac ischemia. In this context, our RNA-seq results reported a total of 350 different exosomal miRNAs, being 58 preferentially represented in the CPC exosomal compartment compared with the whole cell. From these candidates, miR-2110 and miR-1911-3p were the most differentially expressed in the exosomes, followed by miR-199a-3p. Upregulation of miR-2110 has been described in plasma and serum of patients with different types of cancer [386], [387] being its function reported as an onco-suppressor in neuroblastoma [388]. miR-1911-3p upregulation has been also recently determined in the exosomes isolated from the cerebrospinal fluid of patients with neural damage [389] although its functional activity has not been assessed yet. On the other hand, miR-199a-3p was previously shown to be enriched in human amniotic fluid stem cell-exosomes, driving pro-survival and proliferative effects in recipient HDFs [390]. A recent study has also demonstrated miR-199a-3p enrichment in BMSC-derived exosomes and its protective effect against renal I/R injury [391]. Furthermore, it has also been found upregulated in exosomes produced by local fibroblasts in Duchenne muscular dystrophy muscle, increasing the pathological fibrotic response [392]. Interestingly, coinciding with our results, miR-199a has been also described to be up-regulated in CPC-derived exosomes generated under hypoxic conditions. Moreover, their delivery to the heart in an I/R rat model decreased in this case the degree of tissue fibrosis, correlating with an improvement in the cardiac function [393].

Furthermore, we sought to establish the specific miRNA signature of CPC exosomes through a comparative analysis among CPC and MSC and HDF exosomes. In this analysis, 40 exosomal miRNAs were defined to be commonly differentially expressed between CPC and MSC/HDF exosomes. Thirty five % of these miRNAs were up-regulated in CPC exosomes and among them, miR-935, miR-135b and miR-146a presented the highest values. When we compared their expression levels in the exosomal compartment with the whole cell, miR-935, miR-135b and miR-146a showed a differential exosome/cell ratio of 0.5, 2.0 and 3.4,

respectively. miR-146a enrichment has already been reported in CPC exosomes whereas miR-935 and miR-135b have been identified for the first time in this study.

Thus, our analysis revealed a clear overexpression of miR-146a-3p in CPC exosomes when compared with HDF (7.98 log2FC) and MSC (4.46 log2FC) exosomes, being miR-146a-3p one of the few analyzed miRNAs that were preferentially found in the exosomal compartment in comparison with the whole cell. In other studies where the CPC exosomes were anayzed, miR-146a was also identified as one of the most highly enriched miRNA in comparison to fibroblasts-exosomes. Interestingly, *in vivo* studies have reported that injection of the miR-146a mimic into murine infarcted hearts can partially recapitulate the functional effects produced by the transplanted cells. This protective effect was totally exerted by the CPC-exosomes, suggesting that although miR-146a plays an important role in mediating the beneficial effects of CPC exosomes, it does not suffice to confer a robust therapeutic benefit. Other miRNAs in the repertoire may exert similar or even synergistic effects together with this miRNA [240]. Barile *et al.* also analyzed the miRNAs enrichment profile in exosomes secreted by CPC in comparison with fibroblasts, highlighting also the miR-146a-3p as well as other miRNAs like miR-210 and miR-132 [394]. In our study, miR-210 was expressed at low levels in exosomes and its expression was higher in the whole cell. Furthermore, no differential expression was found between CPCs and HDF exosomes. By contrast, our results with miR-132 fully agree with those previously reported, being this miRNA expressed at higher levels in exosomes than in the whole cell and, more importantly, differentially expressed when compared CPC and HDF exosomes. On the contrary, no differential expression was found when we compared with MSC exosomes. Finally, the miRNA content of human CDC exosomes was also recently analyzed by the group of Dr. Marban. Their results revealed a distinct miRNA profile with high expression levels of miR-146a, miR-126 and miR-181b. Comparing with our data, miR-126 was also found differentially expressed between CPC and HDF exosomes, nevertheless, this differential expression was not observed with MSC exosomes so this miRNA was not included in our selection. By contrast, miR-181b, which has been described to mediate polarization of macrophages and modulate the inflammatory processes [395], was not found differentially expressed in our analysis. These variations in miRNAs differential expression are not surprising taking into account that the exosomal content can depend on the method of cells isolation and culture as well as on the state of the donor cell. Biological validation of the results will give a deeper insight about the role and mechanisms of the identified molecules.

Next, among all the miRNAs identified in our study, we focused on miR-935 which despite being not the one with the highest expression, was the most specific for CPC-exosomes,

as presented the greatest differential expression between CPC and MSC/HDF exosomes (10.2 and 7.1 log2FC, respectively). No previous reports have evidenced the expression of miR-935 in the cardiac exosomal compartment and, before our study, the function of miR-935 in the ischemic heart has not been assessed.

Not too much knowledge exists regarding miR-935 biological function, being mainly associated with malignant tumoral processes. Thus, miR-935 expression has been found upregulated in gastric cancer and hepatocellular carcinoma tissues, contributing to cancer cell proliferation by targeting SOX7 gene [396], [397]. Furthermore, its inhibition enhanced the anti-oncogenic effect of paclitaxel, arresting cell growth and apoptosis and increasing SOX7 expression [398]. miR-935 is also found overexpressed in pancreatic carcinoma tissues, promoting cell proliferation and migration and inhibiting cell apoptosis by targeting INPP4A gene [399]. Furthermore, Wang T *et al.* reported that upregulation of miR-935 in non-small cell lung cancer cells could promote their survival and migratory capacity by directly targeting IL-27 expression [400]. Controversial results have been also reported for this non-coding molecule as downregulation of miR-935 has been also reported by other groups in lung cancer cells. Moreover, its *in vitro* overexpression has been shown to suppress cell proliferation and migration by targeting E2F7 [401]. Other studies have also attributed a tumor-suppressive role to miR-935. Thus, up-regulation of miR-935 in gastric signet ring cell carcinoma tissues was reported and demonstrated to inhibit cell growth and metastasis by targeting Notch1 [402] and, in osteosarcoma tissue, miR-935 was found downregulated, being its enforced expression able to reduce cell proliferation and invasion by targeting HMGB1 [403]. Finally, miR-935 has recently been associated with macrophage polarization to an M2-like phenotype in the microenvironment of solid tumors via targeting the TLR4 receptor [404].

Considering the above results, previous studies in our group explored first the potential role of miR-935 for regulating cardiac cells proliferation. However, miR-935 overexpression or inhibition did not significantly affect the proliferative capacity of neither CMs nor cardiac fibroblast cells. Therefore, miR-935 seems not to play a key role for basic cardiac cellular homeostasis, although it could have regulatory functions.

In order to unveil the biological function of miR-935 in the heart, we performed first a global analysis of the functional categories of predicted miR-935 target genes. The predicted analysis revealed miR-935 association with general cardiovascular processes like cardiovascular development, regulation of growth or angiogenesis and more interestingly, with categories related with oxidative stress and response to hypoxia. Oxidative stress is critical in myocardial

ischemia, causing apoptosis of resident cells. Interestingly, other CPC-derived exosomal miRNAs like miR-21 and miR-145 have been already described as main cardioprotective mediators against oxidative stress damage. Thereby, upregulated miR-21 levels can effectively inhibit H_2O_2-induced CMs apoptosis [405]. Also, up-regulation of miR-145 in CPC-derived exosomes has demonstrated their cardioprotective effect under oxidative stress conditions either *in vitro* by inhibiting caspase 3/7, and *in vivo*, in a I/R mouse model [253].

In view of this data, the cardioprotective effect of miR-935 under oxidative stress conditions was first analyzed *in vitro.* miR-935 mimic transfection demonstrated to increase cell survival in H_2O_2-treated CMs, suggesting their potential effect against oxidative stress damage. As expected, opposite results were found with miR-935 inhibitor, showing a decrease in cell survival after RNA transfection. No miR-935 protective effect was observed in the cardiac fibroblasts cell population though. Deeper *in vitro* studies will be performed in order to confirm the cardioprotective role of miR-935 against heart damage and to understand the underlying mechanisms. Analysis of potential predicted gene targets for miR-935 will help also to elucidate its role in such processes.

Interestingly, several miR-935 gene targets like Sox7, IL-27, Notch1 HMGB1 and TLR4 have been already described and validated in different cell types. Surprisingly, some of these target genes, although not all, are related with positive cardiac repair, which contrasts with the potential cardioprotective role hypothesized for our miRNA. For example, it has been recently shown that SOX7 inhibition can induce CMs apoptosis [406]. In the same way, IL-27 was found up-regulated in post-ischemic hearts and its protective role demonstrated both *in vitro* and in a rat model of acute I/R, mediating severe hypoxia-cell damage [407]. On the other hand, the Notch1 pathway plays a critical role in cardiovascular development and vascular diseases [408] as well as in the suppression of cell apoptosis [409]. Inhibition of miR-363 [410] and miR-381 [411] have been reported to *in vivo* protect CMs against hypoxia through the induction of Notch1 expression. On the other hand, the inhibition of extracellular HMGB1 in myocardial I/R injury was reported to reduce inflammation and to be protective. However, on the contrary, administration of HMGB1 after MI demonstrated to ameliorate cardiac performance by promoting tissue regeneration [412]. Finally, TLR4 target has been validated in solid tumors, regulating macrophage polarization to an M2-like phenotype, which could be a potential mechanism to contribute to cardiac repair. Interestingly, another study has recently reported that MSC-derived exosomes attenuated myocardial I/R injury by polarizing inflammatory macrophages. The role of exosomal-miR-182, has been described to modulate macrophage polarization by targeting TLR4 signaling [413].

These different findings demonstrate that, as expected, the expression and biological roles of miR-935 are many and are tissue-specific, exerting a different role depending on the cell type and/or target genes.

Finally, our *in vivo* analysis of miRNA expression in the ischemic hearts showed that miR-935 was severely downregulated after infarction in all different cardiac populations. In view of our *in vitro* data that suggests the cardioprotective role of miR-935 and the *in vivo* regulation of miR-935 expression, we evaluated next the putative therapeutic potential of miR-935 overexpression in a murine model of cardiac ischemia. Our AAV9-TnT-vector was chosen to allow cardiac specific and stable miRNA overexpression. AAV9-TnT vectors carrying miR-935 or miR-Scramble as control were intramyocardially administered to the hearts after infarct induction. miR-935-treated group showed a trend of improvement in cardiac function, although it did not reach statistical significance compared with the control group. In the same way, a positive tendency in heart tissue remodeling, regarding to the infarcted wall thickness and cardiac hypertrophy parameters, was observed in the treated group 2 months post-infarction. These results suggest that despite that miR-935 could have a cardioprotective effect, it was not sufficiently robust for induce a cardiac benefit.

To discard any technical limitation, the overexpression of miR-935 in the hearts was analyzed, confirming the correct overexpression of miR-935 in the treated hearts in comparison with the control group where miR-935 levels were almost not detectable. Furthermore, results showed high miR-935 levels in the injured zone but not in the remote zone, confirming miRNA overexpression at the AAV injection area. Despite the fact that miR-935 was correctly overexpressed in the infarcted hearts, it was not sufficient to improve cardiac function. We do not know if reaching higher levels of miR-935 heart expression, overexpressing the miRNA at earlier time-points (taking into account that AAV maximum-levels are reached after 3-7days of injection) or synergically combining miR-935 with other miRNAs, could promote a stronger therapeutic benefit. To note, many other studies have employed similar AAV9 vectors to allow specific miRNA overexpression and reported an improved cardiac function after MI [166], [343]. In that sense, our biodistribution studies with the AAV9-TnT-vector are consistent with others previous reports The time-course and the expression levels are similar to those reported by other groups, which suggests that the AAV9-TnT-vector was not the limitation in this work. However, as previously commented, it is necessary to consider that even though vector expression is detectable at day 1, it reaches maximum levels between day 3 and 7, so its effect in the first days after ischemia could be very limited. In this context, it is important to better

understand if the miRNA of interest mediates cardiac protection in an immediate early phase of the infarct.

Thus, to fully understand the role of miR-935 in heart dysfunction, further investigations are required. New *in vivo* experiments in our MI mouse model to determine the putative cardioprotective potential of miR-935 at early time-points after MI, could be a key approach. miR-935 overexpression or inhibition would help to determine its pro-survival action at early time-points as well as to determine the signaling pathways involved. In that sense, molecular analysis of the genetic profile of the damaged CMs and cardiac progenitors would be an interesting and very informative approach to elucidate these processes. In addition, we cannot exclude the possibility that miR-935 could directly affect signaling pathways in other cell types such as cardiac fibroblasts, smooth muscle or endothelial cells, since miRNA expression was also found in the healthy hearts.

Overall, miRNA therapeutics is a promising and emerging field. The ability of miRNAs to modulate or target multiple processes related to cardiac remodeling make them an attractive tool. Unlike standard drugs that are directed against a specific target, the existence of multiple targets for each miRNA enable circumvention of cells and tissues regulatory mechanisms that makes them insensitive to certain drugs, which makes miRNAs excellent candidates for developing attractive therapies. However, this property could turn in a limitation, so a thorough understanding of miRNA functions is needed in order to avoid undesired secondary effects. In this context, the use of AAV, with specific and regulatable promoters that allow a sustained and specific expression, could constitute a promising tool. Thus, it has been recently reported that a AAV-miR-199a administered to infarcted pig hearts stimulated cardiac repair. However, in this study, subsequent persistent and uncontrolled expression of the miRNA resulted in sudden arrhythmic death of most of the treated pigs, demonstrating the need of this therapy to be tightly controlled [414]. Other approaches, like the use of nanotechnology, constitute and interesting alternative for therapeutic molecules delivery. Thus, the use of micro/nanoparticles would permit to control the dose applied to the patient (less prolonged than AAV action) and presents mild immunogenicity, being also applicable to all the patients. However, their functionalization to improve their cardiac specificity continues to present some limitations and tissue and cell type specific miRNAs expression is key for its delivery, since off-target expression might lead to pathological side effects. In any case, development of different strategies that allow to regulate miRNAs expression will help to elucidate new alternative treatments for cardiac regulation and/or protection. In that sense, the application of gene therapy in the

cardiovascular field could allow better understanding of specific miRNAs functions and their potential as therapeutic targets.

Conclusions

1. AAV9-EF1α-Luc vector produces higher luciferase expression levels in the liver than in the heart, independently of heart injury. Importantly, heart expression is affected by the AAV-delivery route, being greater when the viral vector is intramiocardially injected than when intravenously delivered.

2. AAV-TnT-Luc vector produces higher cardiac luciferase expression levels in comparison with the AAV-EF1α-Luc vector, reaching the greatest levels when is intramyocardially delivered either in healthy or myocardial infarcted mice. Importantly, minimal expression levels are found in the liver when this vector is used.

3. When intramyocardially injected, AAV9-EF1α and AAV9-TnT vectors expressing luciferase show a similar time-course expression in healthy and infarcted mice that is detectable at day 1, reaches a peak by day 3-7 and is stable for at least 60 days. Importantly, this expression is safe since no significant levels of heart and liver toxicity enzymes are detected after AAV injection.

4. AAV9 cannot be considered a specific cardiotropic vector since, like other AAV serotypes, it mainly transduces the liver, showing in this organ the highest viral genome accumulation in comparison with other major organs like the heart.

5. Myocardial infarction increases AAV-transgene expression in the cardiac tissue independently of the promoter and route of administration. This aspect should be carefully evaluated for clinical applications.

6. AAV9-TnT confines a long-term and CM-specific expression in the heart that is evidenced by the detection of an extensive GFP positive cardiac area, 60 days after AAV9-TnT-GFP intramyocardial injection. Therefore, AAV9-TnT represents, in particular when intramyocardially injected, an effective tool for specific cardiac transgene overexpression in a mouse model of myocardial infarction.

7. Fifty-eight miRNAs are preferentially expressed in the exosomal compartment of CPC in comparison with the whole cell. Interestingly, CPC exosomes cargo contain forty miRNAs differentially expressed in comparison with MSC and HDF exosomes.

8. Despite the fact that miR-935 is not the miRNA with the highest expression in the CPC exosomal compartment, it is the most specific for CPC-exosomes, since it presents the greatest differential expression levels between CPC and MSC/HDF exosomes.

9. Overexpression of miR-935 promotes survival in the murine cardiac cell-line HL1, in response to oxidative stress induced by hydrogen peroxide. As expected, this protective effect is lost after miR-935 inhibition *in vitro.*

10. The levels of miR-935 expression in the heart are regulated by ischemia, being reduced in CMs, cardiac progenitor populations characterized by Bmi1 or Sca1 expression, and non-CM cells, five days post-infarct.

11. In a mouse model of myocardial ischemia, overexpression of miR-935 by intramyocardial injection of AAV9-TnT-miR935 vector does not significantly improve heart function 60 days post-infarct. However, a slight positive trend in the ejection fraction and a decreased adverse cardiac remodeling are observed, suggesting miR-935 putative cardioprotective role.

Bibliography

[1] E. J. Benjamin *et al.*, 'Heart Disease and Stroke Statistics-2019 Update: A Report From the American Heart Association.', *Circulation*, vol. 139, no. 10, pp. e56–e528, Mar. 2019.

[2] A. Deten, H. C. Volz, W. Briest, and H.-G. Zimmer, 'Cardiac cytokine expression is upregulated in the acute phase after myocardial infarction. Experimental studies in rats.', *Cardiovasc. Res.*, vol. 55, no. 2, pp. 329–40, Aug. 2002.

[3] N. G. Frangogiannis, C. W. Smith, and M. L. Entman, 'The inflammatory response in myocardial infarction.', *Cardiovasc. Res.*, vol. 53, no. 1, pp. 31–47, Jan. 2002.

[4] G. Ertl and S. Frantz, 'Healing after myocardial infarction', *Cardiovasc. Res.*, vol. 66, no. 1, pp. 22–32, Apr. 2005.

[5] E. Forte, M. B. Furtado, and N. Rosenthal, 'The interstitium in cardiac repair: role of the immune–stromal cell interplay', *Nat. Rev. Cardiol.*, vol. 15, no. 10, pp. 601–616, Oct. 2018.

[6] M. Nian, P. Lee, N. Khaper, and P. Liu, 'Inflammatory Cytokines and Postmyocardial Infarction Remodeling', *Circ. Res.*, vol. 94, no. 12, pp. 1543–1553, Jun. 2004.

[7] A. Biernacka and N. G. Frangogiannis, 'Aging and Cardiac Fibrosis.', *Aging Dis.*, vol. 2, no. 2, pp. 158–173, Apr. 2011.

[8] A. Leask, 'Potential therapeutic targets for cardiac fibrosis: TGFbeta, angiotensin, endothelin, CCN2, and PDGF, partners in fibroblast activation.', *Circ. Res.*, vol. 106, no. 11, pp. 1675–80, Jun. 2010.

[9] Y. Sun, M. F. Kiani, A. E. Postlethwaite, and K. T. Weber, 'Infarct scar as living tissue', *Basic Res. Cardiol.*, vol. 97, no. 5, pp. 343–347, Sep. 2002.

[10] V. Talman and H. Ruskoaho, 'Cardiac fibrosis in myocardial infarction-from repair and remodeling to regeneration.', *Cell Tissue Res.*, vol. 365, no. 3, pp. 563–81, Sep. 2016.

[11] E. Forte, M. B. Furtado, and N. Rosenthal, 'The interstitium in cardiac repair: role of the immune-stromal cell interplay.', *Nat. Rev. Cardiol.*, vol. 15, no. 10, pp. 601–616, Oct. 2018.

[12] A. Uygur and R. T. Lee, 'Mechanisms of Cardiac Regeneration.', *Dev. Cell*, vol. 36, no. 4, pp. 362–74, Feb. 2016.

[13] S. Durrani, M. Konoplyannikov, M. Ashraf, and K. H. Haider, 'Skeletal myoblasts for cardiac repair.', *Regen. Med.*, vol. 5, no. 6, pp. 919–32, Nov. 2010.

[14] N. Hassan, J. Tchao, and K. Tobita, 'Concise Review: Skeletal Muscle Stem Cells and Cardiac Lineage: Potential for Heart Repair', *Stem Cells Transl. Med.*, vol. 3, no. 2, pp. 183–193, Feb. 2014.

[15] P. Menasché *et al.*, 'The Myoblast Autologous Grafting in Ischemic Cardiomyopathy (MAGIC) trial: first randomized placebo-controlled study of myoblast transplantation.', *Circulation*, vol. 117, no. 9, pp. 1189–200, Mar. 2008.

[16] T. J. Povsic *et al.*, 'A double-blind, randomized, controlled, multicenter study to assess the safety and cardiovascular effects of skeletal myoblast implantation by catheter delivery in patients with chronic heart failure after myocardial infarction.', *Am. Heart J.*, vol. 162, no. 4, pp. 654-662.e1, Oct. 2011.

[17] K. Fouts, B. Fernandes, N. Mal, J. Liu, and K. R. Laurita, 'Electrophysiological

consequence of skeletal myoblast transplantation in normal and infarcted canine myocardium.', *Hear. Rhythm*, vol. 3, no. 4, pp. 452–61, Apr. 2006.

[18] J. J. Gavira *et al.*, 'Repeated implantation of skeletal myoblast in a swine model of chronic myocardial infarction.', *Eur. Heart J.*, vol. 31, no. 8, pp. 1013–21, Apr. 2010.

[19] M. Kudo, Y. Wang, M. A. Wani, M. Xu, A. Ayub, and M. Ashraf, 'Implantation of bone marrow stem cells reduces the infarction and fibrosis in ischemic mouse heart.', *J. Mol. Cell. Cardiol.*, vol. 35, no. 9, pp. 1113–9, Sep. 2003.

[20] C. E. Murry *et al.*, 'Haematopoietic stem cells do not transdifferentiate into cardiac myocytes in myocardial infarcts', *Nature*, vol. 428, no. 6983, pp. 664–668, Apr. 2004.

[21] D. Orlic *et al.*, 'Bone marrow cells regenerate infarcted myocardium', *Nature*, vol. 410, no. 6829, pp. 701–705, Apr. 2001.

[22] K. A. Jackson *et al.*, 'Regeneration of ischemic cardiac muscle and vascular endothelium by adult stem cells', *J. Clin. Invest.*, vol. 107, no. 11, pp. 1395–1402, Jun. 2001.

[23] G. P. Meyer *et al.*, 'Intracoronary bone marrow cell transfer after myocardial infarction: eighteen months' follow-up data from the randomized, controlled BOOST (BOne marrOw transfer to enhance ST-elevation infarct regeneration) trial.', *Circulation*, vol. 113, no. 10, pp. 1287–94, Mar. 2006.

[24] V. Schächinger *et al.*, 'Intracoronary Bone Marrow–Derived Progenitor Cells in Acute Myocardial Infarction', *N. Engl. J. Med.*, vol. 355, no. 12, pp. 1210–1221, Sep. 2006.

[25] J. H. Traverse *et al.*, 'Effect of the Use and Timing of Bone Marrow Mononuclear Cell Delivery on Left Ventricular Function After Acute Myocardial Infarction', *JAMA*, vol. 308, no. 22, pp. 2380–9, Dec. 2012.

[26] E. C. Perin *et al.*, 'Effect of transendocardial delivery of autologous bone marrow mononuclear cells on functional capacity, left ventricular function, and perfusion in chronic heart failure: the FOCUS-CCTRN trial.', *JAMA*, vol. 307, no. 16, pp. 1717–26, Apr. 2012.

[27] D. Sürder *et al.*, 'Intracoronary Injection of Bone Marrow–Derived Mononuclear Cells Early or Late After Acute Myocardial Infarction', *Circulation*, vol. 127, no. 19, pp. 1968–1979, May 2013.

[28] K. W. Yong, J. R. Choi, M. Mohammadi, A. P. Mitha, A. Sanati-Nezhad, and A. Sen, 'Mesenchymal Stem Cell Therapy for Ischemic Tissues', *Stem Cells Int.*, vol. 2018, pp. 1–11, Oct. 2018.

[29] V. Planat-Bénard *et al.*, 'Spontaneous cardiomyocyte differentiation from adipose tissue stroma cells.', *Circ. Res.*, vol. 94, no. 2, pp. 223–9, Feb. 2004.

[30] P. Antonitsis, E. Ioannidou-Papagiannaki, A. Kaidoglou, and C. Papakonstantinou, 'In vitro cardiomyogenic differentiation of adult human bone marrow mesenchymal stem cells. The role of 5-azacytidine', *Interact. Cardiovasc. Thorac. Surg.*, vol. 6, no. 5, pp. 593–597, Jul. 2007.

[31] A. Bayes-Genis *et al.*, 'Human progenitor cells derived from cardiac adipose tissue ameliorate myocardial infarction in rodents.', *J. Mol. Cell. Cardiol.*, vol. 49, no. 5, pp. 771–80, Nov. 2010.

[32] S.-W. Kim *et al.*, 'Mesenchymal stem cells overexpressing GCP-2 improve heart function through enhanced angiogenic properties in a myocardial infarction model.', *Cardiovasc.*

Res., vol. 95, no. 4, pp. 495–506, Sep. 2012.

[33] A. Paul, M. Nayan, A. A. Khan, D. Shum-Tim, and S. Prakash, 'Angiopoietin-1-expressing adipose stem cells genetically modified with baculovirus nanocomplex: investigation in rat heart with acute infarction.', *Int. J. Nanomedicine*, vol. 7, pp. 663–82, Feb. 2012.

[34] X.-Y. Zhu, X.-Z. Zhang, L. Xu, X.-Y. Zhong, Q. Ding, and Y.-X. Chen, 'Transplantation of adipose-derived stem cells overexpressing hHGF into cardiac tissue.', *Biochem. Biophys. Res. Commun.*, vol. 379, no. 4, pp. 1084–90, Feb. 2009.

[35] M. Monguió-Tortajada, S. Roura, C. Gálvez-Montón, M. Franquesa, A. Bayes-Genis, and F. E. Borràs, 'Mesenchymal Stem Cells Induce Expression of CD73 in Human Monocytes In Vitro and in a Swine Model of Myocardial Infarction In Vivo.', *Front. Immunol.*, vol. 8, p. 1577, Nov. 2017.

[36] J. M. Hare *et al.*, 'Comparison of Allogeneic vs Autologous Bone Marrow–Derived Mesenchymal Stem Cells Delivered by Transendocardial Injection in Patients With Ischemic Cardiomyopathy', *JAMA*, vol. 308, no. 22, p. 2369, Dec. 2012.

[37] M. M. Lalu *et al.*, 'Safety of Cell Therapy with Mesenchymal Stromal Cells (SafeCell): A Systematic Review and Meta-Analysis of Clinical Trials', *PLoS One*, vol. 7, no. 10, p. e47559, Oct. 2012.

[38] C. E. Murry and G. Keller, 'Differentiation of embryonic stem cells to clinically relevant populations: lessons from embryonic development.', *Cell*, vol. 132, no. 4, pp. 661–80, Feb. 2008.

[39] S. K. Sanganalmath and R. Bolli, 'Cell Therapy for Heart Failure', *Circ. Res.*, vol. 113, no. 6, pp. 810–834, Aug. 2013.

[40] C. Mummery *et al.*, 'Differentiation of Human Embryonic Stem Cells to Cardiomyocytes', *Circulation*, vol. 107, no. 21, pp. 2733–2740, Jun. 2003.

[41] H. Qiao *et al.*, 'Long-term improvement in postinfarct left ventricular global and regional contractile function is mediated by embryonic stem cell-derived cardiomyocytes.', *Circ. Cardiovasc. Imaging*, vol. 4, no. 1, pp. 33–41, Jan. 2011.

[42] Y. Shiba *et al.*, 'Human ES-cell-derived cardiomyocytes electrically couple and suppress arrhythmias in injured hearts.', *Nature*, vol. 489, no. 7415, pp. 322–5, Sep. 2012.

[43] J. J. H. Chong *et al.*, 'Human embryonic-stem-cell-derived cardiomyocytes regenerate non-human primate hearts', *Nature*, vol. 510, no. 7504, pp. 273–277, Jun. 2014.

[44] P. Menasché *et al.*, 'Transplantation of Human Embryonic Stem Cell–Derived Cardiovascular Progenitors for Severe Ischemic Left Ventricular Dysfunction', *J. Am. Coll. Cardiol.*, vol. 71, no. 4, pp. 429–438, Jan. 2018.

[45] K. Takahashi and S. Yamanaka, 'Induction of Pluripotent Stem Cells from Mouse Embryonic and Adult Fibroblast Cultures by Defined Factors', *Cell*, vol. 126, no. 4, pp. 663–676, Aug. 2006.

[46] K. Takahashi *et al.*, 'Induction of Pluripotent Stem Cells from Adult Human Fibroblasts by Defined Factors', *Cell*, vol. 131, no. 5, pp. 861–872, Nov. 2007.

[47] M. Kawamura *et al.*, 'Feasibility, safety, and therapeutic efficacy of human induced pluripotent stem cell-derived cardiomyocyte sheets in a porcine ischemic cardiomyopathy model.', *Circulation*, vol. 126, no. 11 Suppl 1, pp. S29-37, Sep. 2012.

[48] Y. Shiba *et al.*, 'Allogeneic transplantation of iPS cell-derived cardiomyocytes regenerates primate hearts.', *Nature*, vol. 538, no. 7625, pp. 388–391, Oct. 2016.

[49] K. Miura *et al.*, 'Variation in the safety of induced pluripotent stem cell lines', *Nat. Biotechnol.*, vol. 27, no. 8, pp. 743–745, Aug. 2009.

[50] N. Sougawa *et al.*, 'Immunologic targeting of CD30 eliminates tumourigenic human pluripotent stem cells, allowing safer clinical application of hiPSC-based cell therapy.', *Sci. Rep.*, vol. 8, no. 1, p. 3726, Feb. 2018.

[51] A. Chow *et al.*, 'Human Induced Pluripotent Stem Cell-Derived Cardiomyocyte Encapsulating Bioactive Hydrogels Improve Rat Heart Function Post Myocardial Infarction.', *Stem cell reports*, vol. 9, no. 5, pp. 1415–1422, Nov. 2017.

[52] M. Kawamura *et al.*, 'Enhanced Therapeutic Effects of Human iPS Cell Derived-Cardiomyocyte by Combined Cell-Sheets with Omental Flap Technique in Porcine Ischemic Cardiomyopathy Model.', *Sci. Rep.*, vol. 7, no. 1, p. 8824, Dec. 2017.

[53] S. Tohyama *et al.*, 'Distinct Metabolic Flow Enables Large-Scale Purification of Mouse and Human Pluripotent Stem Cell-Derived Cardiomyocytes', *Cell Stem Cell*, vol. 12, no. 1, pp. 127–137, Jan. 2013.

[54] S. Tohyama *et al.*, 'Efficient Large-Scale 2D Culture System for Human Induced Pluripotent Stem Cells and Differentiated Cardiomyocytes.', *Stem cell reports*, vol. 9, no. 5, pp. 1406–1414, Nov. 2017.

[55] M. A. Laflamme and C. E. Murry, 'Heart regeneration.', *Nature*, vol. 473, no. 7347, pp. 326–35, May 2011.

[56] K. Malliaras *et al.*, 'Cardiomyocyte proliferation and progenitor cell recruitment underlie therapeutic regeneration after myocardial infarction in the adult mouse heart.', *EMBO Mol. Med.*, vol. 5, no. 2, pp. 191–209, Feb. 2013.

[57] A. P. Beltrami *et al.*, 'Adult cardiac stem cells are multipotent and support myocardial regeneration.', *Cell*, vol. 114, no. 6, pp. 763–76, Sep. 2003.

[58] H. Oh *et al.*, 'Cardiac progenitor cells from adult myocardium: Homing, differentiation, and fusion after infarction', *Proc. Natl. Acad. Sci.*, vol. 100, no. 21, pp. 12313–12318, Oct. 2003.

[59] B. G. Galvez *et al.*, 'Cardiac mesoangioblasts are committed, self-renewable progenitors, associated with small vessels of juvenile mouse ventricle.', *Cell Death Differ.*, vol. 15, no. 9, pp. 1417–28, Sep. 2008.

[60] K.-L. Laugwitz *et al.*, 'Postnatal isl1+ cardioblasts enter fully differentiated cardiomyocyte lineages.', *Nature*, vol. 433, no. 7026, pp. 647–53, Feb. 2005.

[61] J. J. H. Chong *et al.*, 'Adult cardiac-resident MSC-like stem cells with a proepicardial origin.', *Cell Stem Cell*, vol. 9, no. 6, pp. 527–40, Dec. 2011.

[62] C. M. Martin *et al.*, 'Persistent expression of the ATP-binding cassette transporter, Abcg2, identifies cardiac SP cells in the developing and adult heart.', *Dev. Biol.*, vol. 265, no. 1, pp. 262–75, Jan. 2004.

[63] G. M. Ellison *et al.*, 'Adult c-kitpos Cardiac Stem Cells Are Necessary and Sufficient for Functional Cardiac Regeneration and Repair', *Cell*, vol. 154, no. 4, pp. 827–842, Aug. 2013.

[64] J. H. van Berlo *et al.*, 'c-kit+ cells minimally contribute cardiomyocytes to the heart.', *Nature*, vol. 509, no. 7500, pp. 337–41, May 2014.

[65] L. He *et al.*, 'Enhancing the precision of genetic lineage tracing using dual recombinases.', *Nat. Med.*, vol. 23, no. 12, pp. 1488–1498, Dec. 2017.

[66] X.-L. Tang *et al.*, 'Long-Term Outcome of Administration of c-kit(POS) Cardiac Progenitor Cells After Acute Myocardial Infarction: Transplanted Cells Do not Become Cardiomyocytes, but Structural and Functional Improvement and Proliferation of Endogenous Cells Persist for at Least One Year.', *Circ. Res.*, vol. 118, no. 7, pp. 1091–105, Apr. 2016.

[67] R. Bolli *et al.*, 'Intracoronary delivery of autologous cardiac stem cells improves cardiac function in a porcine model of chronic ischemic cardiomyopathy.', *Circulation*, vol. 128, no. 2, pp. 122–31, Jul. 2013.

[68] C. Vicinanza *et al.*, 'Adult cardiac stem cells are multipotent and robustly myogenic: c-kit expression is necessary but not sufficient for their identification.', *Cell Death Differ.*, vol. 24, no. 12, pp. 2101–2116, Dec. 2017.

[69] K. Tateishi *et al.*, 'Clonally amplified cardiac stem cells are regulated by Sca-1 signaling for efficient cardiovascular regeneration.', *J. Cell Sci.*, vol. 120, no. Pt 10, pp. 1791–800, May 2007.

[70] H. Wang *et al.*, 'Isolation and characterization of a Sca-1+/CD31- progenitor cell lineage derived from mouse heart tissue.', *BMC Biotechnol.*, vol. 14, no. 1, p. 75, Aug. 2014.

[71] K. Matsuura *et al.*, 'Adult cardiac Sca-1-positive cells differentiate into beating cardiomyocytes.', *J. Biol. Chem.*, vol. 279, no. 12, pp. 11384–91, Mar. 2004.

[72] X. Wang *et al.*, 'The role of the sca-1+/CD31- cardiac progenitor cell population in postinfarction left ventricular remodeling.', *Stem Cells*, vol. 24, no. 7, pp. 1779–88, Jul. 2006.

[73] I. Valiente-Alandi *et al.*, 'Cardiac Bmi1 + cells contribute to myocardial renewal in the murine adult heart', *Stem Cell Res. Ther.*, vol. 6, no. 1, p. 205, Dec. 2015.

[74] N. M. van der Lugt *et al.*, 'Posterior transformation, neurological abnormalities, and severe hematopoietic defects in mice with a targeted deletion of the bmi-1 proto-oncogene.', *Genes Dev.*, vol. 8, no. 7, pp. 757–69, Apr. 1994.

[75] I. Valiente-Alandi, C. Albo-Castellanos, D. Herrero, I. Sanchez, and A. Bernad, 'Bmi1 (+) cardiac progenitor cells contribute to myocardial repair following acute injury.', *Stem Cell Res. Ther.*, vol. 7, no. 1, p. 100, Jul. 2016.

[76] D. Herrero *et al.*, 'Redox-dependent BMI1 activity drives in vivo adult cardiac progenitor cell differentiation.', *Cell Death Differ.*, vol. 25, no. 4, pp. 807–820, Mar. 2018.

[77] D. Herrero *et al.*, 'Bmi1-Progenitor Cell Ablation Impairs the Angiogenic Response to Myocardial Infarction.', *Arterioscler. Thromb. Vasc. Biol.*, vol. 38, no. 9, pp. 2160–2173, Sep. 2018.

[78] K. Cheng, T.-S. Li, K. Malliaras, D. R. Davis, Y. Zhang, and E. Marbán, 'Magnetic targeting enhances engraftment and functional benefit of iron-labeled cardiosphere-derived cells in myocardial infarction.', *Circ. Res.*, vol. 106, no. 10, pp. 1570–81, May 2010.

[79] P. V Johnston *et al.*, 'Engraftment, differentiation, and functional benefits of autologous cardiosphere-derived cells in porcine ischemic cardiomyopathy.', *Circulation*, vol. 120,

no. 12, pp. 1075–83, 7 p following 1083, Sep. 2009.

[80] R. Kannappan *et al.*, 'p53 Modulates the Fate of Cardiac Progenitor Cells Ex Vivo and in the Diabetic Heart In Vivo.', *EBioMedicine*, vol. 16, pp. 224–237, Feb. 2017.

[81] Y. Tokita *et al.*, 'Repeated Administrations of Cardiac Progenitor Cells Are Markedly More Effective Than a Single Administration: A New Paradigm in Cell Therapy.', *Circ. Res.*, vol. 119, no. 5, pp. 635–51, Aug. 2016.

[82] L. Ling, S. Gu, and Y. Cheng, 'Resveratrol activates endogenous cardiac stem cells and improves myocardial regeneration following acute myocardial infarction.', *Mol. Med. Rep.*, vol. 15, no. 3, pp. 1188–1194, Mar. 2017.

[83] R. Yue *et al.*, 'Metformin promotes the survival of transplanted cardiosphere-derived cells thereby enhancing their therapeutic effect against myocardial infarction.', *Stem Cell Res. Ther.*, vol. 8, no. 1, p. 17, Dec. 2017.

[84] F. Limana *et al.*, 'Exogenous high-mobility group box 1 protein induces myocardial regeneration after infarction via enhanced cardiac C-kit+ cell proliferation and differentiation.', *Circ. Res.*, vol. 97, no. 8, pp. e73-83, Oct. 2005.

[85] S. Rignault-Clerc, C. Bielmann, L. Liaudet, B. Waeber, F. Feihl, and N. Rosenblatt-Velin, 'Natriuretic Peptide Receptor B modulates the proliferation of the cardiac cells expressing the Stem Cell Antigen-1.', *Sci. Rep.*, vol. 7, no. 1, p. 41936, Feb. 2017.

[86] The Lancet Editors, 'Expression of concern: the SCIPIO trial.', *Lancet (London, England)*, vol. 383, no. 9925, p. 1279, Apr. 2014.

[87] R. R. Makkar *et al.*, 'Intracoronary cardiosphere-derived cells for heart regeneration after myocardial infarction (CADUCEUS): a prospective, randomised phase 1 trial.', *Lancet (London, England)*, vol. 379, no. 9819, pp. 895–904, Mar. 2012.

[88] 'Late-Breaking Clinical Trial Abstracts', *Circulation*, vol. 126, no. 23, pp. 2776–2799, Dec. 2012.

[89] R. Bolli *et al.*, 'Rationale and Design of the CONCERT-HF Trial (Combination of Mesenchymal and c-kit+ Cardiac Stem Cells As Regenerative Therapy for Heart Failure).', *Circ. Res.*, vol. 122, no. 12, pp. 1703–1715, Jun. 2018.

[90] K. Malliaras *et al.*, 'Safety and efficacy of allogeneic cell therapy in infarcted rats transplanted with mismatched cardiosphere-derived cells.', *Circulation*, vol. 125, no. 1, pp. 100–12, Jan. 2012.

[91] V. Crisostomo *et al.*, 'Delayed administration of allogeneic cardiac stem cell therapy for acute myocardial infarction could ameliorate adverse remodeling: experimental study in swine.', *J. Transl. Med.*, vol. 13, no. 1, p. 156, May 2015.

[92] K. Yee *et al.*, 'Allogeneic cardiospheres delivered via percutaneous transendocardial injection increase viable myocardium, decrease scar size, and attenuate cardiac dilatation in porcine ischemic cardiomyopathy.', *PLoS One*, vol. 9, no. 12, p. e113805, Dec. 2014.

[93] T. Chakravarty *et al.*, 'ALLogeneic Heart STem Cells to Achieve Myocardial Regeneration (ALLSTAR) Trial: Rationale and Design.', *Cell Transplant.*, vol. 26, no. 2, pp. 205–214, Feb. 2017.

[94] E. Tseliou *et al.*, 'Widespread Myocardial Delivery of Heart-Derived Stem Cells by Nonocclusive Triple-Vessel Intracoronary Infusion in Porcine Ischemic Cardiomyopathy:

Superior Attenuation of Adverse Remodeling Documented by Magnetic Resonance Imaging and Histology', *PLoS One*, vol. 11, no. 1, p. e0144523, Jan. 2016.

[95] F. Fernández-Avilés *et al.*, 'Safety and Efficacy of Intracoronary Infusion of Allogeneic Human Cardiac Stem Cells in Patients With ST-Segment Elevation Myocardial Infarction and Left Ventricular Dysfunction.', *Circ. Res.*, vol. 123, no. 5, pp. 579–589, Aug. 2018.

[96] J.-N. Tang *et al.*, 'Concise Review: Is Cardiac Cell Therapy Dead? Embarrassing Trial Outcomes and New Directions for the Future.', *Stem Cells Transl. Med.*, vol. 7, no. 4, pp. 354–359, Apr. 2018.

[97] E. Cambria *et al.*, 'Translational cardiac stem cell therapy: advancing from first-generation to next-generation cell types.', *NPJ Regen. Med.*, vol. 2, no. 1, p. 17, Dec. 2017.

[98] S. Koch and L. Claesson-Welsh, 'Signal transduction by vascular endothelial growth factor receptors.', *Cold Spring Harb. Perspect. Med.*, vol. 2, no. 7, p. a006502, Jul. 2012.

[99] L. Bao *et al.*, 'C-Kit Positive Cardiac Stem Cells and Bone Marrow-Derived Mesenchymal Stem Cells Synergistically Enhance Angiogenesis and Improve Cardiac Function After Myocardial Infarction in a Paracrine Manner.', *J. Card. Fail.*, vol. 23, no. 5, pp. 403–415, May 2017.

[100] K. Huang, S. Hu, and K. Cheng, 'A New Era of Cardiac Cell Therapy: Opportunities and Challenges.', *Adv. Healthc. Mater.*, vol. 8, no. 2, p. e1801011, Jan. 2019.

[101] T. Talwar and M. V. P. Srivastava, 'Role of vascular endothelial growth factor and other growth factors in post-stroke recovery.', *Ann. Indian Acad. Neurol.*, vol. 17, no. 1, pp. 1–6, Jan. 2014.

[102] F. Goto, K. Goto, K. Weindel, and J. Folkman, 'Synergistic effects of vascular endothelial growth factor and basic fibroblast growth factor on the proliferation and cord formation of bovine capillary endothelial cells within collagen gels.', *Lab. Invest.*, vol. 69, no. 5, pp. 508–17, Nov. 1993.

[103] E. De Falco *et al.*, 'SDF-1 involvement in endothelial phenotype and ischemia-induced recruitment of bone marrow progenitor cells.', *Blood*, vol. 104, no. 12, pp. 3472–82, Dec. 2004.

[104] M. E. Mayorga *et al.*, 'Role of SDF-1:CXCR4 in Impaired Post-Myocardial Infarction Cardiac Repair in Diabetes.', *Stem Cells Transl. Med.*, vol. 7, no. 1, pp. 115–124, Jan. 2018.

[105] T. Yoshida, L. Semprun-Prieto, S. Sukhanov, and P. Delafontaine, 'IGF-1 prevents ANG II-induced skeletal muscle atrophy via Akt- and Foxo-dependent inhibition of the ubiquitin ligase atrogin-1 expression.', *Am. J. Physiol. Heart Circ. Physiol.*, vol. 298, no. 5, pp. H1565-70, May 2010.

[106] W. Gan *et al.*, 'The SGK1 inhibitor EMD638683, prevents Angiotensin II-induced cardiac inflammation and fibrosis by blocking NLRP3 inflammasome activation.', *Biochim. Biophys. acta. Mol. basis Dis.*, vol. 1864, no. 1, pp. 1–10, Jan. 2018.

[107] P. Boros and C. M. Miller, 'Hepatocyte growth factor: a multifunctional cytokine.', *Lancet (London, England)*, vol. 345, no. 8945, pp. 293–5, Feb. 1995.

[108] T. Nakamura, S. Mizuno, K. Matsumoto, Y. Sawa, H. Matsuda, and T. Nakamura, 'Myocardial protection from ischemia/reperfusion injury by endogenous and

exogenous HGF.', *J. Clin. Invest.*, vol. 106, no. 12, pp. 1511–9, Dec. 2000.

[109] V. Sala and T. Crepaldi, 'Novel therapy for myocardial infarction: can HGF/Met be beneficial?', *Cell. Mol. Life Sci.*, vol. 68, no. 10, pp. 1703–17, May 2011.

[110] S. Gallo, V. Sala, S. Gatti, and T. Crepaldi, 'HGF/Met Axis in Heart Function and Cardioprotection', *Biomedicines*, vol. 2, no. 4, pp. 247–262, Oct. 2014.

[111] D. Philp and H. K. Kleinman, 'Animal studies with thymosin β4, a multifunctional tissue repair and regeneration peptide', *Ann. N. Y. Acad. Sci.*, vol. 1194, no. 1, pp. 81–86, May 2010.

[112] N. Smart *et al.*, 'De novo cardiomyocytes from within the activated adult heart after injury', *Nature*, vol. 474, no. 7353, pp. 640–644, Jun. 2011.

[113] R. Shah, K. Reyes-Gordillo, Y. Cheng, R. Varatharajalu, J. Ibrahim, and M. R. Lakshman, 'Thymosin β4 Prevents Oxidative Stress, Inflammation, and Fibrosis in Ethanol- and LPS-Induced Liver Injury in Mice.', *Oxid. Med. Cell. Longev.*, vol. 2018, p. 9630175, Jul. 2018.

[114] P. K. Mishra, S. Givvimani, V. Chavali, and S. C. Tyagi, 'Cardiac matrix: A clue for future therapy', *Biochim. Biophys. Acta - Mol. Basis Dis.*, vol. 1832, no. 12, pp. 2271–2276, Dec. 2013.

[115] K. Bersell, S. Arab, B. Haring, and B. Kühn, 'Neuregulin1/ErbB4 signaling induces cardiomyocyte proliferation and repair of heart injury.', *Cell*, vol. 138, no. 2, pp. 257–70, Jul. 2009.

[116] M. Mirotsou, T. M. Jayawardena, J. Schmeckpeper, M. Gnecchi, and V. J. Dzau, 'Paracrine mechanisms of stem cell reparative and regenerative actions in the heart.', *J. Mol. Cell. Cardiol.*, vol. 50, no. 2, pp. 280–9, Feb. 2011.

[117] B. Wightman, I. Ha, and G. Ruvkun, 'Posttranscriptional regulation of the heterochronic gene lin-14 by lin-4 mediates temporal pattern formation in C. elegans.', *Cell*, vol. 75, no. 5, pp. 855–62, Dec. 1993.

[118] A. Kozomara, M. Birgaoanu, and S. Griffiths-Jones, 'miRBase: from microRNA sequences to function.', *Nucleic Acids Res.*, vol. 47, no. D1, pp. D155–D162, Jan. 2019.

[119] F. Sato, S. Tsuchiya, S. J. Meltzer, and K. Shimizu, 'MicroRNAs and epigenetics.', *FEBS J.*, vol. 278, no. 10, pp. 1598–609, May 2011.

[120] V. N. Kim, J. Han, and M. C. Siomi, 'Biogenesis of small RNAs in animals.', *Nat. Rev. Mol. Cell Biol.*, vol. 10, no. 2, pp. 126–39, Feb. 2009.

[121] J. O'Brien, H. Hayder, Y. Zayed, and C. Peng, 'Overview of MicroRNA Biogenesis, Mechanisms of Actions, and Circulation.', *Front. Endocrinol. (Lausanne).*, vol. 9, p. 402, Aug. 2018.

[122] Y.-K. Kim and V. N. Kim, 'Processing of intronic microRNAs', *EMBO J.*, vol. 26, no. 3, pp. 775–783, Feb. 2007.

[123] I. Slezak-Prochazka *et al.*, 'Cellular localization and processing of primary transcripts of exonic microRNAs.', *PLoS One*, vol. 8, no. 9, p. e76647, Sep. 2013.

[124] D. Jevsinek Skok *et al.*, 'Genome-wide *in silico* screening for microRNA genetic variability in livestock species', *Anim. Genet.*, vol. 44, no. 6, pp. 669–677, Dec. 2013.

[125] C. M. Greene, *MicroRNAs and other non-coding RNAs in inflammation*. 2015.

[126] M. Dutka, R. Bobiński, and J. Korbecki, 'The relevance of microRNA in post-infarction left ventricular remodelling and heart failure.', *Heart Fail. Rev.*, Feb. 2019.

[127] Y. Mishima, C. Stahlhut, and A. J. Giraldez, 'miR-1-2 gets to the heart of the matter.', *Cell*, vol. 129, no. 2, pp. 247–9, Apr. 2007.

[128] J. Li, X. Dong, Z. Wang, and J. Wu, 'MicroRNA-1 in Cardiac Diseases and Cancers.', *Korean J. Physiol. Pharmacol.*, vol. 18, no. 5, pp. 359–63, Oct. 2014.

[129] Y. Zhao *et al.*, 'Dysregulation of cardiogenesis, cardiac conduction, and cell cycle in mice lacking miRNA-1-2.', *Cell*, vol. 129, no. 2, pp. 303–17, Apr. 2007.

[130] S. Yan and K. Jiao, 'Functions of miRNAs during Mammalian Heart Development.', *Int. J. Mol. Sci.*, vol. 17, no. 5, May 2016.

[131] L. S. Danielson *et al.*, 'Cardiovascular dysregulation of miR-17-92 causes a lethal hypertrophic cardiomyopathy and arrhythmogenesis.', *FASEB J.*, vol. 27, no. 4, pp. 1460–7, Apr. 2013.

[132] T. E. Callis *et al.*, 'MicroRNA-208a is a regulator of cardiac hypertrophy and conduction in mice.', *J. Clin. Invest.*, vol. 119, no. 9, pp. 2772–86, Sep. 2009.

[133] M. Xin, E. N. Olson, and R. Bassel-Duby, 'Mending broken hearts: cardiac development as a basis for adult heart regeneration and repair', *Nat. Rev. Mol. Cell Biol.*, vol. 14, no. 8, pp. 529–541, Aug. 2013.

[134] Z.-X. Shan *et al.*, 'miR-1/miR-206 regulate Hsp60 expression contributing to glucose-mediated apoptosis in cardiomyocytes', *FEBS Lett.*, vol. 584, no. 16, pp. 3592–3600, Aug. 2010.

[135] B. Zhang *et al.*, 'MicroRNA-92a inhibition attenuates hypoxia/reoxygenation-induced myocardiocyte apoptosis by targeting Smad7.', *PLoS One*, vol. 9, no. 6, p. e100298, Jun. 2014.

[136] R. Hinkel *et al.*, 'Inhibition of microRNA-92a protects against ischemia/reperfusion injury in a large-animal model.', *Circulation*, vol. 128, no. 10, pp. 1066–75, Sep. 2013.

[137] X. Huang *et al.*, 'Expression of microRNA-122 contributes to apoptosis in H9C2 myocytes.', *J. Cell. Mol. Med.*, vol. 16, no. 11, pp. 2637–46, Nov. 2012.

[138] X. Li, M. Kong, D. Jiang, J. Qian, Q. Duan, and A. Dong, 'MicroRNA-150 aggravates H2O2-induced cardiac myocyte injury by down-regulating c-myb gene', *Acta Biochim. Biophys. Sin. (Shanghai).*, vol. 45, no. 9, pp. 734–741, Sep. 2013.

[139] L. Wang *et al.*, 'Effects of downregulation of microRNA-181a on H2O2-induced H9c2 cell apoptosis via the mitochondrial apoptotic pathway.', *Oxid. Med. Cell. Longev.*, vol. 2014, p. 960362, 2014.

[140] Z. Pan *et al.*, 'M3 subtype of muscarinic acetylcholine receptor promotes cardioprotection via the suppression of miR-376b-5p.', *PLoS One*, vol. 7, no. 3, p. e32571, Mar. 2012.

[141] T. G. Hullinger *et al.*, 'Inhibition of miR-15 Protects Against Cardiac Ischemic Injury', *Circ. Res.*, vol. 110, no. 1, pp. 71–81, Jan. 2012.

[142] H. Nishi *et al.*, 'MicroRNA-15b modulates cellular ATP levels and degenerates mitochondria via Arl2 in neonatal rat cardiac myocytes.', *J. Biol. Chem.*, vol. 285, no. 7, pp. 4920–30, Feb. 2010.

[143] H. Zhu, Y. Yang, Y. Wang, J. Li, P. W. Schiller, and T. Peng, 'MicroRNA-195 promotes palmitate-induced apoptosis in cardiomyocytes by down-regulating Sirt1.', *Cardiovasc. Res.*, vol. 92, no. 1, pp. 75–84, Oct. 2011.

[144] R. A. Boon *et al.*, 'MicroRNA-34a regulates cardiac ageing and function', *Nature*, vol. 495, no. 7439, pp. 107–110, Mar. 2013.

[145] B. C. Bernardo *et al.*, 'Therapeutic inhibition of the miR-34 family attenuates pathological cardiac remodeling and improves heart function.', *Proc. Natl. Acad. Sci. U. S. A.*, vol. 109, no. 43, pp. 17615–20, Oct. 2012.

[146] M. Yamakuchi, M. Ferlito, and C. J. Lowenstein, 'miR-34a repression of SIRT1 regulates apoptosis', *Proc. Natl. Acad. Sci.*, vol. 105, no. 36, pp. 13421–13426, Sep. 2008.

[147] J. Li *et al.*, 'Mitofusin 1 is negatively regulated by microRNA 140 in cardiomyocyte apoptosis.', *Mol. Cell. Biol.*, vol. 34, no. 10, pp. 1788–99, May 2014.

[148] X.-P. Ren *et al.*, 'MicroRNA-320 is involved in the regulation of cardiac ischemia/reperfusion injury by targeting heat-shock protein 20.', *Circulation*, vol. 119, no. 17, pp. 2357–2366, May 2009.

[149] B. Li *et al.*, 'MicroRNA-7a/b protects against cardiac myocyte injury in ischemia/reperfusion by targeting poly(ADP-ribose) polymerase.', *PLoS One*, vol. 9, no. 3, p. e90096, Mar. 2014.

[150] D. Frank *et al.*, 'MicroRNA-20a inhibits stress-induced cardiomyocyte apoptosis involving its novel target Egln3/PHD3.', *J. Mol. Cell. Cardiol.*, vol. 52, no. 3, pp. 711–7, Mar. 2012.

[151] S. He *et al.*, 'miR-138 protects cardiomyocytes from hypoxia-induced apoptosis via MLK3/JNK/c-jun pathway.', *Biochem. Biophys. Res. Commun.*, vol. 441, no. 4, pp. 763–9, Nov. 2013.

[152] X. Zhang *et al.*, 'Synergistic effects of the GATA-4-mediated miR-144/451 cluster in protection against simulated ischemia/reperfusion-induced cardiomyocyte death.', *J. Mol. Cell. Cardiol.*, vol. 49, no. 5, pp. 841–50, Nov. 2010.

[153] S. Hu *et al.*, 'MicroRNA-210 as a Novel Therapy for Treatment of Ischemic Heart Disease', *Circulation*, vol. 122, no. 11_suppl_1, pp. S124–S131, Sep. 2010.

[154] J. Wang *et al.*, 'miR-499 protects cardiomyocytes from H 2O 2-induced apoptosis via its effects on Pdcd4 and Pacs2.', *RNA Biol.*, vol. 11, no. 4, pp. 339–50, Apr. 2014.

[155] K. Wang *et al.*, 'miR-874 regulates myocardial necrosis by targeting caspase-8.', *Cell Death Dis.*, vol. 4, no. 7, p. e709, Jul. 2013.

[156] R.-C. Li *et al.*, 'In vivo suppression of microRNA-24 prevents the transition toward decompensated hypertrophy in aortic-constricted mice.', *Circ. Res.*, vol. 112, no. 4, pp. 601–5, Feb. 2013.

[157] L. Qian, L. W. Van Laake, Y. Huang, S. Liu, M. F. Wendland, and D. Srivastava, 'miR-24 inhibits apoptosis and represses Bim in mouse cardiomyocytes.', *J. Exp. Med.*, vol. 208, no. 3, pp. 549–60, Mar. 2011.

[158] M. Meloni *et al.*, 'Local inhibition of microRNA-24 improves reparative angiogenesis and left ventricle remodeling and function in mice with myocardial infarction.', *Mol. Ther.*, vol. 21, no. 7, pp. 1390–402, Jul. 2013.

[159] J. Fiedler *et al.*, 'MicroRNA-24 regulates vascularity after myocardial infarction.', *Circulation*, vol. 124, no. 6, pp. 720–30, Aug. 2011.

[160] G. Lv, S. Shao, H. Dong, X. Bian, X. Yang, and S. Dong, 'MicroRNA-214 protects cardiac myocytes against H2O2-induced injury.', *J. Cell. Biochem.*, vol. 115, no. 1, pp. 93–101, Jan. 2014.

[161] A. B. Aurora *et al.*, 'MicroRNA-214 protects the mouse heart from ischemic injury by controlling Ca^{2+} overload and cell death.', *J. Clin. Invest.*, vol. 122, no. 4, pp. 1222–32, Apr. 2012.

[162] E. R. Porrello *et al.*, 'MiR-15 family regulates postnatal mitotic arrest of cardiomyocytes.', *Circ. Res.*, vol. 109, no. 6, pp. 670–9, Sep. 2011.

[163] N. Liu *et al.*, 'microRNA-133a regulates cardiomyocyte proliferation and suppresses smooth muscle gene expression in the heart.', *Genes Dev.*, vol. 22, no. 23, pp. 3242–54, Dec. 2008.

[164] V. P. Yin, A. Lepilina, A. Smith, and K. D. Poss, 'Regulation of zebrafish heart regeneration by miR-133.', *Dev. Biol.*, vol. 365, no. 2, pp. 319–27, May 2012.

[165] E. R. Porrello *et al.*, 'Regulation of neonatal and adult mammalian heart regeneration by the miR-15 family.', *Proc. Natl. Acad. Sci. U. S. A.*, vol. 110, no. 1, pp. 187–92, Jan. 2013.

[166] A. Eulalio *et al.*, 'Functional screening identifies miRNAs inducing cardiac regeneration.', *Nature*, vol. 492, no. 7429, pp. 376–81, Dec. 2012.

[167] J. Chen *et al.*, 'mir-17-92 cluster is required for and sufficient to induce cardiomyocyte proliferation in postnatal and adult hearts.', *Circ. Res.*, vol. 112, no. 12, pp. 1557–66, Jun. 2013.

[168] A. Bonauer *et al.*, 'MicroRNA-92a Controls Angiogenesis and Functional Recovery of Ischemic Tissues in Mice', *Science (80-.).*, vol. 324, no. 5935, pp. 1710–1713, Jun. 2009.

[169] C. Iaconetti *et al.*, 'Inhibition of miR-92a increases endothelial proliferation and migration in vitro as well as reduces neointimal proliferation in vivo after vascular injury.', *Basic Res. Cardiol.*, vol. 107, no. 5, p. 296, Sep. 2012.

[170] W. Wu *et al.*, 'Flow-Dependent Regulation of Kruppel-Like Factor 2 Is Mediated by MicroRNA-92a.', *Circulation*, vol. 124, no. 5, pp. 633–41, Aug. 2011.

[171] C. Doebele *et al.*, 'Members of the microRNA-17-92 cluster exhibit a cell-intrinsic antiangiogenic function in endothelial cells.', *Blood*, vol. 115, no. 23, pp. 4944–50, Jun. 2010.

[172] A.-L. Pin, F. Houle, M. Guillonneau, E. R. Paquet, M. J. Simard, and J. Huot, 'miR-20a represses endothelial cell migration by targeting MKK3 and inhibiting p38 MAP kinase activation in response to VEGF.', *Angiogenesis*, vol. 15, no. 4, pp. 593–608, Dec. 2012.

[173] Y. Suárez *et al.*, 'Dicer-dependent endothelial microRNAs are necessary for postnatal angiogenesis.', *Proc. Natl. Acad. Sci. U. S. A.*, vol. 105, no. 37, pp. 14082–7, Sep. 2008.

[174] B. Icli *et al.*, 'MicroRNA-26a regulates pathological and physiological angiogenesis by targeting BMP/SMAD1 signaling.', *Circ. Res.*, vol. 113, no. 11, pp. 1231–41, Nov. 2013.

[175] K.-J. Yin, K. Olsen, M. Hamblin, J. Zhang, S. P. Schwendeman, and Y. E. Chen, 'Vascular endothelial cell-specific microRNA-15a inhibits angiogenesis in hindlimb ischemia.', *J. Biol. Chem.*, vol. 287, no. 32, pp. 27055–64, Aug. 2012.

[176] G. Spinetti *et al.*, 'MicroRNA-15a and microRNA-16 impair human circulating proangiogenic cell functions and are increased in the proangiogenic cells and serum of patients with critical limb ischemia.', *Circ. Res.*, vol. 112, no. 2, pp. 335–46, Jan. 2013.

[177] K. R. Cordes *et al.*, 'miR-145 and miR-143 regulate smooth muscle cell fate and plasticity.', *Nature*, vol. 460, no. 7256, pp. 705–10, Aug. 2009.

[178] Y. Yue, Z. Zhang, L. Zhang, S. Chen, Y. Guo, and Y. Hong, 'miR-143 and miR-145 promote hypoxia-induced proliferation and migration of pulmonary arterial smooth muscle cells through regulating ABCA1 expression.', *Cardiovasc. Pathol.*, vol. 37, pp. 15–25, Nov. 2018.

[179] L. Liu, Z. Cheng, and J. Yang, 'miR-23 regulates cell proliferation and apoptosis of vascular smooth muscle cells in coronary heart disease.', *Pathol. Res. Pract.*, vol. 214, no. 11, pp. 1873–1878, Nov. 2018.

[180] E. van Rooij, L. B. Sutherland, X. Qi, J. A. Richardson, J. Hill, and E. N. Olson, 'Control of Stress-Dependent Cardiac Growth and Gene Expression by a MicroRNA', *Science (80-.).*, vol. 316, no. 5824, pp. 575–579, Apr. 2007.

[181] T. Thum *et al.*, 'MicroRNA-21 contributes to myocardial disease by stimulating MAP kinase signalling in fibroblasts.', *Nature*, vol. 456, no. 7224, pp. 980–4, Dec. 2008.

[182] A. V Villar *et al.*, 'Myocardial and circulating levels of microRNA-21 reflect left ventricular fibrosis in aortic stenosis patients.', *Int. J. Cardiol.*, vol. 167, no. 6, pp. 2875–81, Sep. 2013.

[183] S. Roy *et al.*, 'MicroRNA expression in response to murine myocardial infarction: miR-21 regulates fibroblast metalloprotease-2 via phosphatase and tensin homologue', *Cardiovasc. Res.*, vol. 82, no. 1, pp. 21–29, Apr. 2009.

[184] H. Liang *et al.*, 'A novel reciprocal loop between microRNA-21 and TGFβRIII is involved in cardiac fibrosis.', *Int. J. Biochem. Cell Biol.*, vol. 44, no. 12, pp. 2152–60, Dec. 2012.

[185] T. Thum *et al.*, 'Comparison of different miR-21 inhibitor chemistries in a cardiac disease model.', *J. Clin. Invest.*, vol. 121, no. 2, pp. 461–2; author reply 462-3, Feb. 2011.

[186] D. M. Patrick *et al.*, 'Stress-dependent cardiac remodeling occurs in the absence of microRNA-21 in mice', *J. Clin. Invest.*, vol. 120, no. 11, pp. 3912–3916, Nov. 2010.

[187] E. van Rooij *et al.*, 'Dysregulation of microRNAs after myocardial infarction reveals a role of miR-29 in cardiac fibrosis.', *Proc. Natl. Acad. Sci. U. S. A.*, vol. 105, no. 35, pp. 13027–32, Sep. 2008.

[188] H. Qi *et al.*, 'Activation of AMPK Attenuated Cardiac Fibrosis by Inhibiting CDK2 via p21/p27 and miR-29 Family Pathways in Rats.', *Mol. Ther. Nucleic Acids*, vol. 8, pp. 277–290, Sep. 2017.

[189] R. A. Boon *et al.*, 'MicroRNA-29 in aortic dilation: implications for aneurysm formation.', *Circ. Res.*, vol. 109, no. 10, pp. 1115–9, Oct. 2011.

[190] R. Kumarswamy *et al.*, 'SERCA2a gene therapy restores microRNA-1 expression in heart failure via an Akt/FoxO3A-dependent pathway.', *Eur. Heart J.*, vol. 33, no. 9, pp. 1067–75, May 2012.

[191] I. Karakikes *et al.*, 'Therapeutic cardiac-targeted delivery of miR-1 reverses pressure overload-induced cardiac hypertrophy and attenuates pathological remodeling.', *J. Am.*

Heart Assoc., vol. 2, no. 2, p. e000078, Apr. 2013.

[192] G. Castoldi *et al.*, 'MiR-133a regulates collagen 1A1: potential role of miR-133a in myocardial fibrosis in angiotensin II-dependent hypertension.', *J. Cell. Physiol.*, vol. 227, no. 2, pp. 850–6, Feb. 2012.

[193] R. F. Duisters *et al.*, 'miR-133 and miR-30 regulate connective tissue growth factor: implications for a role of microRNAs in myocardial matrix remodeling.', *Circ. Res.*, vol. 104, no. 2, pp. 170–8, 6p following 178, Jan. 2009.

[194] A. Carè *et al.*, 'MicroRNA-133 controls cardiac hypertrophy', *Nat. Med.*, vol. 13, no. 5, pp. 613–618, May 2007.

[195] S. J. Matkovich *et al.*, 'MicroRNA-133a protects against myocardial fibrosis and modulates electrical repolarization without affecting hypertrophy in pressure-overloaded adult hearts.', *Circ. Res.*, vol. 106, no. 1, pp. 166–75, Jan. 2010.

[196] S. Chen, P. Puthanveetil, B. Feng, S. J. Matkovich, G. W. Dorn, and S. Chakrabarti, 'Cardiac miR-133a overexpression prevents early cardiac fibrosis in diabetes', *J. Cell. Mol. Med.*, vol. 18, no. 3, pp. 415–421, Mar. 2014.

[197] E. E. Creemers and E. van Rooij, 'Function and Therapeutic Potential of Noncoding RNAs in Cardiac Fibrosis.', *Circ. Res.*, vol. 118, no. 1, pp. 108–18, Jan. 2016.

[198] F. Xu *et al.*, 'Akt1-Mediated Regulation of Macrophage Polarization in a Murine Model of Staphylococcus aureus Pulmonary Infection', *J. Infect. Dis.*, vol. 208, no. 3, pp. 528–538, Aug. 2013.

[199] C. Wang *et al.*, 'Macrophage-Derived mir-155-Containing Exosomes Suppress Fibroblast Proliferation and Promote Fibroblast Inflammation during Cardiac Injury.', *Mol. Ther.*, vol. 25, no. 1, pp. 192–204, Jan. 2017.

[200] J.-L. Bao and L. Lin, 'MiR-155 and miR-148a reduce cardiac injury by inhibiting NF-κB pathway during acute viral myocarditis.', *Eur. Rev. Med. Pharmacol. Sci.*, vol. 18, no. 16, pp. 2349–56, Aug. 2014.

[201] X.-Q. Wu *et al.*, 'Emerging role of microRNAs in regulating macrophage activation and polarization in immune response and inflammation.', *Immunology*, vol. 148, no. 3, pp. 237–48, Jul. 2016.

[202] S. Banerjee *et al.*, 'miR-125a-5p regulates differential activation of macrophages and inflammation.', *J. Biol. Chem.*, vol. 288, no. 49, pp. 35428–36, Dec. 2013.

[203] S.-W. Kim, K. Ramasamy, H. Bouamar, A.-P. Lin, D. Jiang, and R. C. T. Aguiar, 'MicroRNAs miR-125a and miR-125b constitutively activate the NF-κB pathway by targeting the tumor necrosis factor alpha-induced protein 3 (TNFAIP3, A20).', *Proc. Natl. Acad. Sci. U. S. A.*, vol. 109, no. 20, pp. 7865–70, May 2012.

[204] E. N. Olson, 'MicroRNAs as therapeutic targets and biomarkers of cardiovascular disease.', *Sci. Transl. Med.*, vol. 6, no. 239, p. 239ps3, Jun. 2014.

[205] S. De Rosa, S. Fichtlscherer, R. Lehmann, B. Assmus, S. Dimmeler, and A. M. Zeiher, 'Transcoronary Concentration Gradients of Circulating MicroRNAs', *Circulation*, vol. 124, no. 18, pp. 1936–1944, Nov. 2011.

[206] K. M. Akat *et al.*, 'Comparative RNA-sequencing analysis of myocardial and circulating small RNAs in human heart failure and their utility as biomarkers.', *Proc. Natl. Acad. Sci. U. S. A.*, vol. 111, no. 30, pp. 11151–6, Jul. 2014.

[207] B. Shi, Y. Guo, J. Wang, and W. Gao, 'Altered expression of microRNAs in the myocardium of rats with acute myocardial infarction', *BMC Cardiovasc. Disord.*, vol. 10, no. 1, p. 11, Dec. 2010.

[208] G.-K. Wang *et al.*, 'Circulating microRNA: a novel potential biomarker for early diagnosis of acute myocardial infarction in humans', *Eur. Heart J.*, vol. 31, no. 6, pp. 659–666, Mar. 2010.

[209] Y. Huang, W. Li, J. Wu, M. Han, and B. Li, 'The diagnostic value of circulating microRNAs in heart failure (Review)', *Exp. Ther. Med.*, vol. 17, no. 3, pp. 1985–2003, Jan. 2019.

[210] W. Möbius *et al.*, 'Immunoelectron microscopic localization of cholesterol using biotinylated and non-cytolytic perfringolysin O.', *J. Histochem. Cytochem.*, vol. 50, no. 1, pp. 43–55, Jan. 2002.

[211] A. Ibrahim and E. Marbán, 'Exosomes: Fundamental Biology and Roles in Cardiovascular Physiology', *Annu. Rev. Physiol.*, vol. 78, no. 1, pp. 67–83, Feb. 2016.

[212] C. Raiborg and H. Stenmark, 'The ESCRT machinery in endosomal sorting of ubiquitylated membrane proteins.', *Nature*, vol. 458, no. 7237, pp. 445–52, Mar. 2009.

[213] J. H. Hurley, 'The ESCRT complexes.', *Crit. Rev. Biochem. Mol. Biol.*, vol. 45, no. 6, pp. 463–87, Dec. 2010.

[214] J. H. Hurley and P. I. Hanson, 'Membrane budding and scission by the ESCRT machinery: it's all in the neck.', *Nat. Rev. Mol. Cell Biol.*, vol. 11, no. 8, pp. 556–66, Aug. 2010.

[215] E.-L. Eskelinen, 'Roles of LAMP-1 and LAMP-2 in lysosome biogenesis and autophagy', *Mol. Aspects Med.*, vol. 27, no. 5–6, pp. 495–502, Oct. 2006.

[216] O. Alcazar *et al.*, 'Proteomics Characterization of Cell Membrane Blebs in Human Retinal Pigment Epithelium Cells', *Mol. Cell. Proteomics*, vol. 8, no. 10, pp. 2201–2211, Oct. 2009.

[217] C. Subra *et al.*, 'Exosomes account for vesicle-mediated transcellular transport of activatable phospholipases and prostaglandins.', *J. Lipid Res.*, vol. 51, no. 8, pp. 2105–20, Aug. 2010.

[218] K. Trajkovic *et al.*, 'Ceramide triggers budding of exosome vesicles into multivesicular endosomes.', *Science*, vol. 319, no. 5867, pp. 1244–7, Feb. 2008.

[219] L. Zakharova, M. Svetlova, and A. F. Fomina, 'T cell exosomes induce cholesterol accumulation in human monocytes via phosphatidylserine receptor.', *J. Cell. Physiol.*, vol. 212, no. 1, pp. 174–81, Jul. 2007.

[220] G. Turturici, R. Tinnirello, G. Sconzo, and F. Geraci, 'Extracellular membrane vesicles as a mechanism of cell-to-cell communication: advantages and disadvantages', *Am. J. Physiol. Physiol.*, vol. 306, no. 7, pp. C621–C633, Apr. 2014.

[221] C. He, S. Zheng, Y. Luo, and B. Wang, 'Exosome Theranostics: Biology and Translational Medicine', *Theranostics*, vol. 8, no. 1, pp. 237–255, 2018.

[222] S. Keerthikumar *et al.*, 'ExoCarta: A Web-Based Compendium of Exosomal Cargo.', *J. Mol. Biol.*, vol. 428, no. 4, pp. 688–692, Feb. 2016.

[223] B. K. Thakur *et al.*, 'Double-stranded DNA in exosomes: a novel biomarker in cancer detection', *Cell Res.*, vol. 24, no. 6, pp. 766–769, Jun. 2014.

[224] N. Vyas and J. Dhawan, 'Exosomes: mobile platforms for targeted and synergistic

signaling across cell boundaries.', *Cell. Mol. Life Sci.*, vol. 74, no. 9, pp. 1567–1576, May 2017.

[225] Z. Sun *et al.*, 'Emerging role of exosome-derived long non-coding RNAs in tumor microenvironment', *Mol. Cancer*, vol. 17, no. 1, p. 82, Dec. 2018.

[226] C. Roma-Rodrigues, A. R. Fernandes, and P. V. Baptista, 'Exosome in Tumour Microenvironment: Overview of the Crosstalk between Normal and Cancer Cells', *Biomed Res. Int.*, vol. 2014, pp. 1–10, 2014.

[227] J. Tian *et al.*, 'Extracellular HSP60 induces inflammation through activating and up-regulating TLRs in cardiomyocytes.', *Cardiovasc. Res.*, vol. 98, no. 3, pp. 391–401, Jun. 2013.

[228] C. Bang *et al.*, 'Cardiac fibroblast–derived microRNA passenger strand-enriched exosomes mediate cardiomyocyte hypertrophy', *J. Clin. Invest.*, vol. 124, no. 5, pp. 2136–2146, May 2014.

[229] S. Gupta and A. A. Knowlton, 'HSP60 trafficking in adult cardiac myocytes: role of the exosomal pathway.', *Am. J. Physiol. Heart Circ. Physiol.*, vol. 292, no. 6, pp. H3052-6, Jun. 2007.

[230] J. M. Vicencio *et al.*, 'Plasma Exosomes Protect the Myocardium From Ischemia-Reperfusion Injury', *J. Am. Coll. Cardiol.*, vol. 65, no. 15, pp. 1525–1536, Apr. 2015.

[231] L. Deng *et al.*, 'MicroRNA-143 Activation Regulates Smooth Muscle and Endothelial Cell Crosstalk in Pulmonary Arterial Hypertension', *Circ. Res.*, vol. 117, no. 10, pp. 870–883, Oct. 2015.

[232] H.-J. Sun, X.-X. Zhu, W.-W. Cai, and L.-Y. Qiu, 'Functional roles of exosomes in cardiovascular disorders: a systematic review.', *Eur. Rev. Med. Pharmacol. Sci.*, vol. 21, no. 22, pp. 5197–5206, Nov. 2017.

[233] P.-E. Rautou *et al.*, 'Microparticles from human atherosclerotic plaques promote endothelial ICAM-1-dependent monocyte adhesion and transendothelial migration.', *Circ. Res.*, vol. 108, no. 3, pp. 335–43, Feb. 2011.

[234] F. Jansen *et al.*, 'Endothelial microparticles reduce ICAM-1 expression in a microRNA-222-dependent mechanism.', *J. Cell. Mol. Med.*, vol. 19, no. 9, pp. 2202–14, Sep. 2015.

[235] E. Hergenreider *et al.*, 'Atheroprotective communication between endothelial cells and smooth muscle cells through miRNAs', *Nat. Cell Biol.*, vol. 14, no. 3, pp. 249–256, Mar. 2012.

[236] X. Wang *et al.*, 'Cardiomyocytes mediate anti-angiogenesis in type 2 diabetic rats through the exosomal transfer of miR-320 into endothelial cells.', *J. Mol. Cell. Cardiol.*, vol. 74, pp. 139–50, Sep. 2014.

[237] D. A. Chistiakov, A. N. Orekhov, and Y. V Bobryshev, 'Cardiac Extracellular Vesicles in Normal and Infarcted Heart.', *Int. J. Mol. Sci.*, vol. 17, no. 1, p. 63, Jan. 2016.

[238] F. Arslan *et al.*, 'Mesenchymal stem cell-derived exosomes increase ATP levels, decrease oxidative stress and activate PI3K/Akt pathway to enhance myocardial viability and prevent adverse remodeling after myocardial ischemia/reperfusion injury.', *Stem Cell Res.*, vol. 10, no. 3, pp. 301–12, May 2013.

[239] M. Khan *et al.*, 'Embryonic stem cell-derived exosomes promote endogenous repair mechanisms and enhance cardiac function following myocardial infarction.', *Circ. Res.*,

vol. 117, no. 1, pp. 52–64, Jun. 2015.

[240] A. G.-E. Ibrahim, K. Cheng, and E. Marbán, 'Exosomes as critical agents of cardiac regeneration triggered by cell therapy.', *Stem cell reports*, vol. 2, no. 5, pp. 606–19, May 2014.

[241] L. Barile, G. Milano, and G. Vassalli, 'Beneficial effects of exosomes secreted by cardiac-derived progenitor cells and other cell types in myocardial ischemia', *Stem Cell Investig.*, pp. 93–93, Nov. 2017.

[242] R. Gallet *et al.*, 'Exosomes secreted by cardiosphere-derived cells reduce scarring, attenuate adverse remodelling, and improve function in acute and chronic porcine myocardial infarction.', *Eur. Heart J.*, vol. 38, no. 3, pp. 201–211, Sep. 2017.

[243] J. Mayourian *et al.*, 'Exosomal microRNA-21-5p Mediates Mesenchymal Stem Cell Paracrine Effects on Human Cardiac Tissue Contractility.', *Circ. Res.*, vol. 122, no. 7, pp. 933–944, Mar. 2018.

[244] K. M. Luther *et al.*, 'Exosomal miR-21a-5p mediates cardioprotection by mesenchymal stem cells.', *J. Mol. Cell. Cardiol.*, vol. 119, pp. 125–137, Jun. 2018.

[245] Y. Feng, W. Huang, M. Wani, X. Yu, and M. Ashraf, 'Ischemic preconditioning potentiates the protective effect of stem cells through secretion of exosomes by targeting Mecp2 via miR-22.', *PLoS One*, vol. 9, no. 2, p. e88685, Feb. 2014.

[246] L. Shao *et al.*, 'MiRNA-Sequence Indicates That Mesenchymal Stem Cells and Exosomes Have Similar Mechanism to Enhance Cardiac Repair.', *Biomed Res. Int.*, vol. 2017, p. 4150705, 2017.

[247] H. Park *et al.*, 'Extracellular Vesicles Derived from Hypoxic Human Mesenchymal Stem Cells Attenuate GSK3β Expression via miRNA-26a in an Ischemia-Reperfusion Injury Model.', *Yonsei Med. J.*, vol. 59, no. 6, pp. 736–745, Aug. 2018.

[248] J. Zhu *et al.*, 'Myocardial reparative functions of exosomes from mesenchymal stem cells are enhanced by hypoxia treatment of the cells via transferring microRNA-210 in an nSMase2-dependent way.', *Artif. cells, nanomedicine, Biotechnol.*, vol. 46, no. 8, pp. 1659–1670, Dec. 2018.

[249] Q. Luo, D. Guo, G. Liu, G. Chen, M. Hang, and M. Jin, 'Exosomes from MiR-126-Overexpressing Adscs Are Therapeutic in Relieving Acute Myocardial Ischaemic Injury.', *Cell. Physiol. Biochem.*, vol. 44, no. 6, pp. 2105–2116, 2017.

[250] C. Xiao *et al.*, 'Transplanted Mesenchymal Stem Cells Reduce Autophagic Flux in Infarcted Hearts via the Exosomal Transfer of miR-125b.', *Circ. Res.*, vol. 123, no. 5, pp. 564–578, Aug. 2018.

[251] N. Wang *et al.*, 'Mesenchymal stem cells-derived extracellular vesicles, via miR-210, improve infarcted cardiac function by promotion of angiogenesis', *Biochim. Biophys. Acta - Mol. Basis Dis.*, vol. 1863, no. 8, pp. 2085–2092, Aug. 2017.

[252] J. Xiao *et al.*, 'Cardiac progenitor cell-derived exosomes prevent cardiomyocytes apoptosis through exosomal miR-21 by targeting PDCD4.', *Cell Death Dis.*, vol. 7, no. 6, p. e2277, Jun. 2016.

[253] L. Chen *et al.*, 'Cardiac progenitor-derived exosomes protect ischemic myocardium from acute ischemia/reperfusion injury.', *Biochem. Biophys. Res. Commun.*, vol. 431, no. 3, pp. 566–71, Feb. 2013.

[254] Z. Zhang, J. Yang, W. Yan, Y. Li, Z. Shen, and T. Asahara, 'Pretreatment of Cardiac Stem Cells With Exosomes Derived From Mesenchymal Stem Cells Enhances Myocardial Repair.', *J. Am. Heart Assoc.*, vol. 5, no. 1, Jan. 2016.

[255] J. A. Maring, C. M. Beez, V. Falk, M. Seifert, and C. Stamm, 'Myocardial Regeneration via Progenitor Cell-Derived Exosomes', *Stem Cells Int.*, vol. 2017, pp. 1–10, 2017.

[256] S. M. Davidson and D. M. Yellon, 'Exosomes and cardioprotection – A critical analysis', *Mol. Aspects Med.*, vol. 60, pp. 104–114, Apr. 2018.

[257] D. M. Yellon and S. M. Davidson, 'Exosomes', *Circ. Res.*, vol. 114, no. 2, pp. 325–332, Jan. 2014.

[258] F. Jansen and Q. Li, 'Exosomes as Diagnostic Biomarkers in Cardiovascular Diseases.', *Adv. Exp. Med. Biol.*, vol. 998, pp. 61–70, 2017.

[259] C. M. Boulanger, X. Loyer, P.-E. Rautou, and N. Amabile, 'Extracellular vesicles in coronary artery disease.', *Nat. Rev. Cardiol.*, vol. 14, no. 5, pp. 259–272, May 2017.

[260] S. Matsumoto *et al.*, 'Circulating p53-responsive microRNAs are predictive indicators of heart failure after acute myocardial infarction.', *Circ. Res.*, vol. 113, no. 3, pp. 322–6, Jul. 2013.

[261] M. Y. Rincon, T. VandenDriessche, and M. K. Chuah, 'Gene therapy for cardiovascular disease: advances in vector development, targeting, and delivery for clinical translation', *Cardiovasc. Res.*, vol. 108, no. 1, pp. 4–20, Oct. 2015.

[262] Y. Won, D. A. Bull, and S. Wan, 'Functional polymers of gene delivery for treatment of myocardial infarct', *J. Control. Release*, vol. 195, pp. 110–119, 2014.

[263] N. B. Wasala, J.-H. Shin, and D. Duan, 'The evolution of heart gene delivery vectors.', *J. Gene Med.*, vol. 13, no. 10, pp. 557–65, Oct. 2011.

[264] J. Mátrai, M. K. Chuah, and T. VandenDriessche, 'Recent Advances in Lentiviral Vector Development and Applications', *Mol. Ther.*, vol. 18, no. 3, pp. 477–490, Mar. 2010.

[265] R. W. ATCHISON, B. C. CASTO, and W. M. HAMMON, 'ADENOVIRUS-ASSOCIATED DEFECTIVE VIRUS PARTICLES.', *Science*, vol. 149, no. 3685, pp. 754–6, Aug. 1965.

[266] O.-W. Merten, C. Gény-Fiamma, and A. M. Douar, 'Current issues in adeno-associated viral vector production', *Gene Ther.*, vol. 12, no. S1, pp. S51–S61, Oct. 2005.

[267] M. Salganik, M. L. Hirsch, and R. J. Samulski, 'Adeno-associated Virus as a Mammalian DNA Vector', in *Mobile DNA III*, vol. 3, no. 4, American Society of Microbiology, 2015, pp. 829–851.

[268] F. Sonntag, K. Schmidt, and J. A. Kleinschmidt, 'A viral assembly factor promotes AAV2 capsid formation in the nucleolus', *Proc. Natl. Acad. Sci.*, vol. 107, no. 22, pp. 10220–10225, Jun. 2010.

[269] M. Naumer *et al.*, 'Properties of the Adeno-Associated Virus Assembly-Activating Protein', *J. Virol.*, vol. 86, no. 23, pp. 13038–13048, Dec. 2012.

[270] H. Büning and A. Srivastava, 'Capsid Modifications for Targeting and Improving the Efficacy of AAV Vectors.', *Mol. Ther. Methods Clin. Dev.*, vol. 12, pp. 248–265, Mar. 2019.

[271] J. C. Grieger and R. J. Samulski, 'Adeno-associated virus vectorology, manufacturing, and clinical applications.', *Methods Enzymol.*, vol. 507, pp. 229–54, 2012.

[272] S. Zolotukhin *et al.*, 'Recombinant adeno-associated virus purification using novel methods improves infectious titer and yield.', *Gene Ther.*, vol. 6, no. 6, pp. 973–85, Jun. 1999.

[273] N. Brument *et al.*, 'A versatile and scalable two-step ion-exchange chromatography process for the purification of recombinant adeno-associated virus serotypes-2 and -5.', *Mol. Ther.*, vol. 6, no. 5, pp. 678–86, Nov. 2002.

[274] N. Kaludov, B. Handelman, and J. A. Chiorini, 'Scalable purification of adeno-associated virus type 2, 4, or 5 using ion-exchange chromatography.', *Hum. Gene Ther.*, vol. 13, no. 10, pp. 1235–43, Jul. 2002.

[275] A. Srivastava, 'In vivo tissue-tropism of adeno-associated viral vectors', *Curr. Opin. Virol.*, vol. 21, pp. 75–80, Dec. 2016.

[276] C. L. Bell, B. L. Gurda, K. Van Vliet, M. Agbandje-McKenna, and J. M. Wilson, 'Identification of the galactose binding domain of the adeno-associated virus serotype 9 capsid.', *J. Virol.*, vol. 86, no. 13, pp. 7326–33, Jul. 2012.

[277] H. Zhang *et al.*, 'Several rAAV vectors efficiently cross the blood-brain barrier and transduce neurons and astrocytes in the neonatal mouse central nervous system.', *Mol. Ther.*, vol. 19, no. 8, pp. 1440–8, Aug. 2011.

[278] S. F. Merkel *et al.*, 'Trafficking of adeno-associated virus vectors across a model of the blood-brain barrier; a comparative study of transcytosis and transduction using primary human brain endothelial cells', *J. Neurochem.*, vol. 140, no. 2, pp. 216–230, Jan. 2017.

[279] S. Pillay *et al.*, 'An essential receptor for adeno-associated virus infection', *Nature*, vol. 530, no. 7588, pp. 108–112, Feb. 2016.

[280] M. A. Bartel, J. R. Weinstein, and D. V Schaffer, 'Directed evolution of novel adeno-associated viruses for therapeutic gene delivery.', *Gene Ther.*, vol. 19, no. 6, pp. 694–700, Jun. 2012.

[281] M. A. Kotterman and D. V. Schaffer, 'Engineering adeno-associated viruses for clinical gene therapy', *Nat. Rev. Genet.*, vol. 15, no. 7, pp. 445–451, Jul. 2014.

[282] D. Dalkara *et al.*, 'In vivo-directed evolution of a new adeno-associated virus for therapeutic outer retinal gene delivery from the vitreous.', *Sci. Transl. Med.*, vol. 5, no. 189, p. 189ra76, Jun. 2013.

[283] R. C. Münch *et al.*, 'Displaying High-affinity Ligands on Adeno-associated Viral Vectors Enables Tumor Cell-specific and Safe Gene Transfer', *Mol. Ther.*, vol. 21, no. 1, pp. 109–118, Jan. 2013.

[284] B. Balakrishnan and G. R. Jayandharan, 'Basic biology of adeno-associated virus (AAV) vectors used in gene therapy.', *Curr. Gene Ther.*, vol. 14, no. 2, pp. 86–100, 2014.

[285] R. J. Samulski *et al.*, 'Targeted integration of adeno-associated virus (AAV) into human chromosome 19.', *EMBO J.*, vol. 10, no. 12, pp. 3941–50, Dec. 1991.

[286] F. Mingozzi *et al.*, 'Pharmacological modulation of humoral immunity in a nonhuman primate model of AAV gene transfer for hemophilia B.', *Mol. Ther.*, vol. 20, no. 7, pp. 1410–6, Jul. 2012.

[287] F. Mingozzi *et al.*, 'Prevalence and pharmacological modulation of humoral immunity to AAV vectors in gene transfer to synovial tissue.', *Gene Ther.*, vol. 20, no. 4, pp. 417–24, Apr. 2013.

[288] F. Mingozzi *et al.*, 'Overcoming preexisting humoral immunity to AAV using capsid decoys.', *Sci. Transl. Med.*, vol. 5, no. 194, p. 194ra92, Jul. 2013.

[289] N. A. Huttner *et al.*, 'Genetic modifications of the adeno-associated virus type 2 capsid reduce the affinity and the neutralizing effects of human serum antibodies.', *Gene Ther.*, vol. 10, no. 26, pp. 2139–47, Dec. 2003.

[290] K. Adachi, T. Enoki, Y. Kawano, M. Veraz, and H. Nakai, 'Drawing a high-resolution functional map of adeno-associated virus capsid by massively parallel sequencing.', *Nat. Commun.*, vol. 5, no. 1, p. 3075, May 2014.

[291] I. Kwon and D. V Schaffer, 'Designer gene delivery vectors: molecular engineering and evolution of adeno-associated viral vectors for enhanced gene transfer.', *Pharm. Res.*, vol. 25, no. 3, pp. 489–99, Mar. 2008.

[292] N. Maheshri, J. T. Koerber, B. K. Kaspar, and D. V Schaffer, 'Directed evolution of adeno-associated virus yields enhanced gene delivery vectors', *Nat. Biotechnol.*, vol. 24, no. 2, pp. 198–204, Feb. 2006.

[293] 'Abstract 15439: AAV-Containing Exosomes as a Novel Vector to Improve AAV-Mediated Myocardial Gene Delivery in Resistance to Neutralizing Antibody | Circulation'. [Online]. Available: https://www.ahajournals.org/doi/10.1161/circ.136.suppl_1.15439. [Accessed: 20-May-2019].

[294] C. Zincarelli, S. Soltys, G. Rengo, W. J. Koch, and J. E. Rabinowitz, 'Comparative Cardiac Gene Delivery of Adeno-Associated Virus Serotypes 1–9 reveals that AAV6 Mediates the Most Efficient Transduction in Mouse Heart'.

[295] G. Gao *et al.*, 'Transendocardial Delivery of AAV6 Results in Highly Efficient and Global Cardiac Gene Transfer in Rhesus Macaques', *Hum. Gene Ther.*, vol. 22, no. 8, pp. 979–984, Aug. 2011.

[296] O. J. Müller *et al.*, 'Improved cardiac gene transfer by transcriptional and transductional targeting of adeno-associated viral vectors.', *Cardiovasc. Res.*, vol. 70, no. 1, pp. 70–8, Apr. 2006.

[297] C. A. Pacak *et al.*, 'Recombinant adeno-associated virus serotype 9 leads to preferential cardiac transduction in vivo.', *Circ. Res.*, vol. 99, no. 4, pp. e3-9, Aug. 2006.

[298] A. Asokan *et al.*, 'Reengineering a receptor footprint of adeno-associated virus enables selective and systemic gene transfer to muscle', *Nat. Biotechnol.*, vol. 28, no. 1, pp. 79–82, Jan. 2010.

[299] N. Pulicherla *et al.*, 'Engineering liver-detargeted AAV9 vectors for cardiac and musculoskeletal gene transfer.', *Mol. Ther.*, vol. 19, no. 6, pp. 1070–8, Jun. 2011.

[300] L. Yang *et al.*, 'A myocardium tropic adeno-associated virus (AAV) evolved by DNA shuffling and in vivo selection.', *Proc. Natl. Acad. Sci. U. S. A.*, vol. 106, no. 10, pp. 3946–51, 2009.

[301] L. Damdindorj *et al.*, 'A comparative analysis of constitutive promoters located in adeno-associated viral vectors.', *PLoS One*, vol. 9, no. 8, p. e106472, Aug. 2014.

[302] C. A. Pacak, Y. Sakai, B. D. Thattaliyath, C. S. Mah, and B. J. Byrne, 'Tissue specific promoters improve specificity of AAV9 mediated transgene expression following intra-vascular gene delivery in neonatal mice.', *Genet. Vaccines Ther.*, vol. 6, no. 1, p. 13, Sep.

2008.

[303] S. T. Pleger *et al.*, 'Cardiac AAV9-S100A1 gene therapy rescues post-ischemic heart failure in a preclinical large animal model.', *Sci. Transl. Med.*, vol. 3, no. 92, p. 92ra64, Jul. 2011.

[304] P. W. J. Raake *et al.*, 'AAV6.βARKct cardiac gene therapy ameliorates cardiac function and normalizes the catecholaminergic axis in a clinically relevant large animal heart failure model.', *Eur. Heart J.*, vol. 34, no. 19, pp. 1437–47, May 2013.

[305] S. C. Kolwicz *et al.*, 'AAV6-mediated Cardiac-specific Overexpression of Ribonucleotide Reductase Enhances Myocardial Contractility.', *Mol. Ther.*, vol. 24, no. 2, pp. 240–250, Feb. 2016.

[306] S. L. Teichman, K. S. Thomson, and M. Regnier, 'Cardiac Myosin Activation with Gene Therapy Produces Sustained Inotropic Effects and May Treat Heart Failure with Reduced Ejection Fraction.', *Handb. Exp. Pharmacol.*, vol. 243, pp. 447–464, 2017.

[307] G. Mearini *et al.*, 'Mybpc3 gene therapy for neonatal cardiomyopathy enables long-term disease prevention in mice.', *Nat. Commun.*, vol. 5, no. 1, p. 5515, Dec. 2014.

[308] F. Woitek *et al.*, 'Intracoronary Cytoprotective Gene Therapy: A Study of VEGF-B167 in a Pre-Clinical Animal Model of Dilated Cardiomyopathy.', *J. Am. Coll. Cardiol.*, vol. 66, no. 2, pp. 139–53, Jul. 2015.

[309] R. J. Samulski, A. Srivastava, K. I. Berns, and N. Muzyczka, 'Rescue of adeno-associated virus from recombinant plasmids: gene correction within the terminal repeats of AAV.', *Cell*, vol. 33, no. 1, pp. 135–43, May 1983.

[310] Q. Zhou, W. Tian, C. Liu, Z. Lian, X. Dong, and X. Wu, 'Deletion of the B-B' and C-C' regions of inverted terminal repeats reduces rAAV productivity but increases transgene expression.', *Sci. Rep.*, vol. 7, no. 1, p. 5432, Dec. 2017.

[311] A. Geisler and H. Fechner, 'MicroRNA-regulated viral vectors for gene therapy', *World J. Exp. Med.*, vol. 6, no. 2, p. 37, May 2016.

[312] D. M. McCarty, 'Self-complementary AAV vectors; advances and applications.', *Mol. Ther.*, vol. 16, no. 10, pp. 1648–56, Oct. 2008.

[313] M. Jessup *et al.*, 'Calcium Upregulation by Percutaneous Administration of Gene Therapy in Cardiac Disease (CUPID)', *Circulation*, vol. 124, no. 3, pp. 304–313, Jul. 2011.

[314] K. Zsebo *et al.*, 'Long-term effects of AAV1/SERCA2a gene transfer in patients with severe heart failure: analysis of recurrent cardiovascular events and mortality.', *Circ. Res.*, vol. 114, no. 1, pp. 101–8, Jan. 2014.

[315] B. Greenberg *et al.*, 'Calcium upregulation by percutaneous administration of gene therapy in patients with cardiac disease (CUPID 2): a randomised, multinational, double-blind, placebo-controlled, phase 2b trial.', *Lancet (London, England)*, vol. 387, no. 10024, pp. 1178–86, Mar. 2016.

[316] P. Boekstegers *et al.*, 'Myocardial gene transfer by selective pressure-regulated retroinfusion of coronary veins', *Gene Ther.*, vol. 7, no. 3, pp. 232–240, Feb. 2000.

[317] G. Vassalli, H. Büeler, J. Dudler, L. K. von Segesser, and L. Kappenberger, 'Adeno-associated virus (AAV) vectors achieve prolonged transgene expression in mouse myocardium and arteries in vivo: a comparative study with adenovirus vectors.', *Int. J. Cardiol.*, vol. 90, no. 2–3, pp. 229–38, Aug. 2003.

[318] A. Bera and D. Sen, 'Promise of adeno-associated virus as a gene therapy vector for cardiovascular diseases', *Heart Fail. Rev.*, vol. 22, no. 6, pp. 795–823, Nov. 2017.

[319] S. Bass-Stringer, B. C. Bernardo, C. N. May, C. J. Thomas, K. L. Weeks, and J. R. McMullen, 'Adeno-Associated Virus Gene Therapy: Translational Progress and Future Prospects in the Treatment of Heart Failure.', *Heart. Lung Circ.*, vol. 27, no. 11, pp. 1285–1300, Nov. 2018.

[320] M. Ferrarini *et al.*, 'Adeno-associated virus-mediated transduction of VEGF165 improves cardiac tissue viability and functional recovery after permanent coronary occlusion in conscious dogs.', *Circ. Res.*, vol. 98, no. 7, pp. 954–61, Apr. 2006.

[321] Z. Tao *et al.*, 'Coexpression of VEGF and angiopoietin-1 promotes angiogenesis and cardiomyocyte proliferation reduces apoptosis in porcine myocardial infarction (MI) heart.', *Proc. Natl. Acad. Sci. U. S. A.*, vol. 108, no. 5, pp. 2064–9, Feb. 2011.

[322] C. Kupatt *et al.*, 'Cotransfection of Vascular Endothelial Growth Factor-A and Platelet-Derived Growth Factor-B Via Recombinant Adeno-Associated Virus Resolves Chronic Ischemic Malperfusion', *J. Am. Coll. Cardiol.*, vol. 56, no. 5, pp. 414–422, Jul. 2010.

[323] Y. Kawase *et al.*, 'Reversal of cardiac dysfunction after long-term expression of SERCA2a by gene transfer in a pre-clinical model of heart failure.', *J. Am. Coll. Cardiol.*, vol. 51, no. 11, pp. 1112–9, Mar. 2008.

[324] L. Hadri *et al.*, 'SERCA2a gene transfer enhances eNOS expression and activity in endothelial cells.', *Mol. Ther.*, vol. 18, no. 7, pp. 1284–92, Jul. 2010.

[325] M. J. Byrne, J. M. Power, A. Preovolos, J. A. Mariani, R. J. Hajjar, and D. M. Kaye, 'Recirculating cardiac delivery of AAV2/1SERCA2a improves myocardial function in an experimental model of heart failure in large animals.', *Gene Ther.*, vol. 15, no. 23, pp. 1550–7, Dec. 2008.

[326] R. Beeri *et al.*, 'Gene Delivery of Sarcoplasmic Reticulum Calcium ATPase Inhibits Ventricular Remodeling in Ischemic Mitral Regurgitation', *Circ. Hear. Fail.*, vol. 3, no. 5, pp. 627–634, Sep. 2010.

[327] J. A. Mariani, A. Smolic, A. Preovolos, M. J. Byrne, J. M. Power, and D. M. Kaye, 'Augmentation of left ventricular mechanics by recirculation-mediated AAV2/1-SERCA2a gene delivery in experimental heart failure.', *Eur. J. Heart Fail.*, vol. 13, no. 3, pp. 247–53, Mar. 2011.

[328] A. S. Fargnoli *et al.*, 'Cardiac surgical delivery of the sarcoplasmic reticulum calcium ATPase rescues myocytes in ischemic heart failure.', *Ann. Thorac. Surg.*, vol. 96, no. 2, pp. 586–95, Aug. 2013.

[329] M. G. Katz *et al.*, 'Mitigation of myocardial fibrosis by molecular cardiac surgery-mediated gene overexpression.', *J. Thorac. Cardiovasc. Surg.*, vol. 151, no. 4, pp. 1191–200.e3, Apr. 2016.

[330] M. G. Katz *et al.*, 'Safety and efficacy of high-dose adeno-associated virus 9 encoding sarcoplasmic reticulum Ca(2+) adenosine triphosphatase delivered by molecular cardiac surgery with recirculating delivery in ovine ischemic cardiomyopathy.', *J. Thorac. Cardiovasc. Surg.*, vol. 148, no. 3, pp. 1065–72, 1073e1-2; discussion1072-3, Sep. 2014.

[331] Y.-F. Mi, X.-Y. Li, L.-J. Tang, X.-C. Lu, Z.-Q. Fu, and W.-H. Ye, 'Improvement in cardiac function after sarcoplasmic reticulum Ca2+-ATPase gene transfer in a beagle heart failure model.', *Chin. Med. J. (Engl).*, vol. 122, no. 12, pp. 1423–8, Jun. 2009.

[332] X. Zhu *et al.*, 'Immunosuppression Decreases Inflammation and Increases AAV6-hSERCA2a-Mediated SERCA2a Expression', *Hum. Gene Ther.*, vol. 23, no. 7, pp. 722–732, Jul. 2012.

[333] L. Tilemann *et al.*, 'SUMO-1 gene transfer improves cardiac function in a large-animal model of heart failure.', *Sci. Transl. Med.*, vol. 5, no. 211, p. 211ra159, Nov. 2013.

[334] C. Weber *et al.*, 'Therapeutic safety of high myocardial expression levels of the molecular inotrope S100A1 in a preclinical heart failure model.', *Gene Ther.*, vol. 21, no. 2, pp. 131–8, Feb. 2014.

[335] K. M. Fish *et al.*, 'AAV9.I-1c delivered via direct coronary infusion in a porcine model of heart failure improves contractility and mitigates adverse remodeling.', *Circ. Heart Fail.*, vol. 6, no. 2, pp. 310–7, Mar. 2013.

[336] K. Ishikawa *et al.*, 'Cardiac I-1c overexpression with reengineered AAV improves cardiac function in swine ischemic heart failure.', *Mol. Ther.*, vol. 22, no. 12, pp. 2038–45, Dec. 2014.

[337] R. Hinkel *et al.*, 'Heme Oxygenase-1 Gene Therapy Provides Cardioprotection Via Control of Post-Ischemic Inflammation: An Experimental Study in a Pre-Clinical Pig Model.', *J. Am. Coll. Cardiol.*, vol. 66, no. 2, pp. 154–65, Jul. 2015.

[338] L. T. Bish *et al.*, 'Cardiac gene transfer of short hairpin RNA directed against phospholamban effectively knocks down gene expression but causes cellular toxicity in canines.', *Hum. Gene Ther.*, vol. 22, no. 8, pp. 969–77, Aug. 2011.

[339] B. E. Jaski *et al.*, 'Calcium Upregulation by Percutaneous Administration of Gene Therapy in Cardiac Disease (CUPID Trial), a First-in-Human Phase 1/2 Clinical Trial', *J. Card. Fail.*, vol. 15, no. 3, pp. 171–181, Apr. 2009.

[340] J.-S. Hulot *et al.*, 'Effect of intracoronary administration of AAV1/SERCA2a on ventricular remodelling in patients with advanced systolic heart failure: results from the AGENT-HF randomized phase 2 trial.', *Eur. J. Heart Fail.*, vol. 19, no. 11, pp. 1534–1541, Nov. 2017.

[341] J. Ganesan *et al.*, 'MiR-378 controls cardiac hypertrophy by combined repression of mitogen-activated protein kinase pathway factors.', *Circulation*, vol. 127, no. 21, pp. 2097–106, May 2013.

[342] A. Borden *et al.*, 'Transient Introduction of miR-294 in the Heart Promotes Cardiomyocyte Cell Cycle Reentry After Injury.', *Circ. Res.*, p. CIRCRESAHA.118.314223, Apr. 2019.

[343] F. Gao *et al.*, 'Therapeutic role of miR-19a/19b in cardiac regeneration and protection from myocardial infarction.', *Nat. Commun.*, vol. 10, no. 1, p. 1802, Dec. 2019.

[344] M. Quattrocelli *et al.*, 'Long-term miR-669a therapy alleviates chronic dilated cardiomyopathy in dystrophic mice.', *J. Am. Heart Assoc.*, vol. 2, no. 4, p. e000284, Aug. 2013.

[345] C. Wahlquist *et al.*, 'Inhibition of miR-25 improves cardiac contractility in the failing heart.', *Nature*, vol. 508, no. 7497, pp. 531–5, Apr. 2014.

[346] K.-M. R. Prasad, Y. Xu, Z. Yang, S. T. Acton, and B. A. French, 'Robust cardiomyocyte-specific gene expression following systemic injection of AAV: in vivo gene delivery follows a Poisson distribution.', *Gene Ther.*, vol. 18, no. 1, pp. 43–52, Jan. 2011.

[347] J. E. Loeb, W. S. Cordier, M. E. Harris, M. D. Weitzman, and T. J. Hope, 'Enhanced expression of transgenes from adeno-associated virus vectors with the woodchuck hepatitis virus posttranscriptional regulatory element: implications for gene therapy.', *Hum. Gene Ther.*, vol. 10, no. 14, pp. 2295–305, Sep. 1999.

[348] O. Iglesias-García *et al.*, 'Neuregulin-1β induces mature ventricular cardiac differentiation from induced pluripotent stem cells contributing to cardiac tissue repair.', *Stem Cells Dev.*, vol. 24, no. 4, pp. 484–96, Feb. 2015.

[349] J. L. Torán *et al.*, 'CXCL6 is an important paracrine factor in the pro-angiogenic human cardiac progenitor-like cell secretome.', *Sci. Rep.*, vol. 7, no. 1, p. 12490, Dec. 2017.

[350] C. Théry, S. Amigorena, G. Raposo, and A. Clayton, 'Isolation and Characterization of Exosomes from Cell Culture Supernatants and Biological Fluids', *Curr. Protoc. Cell Biol.*, vol. 30, no. 1, pp. 3.22.1-3.22.29, Mar. 2006.

[351] E. Sangiorgi and M. R. Capecchi, 'Bmi1 is expressed in vivo in intestinal stem cells', *Nat. Genet.*, vol. 40, no. 7, pp. 915–920, Jul. 2008.

[352] T. D. Schmittgen, E. J. Lee, and J. Jiang, 'High-Throughput Real-Time PCR', in *Methods in molecular biology (Clifton, N.J.)*, vol. 429, 2008, pp. 89–98.

[353] G. Yu, L.-G. Wang, Y. Han, and Q.-Y. He, 'clusterProfiler: an R Package for Comparing Biological Themes Among Gene Clusters', *Omi. A J. Integr. Biol.*, vol. 16, no. 5, pp. 284–287, May 2012.

[354] J. L. McBride *et al.*, 'Artificial miRNAs mitigate shRNA-mediated toxicity in the brain: implications for the therapeutic development of RNAi.', *Proc. Natl. Acad. Sci. U. S. A.*, vol. 105, no. 15, pp. 5868–73, Apr. 2008.

[355] R. L. Boudreau, I. Martins, and B. L. Davidson, 'Artificial MicroRNAs as siRNA Shuttles: Improved Safety as Compared to shRNAs In vitro and In vivo', *Mol. Ther.*, vol. 17, no. 1, pp. 169–175, Jan. 2009.

[356] A. Georgiadis *et al.*, 'AAV-mediated knockdown of peripherin-2 in vivo using miRNA-based hairpins.', *Gene Ther.*, vol. 17, no. 4, pp. 486–93, Apr. 2010.

[357] X. Yang, K. Marcucci, X. Anguela, and L. B. Couto, 'Preclinical Evaluation of An Anti-HCV miRNA Cluster for Treatment of HCV Infection', *Mol. Ther.*, vol. 21, no. 3, pp. 588–601, Mar. 2013.

[358] L. A. Aagaard *et al.*, 'Engineering and optimization of the miR-106b cluster for ectopic expression of multiplexed anti-HIV RNAs', *Gene Ther.*, vol. 15, no. 23, pp. 1536–1549, Dec. 2008.

[359] K. Chang, K. Marran, A. Valentine, and G. J. Hannon, 'Generation of transgenic Drosophila expressing shRNAs in the miR-1 backbone.', *Cold Spring Harb. Protoc.*, vol. 2014, no. 5, p. pdb.prot080762-pdb.prot080762, May 2014.

[360] Y. P. Liu, J. Haasnoot, O. ter Brake, B. Berkhout, and P. Konstantinova, 'Inhibition of HIV-1 by multiple siRNAs expressed from a single microRNA polycistron.', *Nucleic Acids Res.*, vol. 36, no. 9, pp. 2811–24, May 2008.

[361] S. C.-Y. Chen, P. Stern, Z. Guo, and J. Chen, 'Expression of multiple artificial microRNAs from a chicken miRNA126-based lentiviral vector.', *PLoS One*, vol. 6, no. 7, p. e22437, Jul. 2011.

[362] Y. Zeng, E. J. Wagner, and B. R. Cullen, 'Both natural and designed micro RNAs can

inhibit the expression of cognate mRNAs when expressed in human cells.', *Mol. Cell*, vol. 9, no. 6, pp. 1327–33, Jun. 2002.

[363] K.-H. Chung *et al.*, 'Polycistronic RNA polymerase II expression vectors for RNA interference based on BIC/miR-155.', *Nucleic Acids Res.*, vol. 34, no. 7, p. e53, Apr. 2006.

[364] K. N. Heller, J. T. Mendell, J. R. Mendell, and L. R. Rodino-Klapac, 'MicroRNA-29 overexpression by adeno-associated virus suppresses fibrosis and restores muscle function in combination with micro-dystrophin.', *JCI insight*, vol. 2, no. 9, May 2017.

[365] C. Benavides-Vallve *et al.*, 'New strategies for echocardiographic evaluation of left ventricular function in a mouse model of long-term myocardial infarction.', *PLoS One*, vol. 7, no. 7, p. e41691, Jul. 2012.

[366] L. T. Bish *et al.*, 'Adeno-associated virus (AAV) serotype 9 provides global cardiac gene transfer superior to AAV1, AAV6, AAV7, and AAV8 in the mouse and rat.', *Hum. Gene Ther.*, vol. 19, no. 12, pp. 1359–68, Dec. 2008.

[367] C. A. Pacak *et al.*, 'Recombinant adeno-associated virus serotype 9 leads to preferential cardiac transduction in vivo.', *Circ. Res.*, vol. 99, no. 4, pp. e3-9, Aug. 2006.

[368] K. Inagaki *et al.*, 'Robust systemic transduction with AAV9 vectors in mice: efficient global cardiac gene transfer superior to that of AAV8', *Mol. Ther.*, vol. 14, no. 1, pp. 45–53, 2006.

[369] K. Gabisonia and F. A. Recchia, 'Gene Therapy for Heart Failure: New Perspectives', *Curr. Heart Fail. Rep.*, vol. 15, no. 6, pp. 340–349, Dec. 2018.

[370] L. T. Bish *et al.*, 'Adeno-Associated Virus (AAV) Serotype 9 Provides Global Cardiac Gene Transfer Superior to AAV1, AAV6, AAV7, and AAV8 in the Mouse and Rat', *Hum. Gene Ther.*, vol. 19, pp. 1359–1368, 2008.

[371] C. Zincarelli, S. Soltys, G. Rengo, and J. E. Rabinowitz, 'Analysis of AAV serotypes 1-9 mediated gene expression and tropism in mice after systemic injection.', *Mol. Ther.*, vol. 16, no. 6, pp. 1073–1080, 2008.

[372] H. Fang *et al.*, 'Comparison of Adeno-Associated Virus Serotypes and Delivery Methods for Cardiac Gene Transfer', *Hum. Gene Ther. Methods*, vol. 23, no. 4, pp. 234–241, Aug. 2012.

[373] M. Merentie *et al.*, 'Efficacy and safety of myocardial gene transfer of adenovirus, adeno-associated virus and lentivirus vectors in the mouse heart', *Gene Ther.*, vol. 23, no. 3, pp. 296–305, Mar. 2016.

[374] C. Bär *et al.*, 'Telomerase expression confers cardioprotection in the adult mouse heart after acute myocardial infarction.', *Nat. Commun.*, vol. 5, p. 5863, Dec. 2014.

[375] K. Chamberlain, J. M. Riyad, and T. Weber, 'Cardiac gene therapy with adeno-associated virus-based vectors', *Curr. Opin. Cardiol.*, vol. 32, no. 3, pp. 275–282, May 2017.

[376] A. Geisler *et al.*, 'microRNA122-regulated transgene expression increases specificity of cardiac gene transfer upon intravenous delivery of AAV9 vectors.', *Gene Ther.*, vol. 18, no. 2, pp. 199–209, Feb. 2011.

[377] A. Geisler *et al.*, 'Application of mutated miR-206 target sites enables skeletal muscle-specific silencing of transgene expression of cardiotropic AAV9 vectors.', *Mol. Ther.*, vol. 21, no. 5, pp. 924–33, May 2013.

[378] S. T. Pleger *et al.*, 'Stable myocardial-specific AAV6-S100A1 gene therapy results in chronic functional heart failure rescue.', *Circulation*, vol. 115, no. 19, pp. 2506–15, May 2007.

[379] K.-M. R. Prasad, Y. Xu, Z. Yang, S. T. Acton, and B. A. French, 'Robust cardiomyocyte-specific gene expression following systemic injection of AAV: in vivo gene delivery follows a Poisson distribution.', *Gene Ther.*, vol. 18, no. 1, pp. 43–52, Jan. 2011.

[380] J. Ai *et al.*, 'Cellular Physiology and Biochemistry Cellular Physiology and Biochemistry Characterization of Recombinant Adeno-Associated Viral Transduction and Safety Profiles in Cardiomyocytes', *Cell Physiol Biochem*, vol. 48, pp. 1894–1900, 2018.

[381] K.-M. R. Prasad, R. S. Smith, Y. Xu, and B. A. French, 'A single direct injection into the left ventricular wall of an adeno-associated virus 9 (AAV9) vector expressing extracellular superoxide dismutase from the cardiac troponin-T promoter protects mice against myocardial infarction.', *J. Gene Med.*, vol. 13, no. 6, pp. 333–41, Jun. 2011.

[382] P. R. Konkalmatt, R. J. Beyers, D. M. O'Connor, Y. Xu, M. E. Seaman, and B. A. French, 'Cardiac-Selective Expression of Extracellular Superoxide Dismutase After Systemic Injection of Adeno-Associated Virus 9 Protects the Heart Against Post–Myocardial Infarction Left Ventricular Remodeling', *Circ. Cardiovasc. Imaging*, vol. 6, no. 3, pp. 478–486, May 2013.

[383] T. Cervelli *et al.*, 'Processing of recombinant AAV genomes occurs in specific nuclear structures that overlap with foci of DNA-damage-response proteins', *J. Cell Sci.*, vol. 121, no. 3, pp. 349–357, Jan. 2008.

[384] R. S. Traister, S. Fabre, Z. Wang, X. Xiao, and R. Hirsch, 'Inflammatory cytokine regulation of transgene expression in human fibroblast-like synoviocytes infected with adeno-associated virus.', *Arthritis Rheum.*, vol. 54, no. 7, pp. 2119–26, Jul. 2006.

[385] C. Collesi and M. Giacca, 'Gene transfer to promote cardiac regeneration', *Crit. Rev. Clin. Lab. Sci.*, vol. 53, no. 6, pp. 359–369, Nov. 2016.

[386] M. Ferracin *et al.*, 'Absolute quantification of cell-free microRNAs in cancer patients', *Oncotarget*, vol. 6, no. 16, pp. 14545–55, Jun. 2015.

[387] Z. Zhao *et al.*, 'A combined gene expression and functional study reveals the crosstalk between N-Myc and differentiation-inducing microRNAs in neuroblastoma cells.', *Oncotarget*, vol. 7, no. 48, pp. 79372–79387, Nov. 2016.

[388] Z. Zhao *et al.*, 'microRNA-2110 functions as an onco-suppressor in neuroblastoma by directly targeting Tsukushi.', *PLoS One*, vol. 13, no. 12, p. e0208777, Dec. 2018.

[389] R. Spaull *et al.*, 'Exosomes populate the cerebrospinal fluid of preterm infants with post-haemorrhagic hydrocephalus.', *Int. J. Dev. Neurosci.*, vol. 73, pp. 59–65, Apr. 2019.

[390] C. Balbi *et al.*, 'First Characterization of Human Amniotic Fluid Stem Cell Extracellular Vesicles as a Powerful Paracrine Tool Endowed with Regenerative Potential.', *Stem Cells Transl. Med.*, vol. 6, no. 5, pp. 1340–1355, May 2017.

[391] C. Wang *et al.*, 'BMSCs protect against renal ischemia-reperfusion injury by secreting exosomes loaded with miR-199a-5p that target BIP to inhibit endoplasmic reticulum stress at the very early reperfusion stages', *FASEB J.*, vol. 33, no. 4, pp. 5440–5456, Apr. 2019.

[392] S. Zanotti *et al.*, 'Exosomes and exosomal miRNAs from muscle-derived fibroblasts

promote skeletal muscle fibrosis.', *Matrix Biol.*, vol. 74, pp. 77–100, Dec. 2018.

[393] W. D. Gray *et al.*, 'Identification of therapeutic covariant microRNA clusters in hypoxia-treated cardiac progenitor cell exosomes using systems biology.', *Circ. Res.*, vol. 116, no. 2, pp. 255–63, Jan. 2015.

[394] L. Barile *et al.*, 'Extracellular vesicles from human cardiac progenitor cells inhibit cardiomyocyte apoptosis and improve cardiac function after myocardial infarction.', *Cardiovasc. Res.*, vol. 103, no. 4, pp. 530–41, Sep. 2014.

[395] G. de Couto *et al.*, 'Exosomal MicroRNA Transfer Into Macrophages Mediates Cellular Postconditioning', *Circulation*, vol. 136, no. 2, pp. 200–214, Jul. 2017.

[396] M. Yang *et al.*, 'miR-935 promotes gastric cancer cell proliferation by targeting SOX7.', *Biomed. Pharmacother.*, vol. 79, pp. 153–8, Apr. 2016.

[397] X. Liu, J. Li, Z. Yu, J. Li, R. Sun, and Q. Kan, 'miR-935 Promotes Liver Cancer Cell Proliferation and Migration by Targeting SOX7.', *Oncol. Res.*, vol. 25, no. 3, pp. 427–435, Mar. 2017.

[398] B. Peng, C. Li, P. Cai, L. Yu, B. Zhao, and G. Chen, 'Knockdown of miR-935 increases paclitaxel sensitivity via regulation of SOX7 in non-small-cell lung cancer.', *Mol. Med. Rep.*, vol. 18, no. 3, pp. 3397–3402, Sep. 2018.

[399] C. Wang, Z. Feng, K. Jiang, and X. Zuo, 'Upregulation of MicroRNA-935 Promotes the Malignant Behaviors of Pancreatic Carcinoma PANC-1 Cells via Targeting Inositol Polyphosphate 4-Phosphatase Type I Gene (INPP4A).', *Oncol. Res.*, vol. 25, no. 4, pp. 559–569, Apr. 2017.

[400] T. Wang, Y. Chen, H. Nie, Y. Huang, Y. Zhao, and J. Yang, 'IL-27 inhibits non-small-cell lung cancer cell metastasis by miR-935 in vitro.', *Onco. Targets. Ther.*, vol. 12, pp. 1447–1454, Feb. 2019.

[401] C. Wang, S. Li, J. Xu, W. Niu, and S. Li, 'microRNA-935 is reduced in non-small cell lung cancer tissue, is linked to poor outcome, and acts on signal transduction mediator E2F7 and the AKT pathway.', *Br. J. Biomed. Sci.*, vol. 76, no. 1, pp. 17–23, Jan. 2019.

[402] C. Yan, J. Yu, W. Kang, Y. Liu, Z. Ma, and L. Zhou, 'miR-935 suppresses gastric signet ring cell carcinoma tumorigenesis by targeting Notch1 expression.', *Biochem. Biophys. Res. Commun.*, vol. 470, no. 1, pp. 68–74, Jan. 2016.

[403] Z. Liu, Q. Li, X. Zhao, B. Cui, L. Zhang, and Q. Wang, 'MicroRNA-935 inhibits proliferation and invasion of osteosarcoma cells by directly targeting High mobility group box 1', *Oncol. Res. Featur. Preclin. Clin. Cancer Ther.*, 2018.

[404] B. Zhang *et al.*, 'INT-HA induces M2-like macrophage differentiation of human monocytes via TLR4-miR-935 pathway.', *Cancer Immunol. Immunother.*, vol. 68, no. 2, pp. 189–200, Feb. 2019.

[405] J. Xiao *et al.*, 'Cardiac progenitor cell-derived exosomes prevent cardiomyocytes apoptosis through exosomal miR-21 by targeting PDCD4', *Cell Death Dis.*, vol. 7, no. 6, pp. e2277–e2277, Jun. 2016.

[406] J. Yang, F. Hu, X. Fu, Z. Jiang, W. Zhang, and K. Chen, 'MiR-128/SOX7 alleviates myocardial ischemia injury by regulating IL-33/sST2 in acute myocardial infarction.', *Biol. Chem.*, vol. 400, no. 4, pp. 533–544, Mar. 2019.

[407] M.-C. Ma *et al.*, 'Interleukin-27, a novel cytokine induced by ischemia-reperfusion injury

in rat hearts, mediates cardioprotective effects via the gp130/STAT3 pathway.', *Basic Res. Cardiol.*, vol. 110, no. 3, p. 22, May 2015.

[408] K. Niessen and A. Karsan, 'Notch signaling in the developing cardiovascular system.', *Am. J. Physiol. Cell Physiol.*, vol. 293, no. 1, pp. C1-11, Jul. 2007.

[409] W.-H. Liu, H.-W. Hsiao, W.-I. Tsou, and M.-Z. Lai, 'Notch inhibits apoptosis by direct interference with XIAP ubiquitination and degradation.', *EMBO J.*, vol. 26, no. 6, pp. 1660–9, Mar. 2007.

[410] X. Meng *et al.*, 'Inhibition of miR-363 protects cardiomyocytes against hypoxia-induced apoptosis through regulation of Notch signaling.', *Biomed. Pharmacother.*, vol. 90, pp. 509–516, Jun. 2017.

[411] L. Lu, H. Zhang, W. Dong, W. Peng, and J. Yang, 'MiR-381 negatively regulates cardiomyocyte survival by suppressing Notch signaling.', *In Vitro Cell. Dev. Biol. Anim.*, vol. 54, no. 8, pp. 610–619, Sep. 2018.

[412] A. Raucci, S. Di Maggio, F. Scavello, A. D'Ambrosio, M. E. Bianchi, and M. C. Capogrossi, 'The Janus face of HMGB1 in heart disease: a necessary update.', *Cell. Mol. Life Sci.*, vol. 76, no. 2, pp. 211–229, Jan. 2019.

[413] J. Zhao *et al.*, 'Mesenchymal Stromal Cell-Derived Exosomes Attenuate Myocardial Ischemia-Reperfusion Injury through miR-182-Regulated Macrophage Polarization.', *Cardiovasc. Res.*, Feb. 2019.

[414] K. Gabisonia *et al.*, 'MicroRNA therapy stimulates uncontrolled cardiac repair after myocardial infarction in pigs', *Nature*, vol. 569, no. 7756, pp. 418–422, May 2019.